Comparative study in clearing of transient faults in medium voltage networks by means of neutral or single-phase tripping

CJ van der Mescht

20255616

Dissertation submitted in fulfilment of the requirements for the degree Magister in Electrical and Electronic Engineering at the Potchefstroom Campus of the North-West University

Supervisor: Dr L Lamont

November 2016

Abstract

Within power utility networks, transient and permanent faults cause power interruptions to customers. Research has indicated that most faults that result in breakers tripping within MV networks are temporary in nature. Other sources have also indicated that approximately 30% of permanent faults started as a transient fault. All types of faults in an electrical network do put strain on electrical equipment to a certain degree.

A need therefore arises to explore alternative ways of clearing transient faults in order to increase network reliability. If transient faults are cleared more effectively, it will influence power quality positively by reducing the length of voltage dips and limiting voltage dip propagation.

This dissertation contains research performed on the effectiveness of methods that aims to clear transient faults on MV networks (11 kV and 22 kV) without causing momentary supply loss to customers due to breaker ARC operations. Transient fault clearing is achieved by interrupting fault currents very quickly.

For transient earth faults, this can be achieved by momentarily disconnecting the neutral earth connection of the NECR. For transient phase-to-phase faults, this can be achieved by single-phase tripping - which will open only one of the two affected phase breakers within 30 ms. The fast operation greatly reduces the amount of ionised air and damage that is formed during a fault condition. This, in turn, improves the overall success rate of both schemes.

MV line - and transformer models were created, verified and validated by means of calculations, simulations and field testing. The validated line and transformer models were used to develop integrated models for each of the two fault-clearing schemes. The integrated models were used to simulate the expected network response under different fault conditions. After implementing both fault-clearing schemes on actual MV networks, the simulated results of the integrated models were validated with measurements.

Neutral tripping is effective in the clearing of high and low impedance earth faults. It was found that by implementing neutral tripping, as many as 83.4% of earth faults were successfully cleared. The fault-clearing effectiveness of neutral tripping is primarily determined by the capacitive coupling of the MV network. Single-phase tripping is effective in the clearing of earth faults and phase-to-phase faults. It was found that by implementing single-phase tripping, 58% of earth faults and 94% of phase-to-phase faults were successfully cleared. The fault-clearing

effectiveness of single-phase tripping is primarily determined by the feedback current magnitudes of Δ/Y transformers as well as the capacitive coupling on the MV line.

Implementing these methods of transient fault clearing results in less stress being placed on breakers, conductors and transformers within the MV network. The efficiency with which transient faults are cleared positively influences network reliability as transient faults will not result in permanent faults. The speed with which transient faults are cleared improves the power quality of the MV network with regards to voltage dips, sustained and momentary interruptions.

Lastly, the neutral breaker and single-phase breaker schemes will result in up to 50 times fewer burn wounds on people or animals in the unfortunate case where inadvertent contact is made with the MV network due to the fast tripping capabilities of both schemes.

Key words: Single-phase tripping, neutral tripping, transient fault, capacitive coupling, medium voltage, power quality

Opsomming

Tydelike en permanente elektriese foute veroorsaak ongewenste kragonderbrekings in elektriese verspreidingsnetwerke. Navorsing toon dat die meerderheid foute wat veroorsaak dat stroombrekers in 11kV- en 22kV-distribusienetwerke klink, tydelik van aard is. Ongeveer 30% van permanente foute het begin as gevolg van ‘n tydelike fout. Alle elektriese foute veroorsaak egter stremming op verskeie elektriese komponente.

Daar is dus ’n behoefte om alternatiewe oplossings te ondersoek wat tydelike foute effektief kan blus en sodoende netwerkbetroubaarheid verbeter. Indien tydelike foute effektief geblus kan word, sal die toevoerkwaliteit verbeter omdat spanningsknikke verkort word.

Hierdie verhandeling omvat navorsing oor die effektiwiteit van verskeie tegnieke om tydelike foute in 11kV- en 22kV-kragnetwerke te blus sonder om ’n drie-fase toevoeronderbreking te veroorsaak. Tydelike foute kan geblus word deur die foutstroomvloei so gou moontlik te onderbreek.

Tydelike aardfoute kan geblus word deur die neutrale aardverbindingspunt van die neutraleaardingskompensator (NECR) tydelik te onderbreek. Fase-na-fase foute kan geblus word deur enkel-fase klinking, waarna slegs een van die twee geaffekteerde fases binne 30 ms sal klink. As gevolg van die hoë spoed waarteen die breker klink, sal die hoeveelheid geïoniseerde lug en skade aan die elektriese netwerk wat tydens ’n fouttoestand veroorsaak word, verminder.

Die 11kV- en 22kV-kraglyn en transformatormodelle is ontwerp en gestaaf deur middel van berekeninge, simulasies en praktiese toetse. Die gestaafde lyn- en transformatormodelle is gebruik om geïntegreerde modelle vir elk van die twee foutklinkingtegnieke te ontwerp. Die geïntegreerde modelle is gebruik om die kragnetwerk se reaksie onder verskeie fouttoestande te bepaal. Al twee foutklinkingtegnieke is op bestaande 11kV- en 22kV-kragnetwerke geïmplementeer en die gemete resultate is vergelyk met die simulasie resultate van die geïntegreerde modelle.

Neutrale klinking is effektief om hoë en lae impedansie aardfoute te blus. Gedurende die navorsing is bevind dat 83.4% van al die aardfoute suksesvol geblus het ná die implementering van die neutrale klinkingtegniek. Die effektiwiteit van neutrale klinking is hoofsaaklik afhanklik van die kapasitiewe-koppeling van die kragnetwerk. Enkel-fase klinking is effektief om aardfoute sowel as fase-na-fase foute te blus. Gedurende die navorsing is bevind dat 58% van

alle aardfoute en 94% van alle fase-na-fase foute suksesvol geblus het ná die implementering van die enkel-fase klinkingtegniek. Die effektiwiteit van enkel-fase klinking is hoofsaaklik afhanklik van die Δ/Y-transformators se terugvoerstroom, sowel as die kapasitiewe-koppeling van die kraglyn.

Die implementering van die twee bogenoemde foutklinkingtegnieke het gelei tot minder stremming op stroombrekers, geleiers en transformators in die elektriese kragnetwerk. Die effektiwiteit waarmee foute blus, dra by tot die betroubaarheid van die elektriese kragnetwerk omdat tydelike foute nie ontwikkel in permanente foute nie. Die spoed waarteen foute geblus word, dra ook by tot ’n verbetering in toevoerkwaliteit ten opsigte van spanningsknikke, en tydelike sowel as permanente kragtoevoeronderbrekings.

As gevolg van die hoë klinkingspoed van al twee foutklinkingtegnieke sal tot 50 maal minder brandwonde veroorsaak word in ongewenste gevalle waar ’n mens of dier kontak met ’n elektriese kragnetwerk maak.

Sleutel woorde: Enkel-fase klinking, neutrale klinking, tydelike fout, kapasitiewe-koppeling, toevoerkwaliteit

Acknowledgments

I would like to thank the following people and institutions for affording me the opportunity to pursue a Master's degree:

- North-West University, for affording me the opportunity to pursue a Master's degree
- Eskom Holdings, for the financial support with experimental equipment
- My Eskom colleagues, who supported me during my endeavours
- My supervisor, Dr Lafras Lamont, for his guidance and time
- Prof George van Schoor, who assisted with the layout of this dissertation
- Dr Luna Bergh, for helping me with the proof-reading and editing of my dissertation
- My friends and family for all their prayers
- Willem Dirkse van Schalkwyk, for his mentorship, friendship and encouragement throughout my Electrical Engineering career
- Mandri van der Mescht, my loving wife, for all your prayers, support and heart-to-heart sessions we had during this journey. If it was not for you, this dissertation would not have materialised at all.

All honour and glory be to God for helping me to complete this dissertation. Without You I am nothing, but because I have You, I have everything.

Psalm 16: 5 - 11

Table of Contents

List of figures and tables

List of abbreviations

BIL	-	Basic insulation level
QOS	-	Quality of supply
V	-	Volts
A	-	Amperes
W	-	Watts
F	-	Farads
LV	-	Low Voltage (up to 1000V)
MV	-	Medium Voltage (1 kV<MV<= 44 kV)
HV	-	High Voltage (44 kV<HV<=220 kV)
EHV	-	Extra High Voltage (220 kV<EHV<=400 kV)
UHV	-	Extra High Voltage (UHV>400 kV)
E/F	-	Earth Fault
O/C	-	Over Current
IDMT	-	Inverse Definite Minimum Time
NERSA	-	National Energy Regulator of South Africa
FALLS	-	Fault Analysis and Lightning Locating System
GSD	-	Ground Stroke Density
ARC	-	Auto Reclose Cycle
FSOU	-	Free State Operating Unit
m	-	Meter
rms	-	Root Mean Square
CT	-	Current Transformer
NEC	-	Neutral Earthing Compensator
NER	-	Neutral Earthing Resistor
NECR	-	Neutral Earthing Compensator with Neutral Resistor
SPAR	-	Single-phase Auto Reclosing

--- Chapter 1 ---

Introduction

1.1 Background

Eskom, being the largest electricity supplier in South Africa, has quite an extensive medium voltage (MV) network. Figures in the Eskom annual report of 2015 indicated that the total length of power lines equate to 368331 kilometres. More than 75% of these power lines are overhead MV power lines (6.6 kV, 11 kV, 22 kV and 33 kV) [1]. MV overhead lines are more prone to transient faults when compared to HV and EHV lines, due to the following reasons [2]:

- The BIL of the insulators on MV lines are much lower than on HV lines
- The footing resistance of MV structures are higher, which could lead to back flashovers during lightning storms
- HV structures are primarily constructed from steel as compared to wooden MV structures.

Currently, the majority of breaker operations within MV networks can be ascribed to transient faults caused by lightning, animals, vegetation and wind [3], [4]. Phase-to-phase fault current magnitudes are generally much higher on MV networks as compared to earth faults when NECR's are installed. For this reason, it is more difficult to quench a phase-to-phase fault without a breaker operation. Secondly, with phase-to-phase faults there is no way of clearing the fault current path without causing a supply interruption to customers. In the case of earth faults, the fault current path can be interrupted by temporarily ungrounding the MV network [4]. If the fault current path is removed, the electric arc will quench - provided that the capacitive coupling of the MV network is such that the capacitive current is lower than 35 A [5].

1.1.1 Electrical faults

The energy associated with an open air electrical arc can cause an enormous amount of electrical and mechanical stress on an overhead MV network. The heat generated by an electrical arc could range roughly anywhere from 7000 $^{\circ}$C up to 18000 $^{\circ}$C [6]. It is, therefore, imperative to limit the total amount of energy that could arise during an electrical arc. Electrical network components that are generally the most exposed to damage caused by repeated network faults are [7]:

- Breakers
- Conductors
- Transformers, and
- Isolators.

The amount of arc energy generated during a fault condition is dependent on the system voltage, fault current magnitude and the time the fault remains on the electrical network [8]. When a transient fault occurs on an MV overhead line, an upstream breaker is required to trip in order to clear the fault from the electrical network. If the transient fault was to remain on the electrical network for a prolonged period of time, it can result in the failure of upstream equipment [7]. This will cause a sustained interruption to all the customers connected downstream from the breaker that tripped. Figure 1-1 shows an example where a conductor failure occurred due to a transient fault remaining on the electrical network for a prolonged period of time.

Figure 1-1 Conductor failures on MV overhead line due to initial temporary fault (lightning)

1.1.2 Power quality

Eskom, which is currently the largest power utility in South Africa, is governed by the National Energy Regulator of South Africa (NERSA). One of the aspects that NERSA governs is power quality. The power quality of an electrical network refers to voltage continuity, voltage disturbances and waveform quality. The main focus areas of this dissertation with regards to power quality are voltage dips as well as momentary and sustained interruptions. Voltage dips represent a very important aspect within the power quality field due to the impact it can have on plant operations [9]. Severe voltage dips are generally caused by faults on the electrical network. The duration of such dips depends on the fault-clearing capabilities of protection equipment [10]. In the event that a voltage dip is short and small in magnitude, some plant equipment might be able to ride through the duration of the voltage dip successfully. However, for more severe voltage dips that are deeper and longer in nature, the chances for plant equipment to ride through such dips are quite slim [11]. Guidelines have been given in the NRS 048-2 as to what the acceptable limits are with regards to voltage dips (Figure 1-2).

1	2	3	4	5	6	7
Network voltage range (nominal voltages)	**Number of voltage dips per year**					
	Dip window category					
	X1	**X2**	**T**	**S**	**Z1**	**Z2**
6,6 kV to ≤ 44 kV extended overhead	85	210	115	400	450	450
6,6 kV to ≤ 44 kV	20	30	110	30	20	45
> 44 kV to ≤ 220 kV	35	35	25	40	40	10
220 kV to ≤ 765 kV	30	30	20	20	10	5

Figure 1-2 Number of allowable voltage dips per year [12]

Even when a transient fault does not develop into a permanent fault, the power quality of an electrical network is still affected in terms of dip performance and momentary interruptions [13]. Consider the single line diagram shown in Figure 1-3.

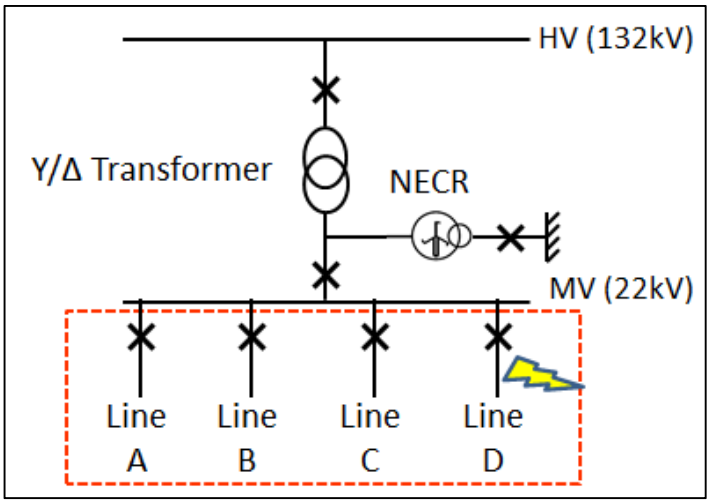

Figure 1-3 Single line electrical network diagram

For a fault occurring on Line D, the relevant line breaker will trip to isolate the faulty section of line from the electrical network. The voltage dip caused by the fault will propagate to all neighbouring lines that are connected on the same busbar. Depending on the location of the fault and the fault level at the substation, the voltage dip encountered on the MV line can propagate to the HV line.

An MV breaker opens all three its poles when tripping for a fault on the MV distribution network, regardless of whether the fault is a multi-phase fault or earth fault. This causes a momentary three-phase interruption which results in motors stalling as contactors drops out. This in turn results in an interruption of plant production, although the three-phase breaker may have successfully reclosed three-seconds later due to the fault being temporary in nature. Guidelines have been given in the NRS048-2 as to what acceptable limits are with regards to sustained interruptions. The limits are shown in Figure 1-4.

1	2	3
Network category	**Unplanned interruptions, number**	**Planned interruptions, number**
A	3 (6)	< 1 (3)
B	18 (75)	4 (11)
NOTE 1 The values for 50 % of customers reflect the number of events per annum that are generally not exceeded in the case of 50 % of customers in South Africa. NOTE 2 The values for 95 % of customers reflect the number of events per annum that are generally not exceeded in the case of 95 % of customers in South Africa. NOTE 3 Characteristic values for category C networks will generally be between those of category A and category B networks.		

Figure 1-4 Number of allowable sustained interruptions per year [12]

1.2 Problem statement

Within power utility networks, transient and permanent faults cause power interruptions to customers. Research has indicated that most faults that result in breakers tripping within MV networks are temporary in nature [14], [15]. Other sources have also indicated that approximately 30% of permanent faults started as a transient fault [16]. All types of faults in an electrical network do put strain on electrical equipment to a certain degree.

During the 2014/2015 and 2015/2016 financial years, the majority of breaker operations within the Eskom Distribution Free State Operating Unit were due to transient faults, as shown in Figure 1-5. The raw data was obtained by compiling a pivot table from historical fault data captured within the Eskom network equipment and performance system database [17]. The following root causes in Figure 1-5 can be classified as being transient faults and have a combined weight of approximately 61%:

- Overhead line problem
- Fault not found
- Conductor problem
- Adverse weather.

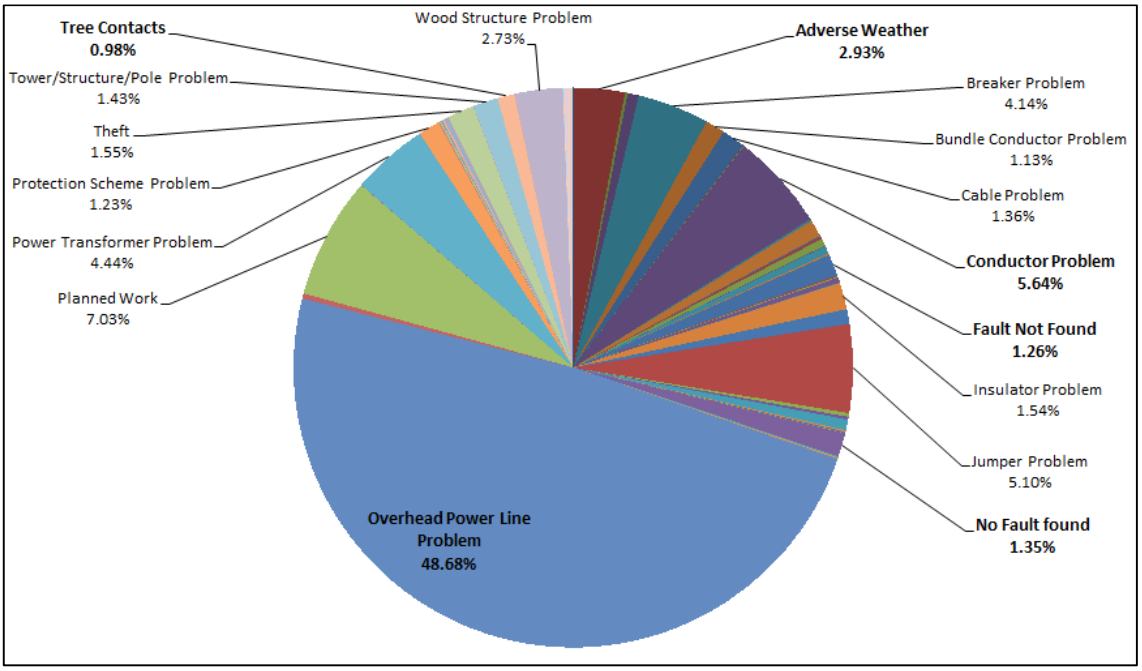

Figure 1-5 Root causes resulting in customer interruptions for the period April 2014 – March 2016 [17]

A need therefore arises to explore alternative ways of clearing transient faults in order to increase network reliability. If transient faults are cleared more effectively, it will influence power quality positively by reducing the length of voltage dips and limiting voltage dip propagation [10], [11].

In order of frequency of occurrence, phase-to-earth faults occurs the most, followed by phase-to-phase, phase-to-phase-to-earth and, lastly, balanced three-phase faults [18]. It follows from the literature available that earth faults on HV networks account for 70% of all faults and earth faults on EHV networks for 90% of all faults [19].

The two types of fault-clearing methodologies that are studied during the course of this dissertation are:

- Neutral tripping
- Single-phase tripping.

The objective of this dissertation is to conduct a comparative study between neutral tripping and single-phase tripping in medium voltage networks for the purpose of clearing transient faults.

1.3 Challenges to address

The challenges listed in this section form an integral part of the overall research methodology of this dissertation.

1.3.1 Protection philosophy

To integrate the neutral breaker scheme and the single-phase breaker scheme into the protection philosophy of an existing electrical network could prove to be challenging. A protection operating philosophy is developed for each scheme such that it does not negatively impact the overall functioning of the existing protection philosophy of equipment. The protection philosophies of the schemes are designed to limit the amount of arc energy and ionised air during fault conditions. The safety of humans, animals and equipment are important factors that are taken into consideration when designing and practically implementing the schemes.

1.3.2 Line model

The accuracy of the line model used in this dissertation is of utmost importance. The line model influences the magnitude of the secondary arc current, which exists as soon as the primary arc quenches. The secondary arc current can be defined as the current that continues to flow in the electrical arc after interrupting the primary fault current path. The secondary arc current is applicable to both the neutral breaker and single-phase breaker schemes. The secondary arc current is the sum of the electromagnetic (inductive) and electrostatic (capacitive) currents [20]. If the capacitive and inductive coupling between the faulty and healthy phases is strong enough the secondary arc current will sustain the electrical arc [21]. In order to quench an electrical arc successfully, the fault current needs to be lower than 35 A [5].

It is, therefore, imperative that accurate calculations be performed and verified with the help of line model simulations. The results of these calculations and simulations will provide the magnitude of the capacitive current, which could be expected during fault conditions. The overall effectiveness of the arc-quenching capabilities of both the neutral breaker and single-phase breaker schemes are dependent on the capacitive current.

1.3.3 Transformer model

The transformer model also influences the magnitude of the secondary arc current. As mentioned, the magnitude of the secondary arc current determines whether or not a fault will quench [5]. The accuracy of the transformer model is more applicable to the single-phase breaker scheme. The validation of the transformer model will be done by means of field tests that will be performed.

1.3.4 Integrated models

Both the verified line - and transformer models are combined to develop integrated models that simulate the response of an electrical network under fault conditions. It is vital that the integrated models yield valid results to ensure that no undesirable results occur during the implementation of the neutral breaker and single-phase breaker schemes on actual MV networks.

1.4 Methodology

The methodology of the dissertation is shown in Figure 1-6. The outline of the methodology was primarily guided by the challenges that need to be addressed.

Firstly, a detailed literature study was conducted in order to fully understand the principles of electrical arcs, electrical faults, power quality and the effects of capacitive coupling. After a better understanding of fault-clearing fundamentals had been obtained, a unique protection philosophy per fault-clearing scheme was developed.

Before work could commence on developing an integrated model for each of the two fault-clearing schemes, the parameters of the line and transformer models within ATPdraw needed to be verified and validated. The verification of the line model is done by means of calculations and is afterwards validated with field test measurements. The validation of the transformer model is also done by means of field test measurements.

Information gathered from the line and transformer models are then used to identify suitable trial sites where the single-phase breaker and neutral breaker schemes are implemented.

The verified and validated line - and transformer models are combined to develop integrated models for the neutral breaker and single-phase breaker schemes. The integrated models are used to simulate the operation and fault-quenching capabilities of the neutral breaker and single-phase breaker schemes.

After the successful simulation of both fault-clearing schemes, the schemes are practically implemented at the identified trail sites. The simulated results are then compared to actual measured results, which form part of the validating process with regards to the developed integrated models.

Lastly, a comparison is made between the neutral tripping and single-phase tripping fault-clearing philosophies.

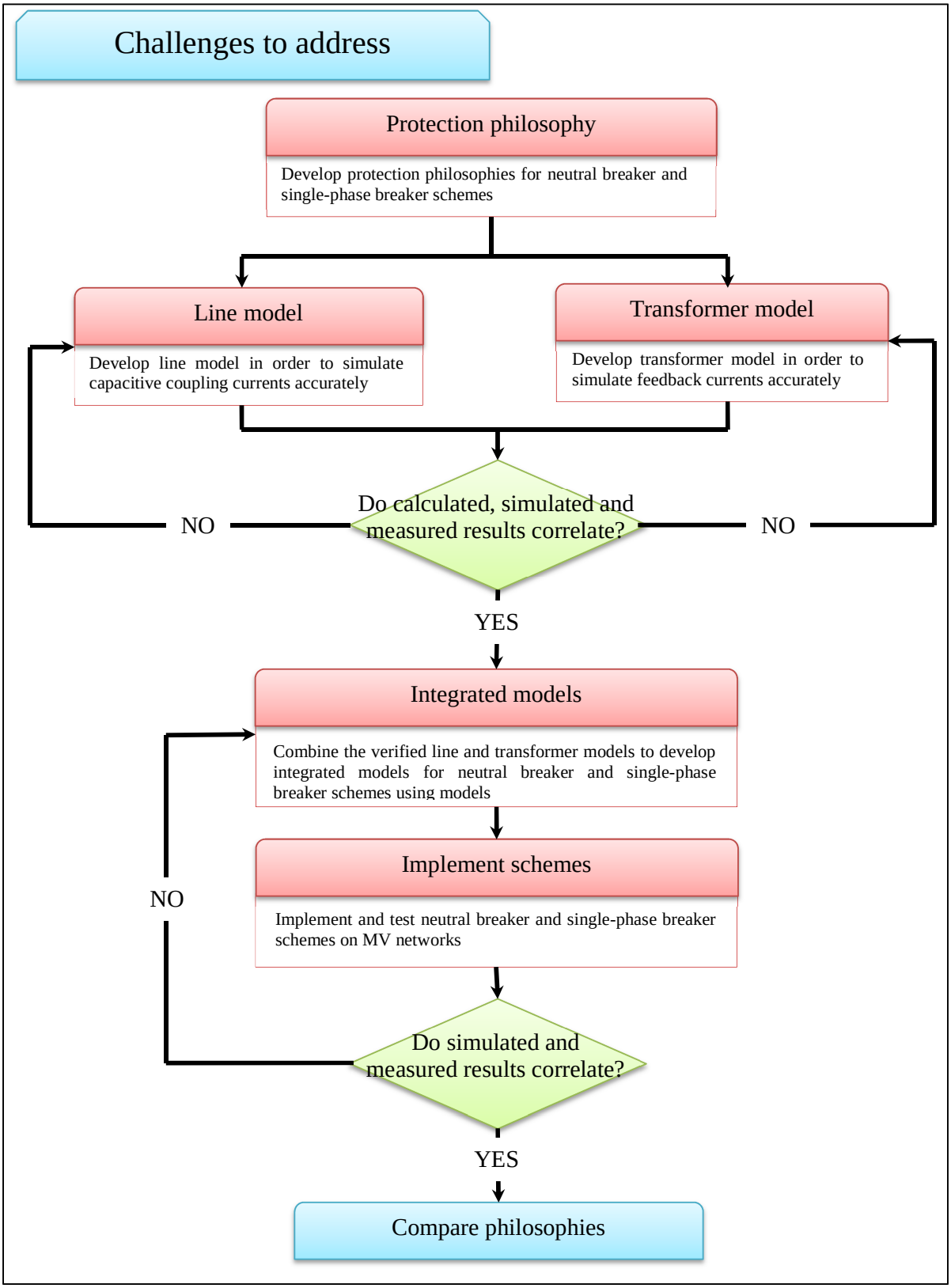

Figure 1-6 Dissertation methodology

1.5 Dissertation overview

Chapter 2 provides a brief overview of literature regarding electrical faults and ways of limiting and reducing electrical arc energy. Arc quenching methods are also discussed. The nature and importance of transient faults, and ways of mitigating such faults are reviewed. Furthermore, the effects which transient faults have on power quality in terms of voltage dips and supply interruptions are also discussed. Chapter 2 discloses the theory regarding capacitive coupling as this is one of the fundamental issues that influences the quenching of electrical arcs.

Chapter 3 gives an overview of the development of protection philosophies regarding the two proposed transient fault-clearing schemes. These two schemes being:

- Neutral breaker scheme on MV networks
- Single-phase breaker scheme on radial MV lines.

The proposed operating philosophies of both schemes are also established in Chapter 3.

Chapter 4 focusses on creating, verifying and validating a line model. The accuracy of the line model has a direct influence on the magnitude of the secondary arc current which could sustain an electrical arc. Therefore, a comparison is done between the calculation and simulation results in order to verify the accuracy of the line model used in the ATPDraw simulation package. The calculation and simulation results are validated with two sets of measured results. The results and validated line model is then further used in the integrated models, which is discussed in Chapter 6 of this dissertation.

Chapter 5 focusses on validating a transformer model. The accuracy of the transformer model has a direct influence on the magnitude of the secondary arc current that could sustain an electrical arc. Therefore, a comparison is done between two sets of simulation and measured results in order to verify the accuracy of the transformer model used in the ATPdraw simulation package. The validated transformer model, is then further used in the integrated models, which is discussed in Chapter 6 of this dissertation.

Chapter 6 focusses on selecting suitable locations where the neutral breaker and single-phase breaker schemes will be implemented. Simulations of both schemes are done and the results analysed in order to determine whether it is possible to implement both schemes. Based on the simulation results obtained, each scheme's advantages and limitations are also briefly discussed.

Chapter 7 contains measured results of both implemented schemes. The measured results are discussed and compared to the simulated results in order to validate the integrated models that were created in Chapter 6.

Chapter 8 aims to compare the neutral breaker and single-phase breaker philosophies with each other. The comparison includes the following:

- Transient earth fault-clearing capabilities
- Transient phase-to-phase fault-clearing capabilities
- Impact on power quality
- Advantages of each philosophy
- Limitations of each philosophy
- Proposed locations to implement each scheme.

Chapter 8 also includes relevant recommendations that are made with regards to improving the operation of both schemes and in view of future research.

--- Chapter 2 ---

Literature study

As basis to explore the problem statement described in Chapter 1, the theory around electrical arcs, electrical faults, single-phase tripping, power quality and the effects of capacitive coupling needs to be reviewed.

2.1 Electrical arcs

2.1.1 Background

An electric arc can be described as a rapid release of energy due to insulation breakdown. Insulation breakdown occurs between a live electrical conductor and earth, or between two live conductors at different potentials [6], [8]. The rapid release of arc energy can be in the form of [6]:

- Heat energy
- Light energy
- Mechanical energy - Shockwave
- Sound energy.

There are numerous factors that can result in an electrical arc forming within an electrical network. Some of the factors are [2], [6]:

- Insulation breakdown of equipment due to pollution, corrosion, condensation or mechanical failure
- Overvoltage conditions that exceed the basic insulation levels of equipment
- Foreign objects like animals and vegetation that create a fault path between two conductors or a conductor and earth.

2.1.2 Arc energy

The energy associated with an open air electrical arc places an enormous amount of electrical and mechanical stress on an overhead MV network. The heat generated by an electrical arc could range roughly anywhere from 7000 °C up to 18000 °C [6]. It is, therefore, imperative to limit the amount of energy generated during an electrical arc.

According to IEEE standard 1584 of 2002 [8] the available incident energy of an electrical arc, to which a person might be exposed, for a phase-to-phase system voltages up to 15 kV is calculated as

$$\mathrm{E} = \mathrm{C_f E_n}\left(\frac{\mathrm{t}}{0.2}\right)\left(\frac{610^{\mathrm{x}}}{\mathrm{D^x}}\right), \tag{1}$$

and the incident energy of an electrical arc, for phase-to-phase system voltages above 15 kV, is calculated as

$$\mathrm{E} = 5.12\mathrm{x}10^{5}\mathrm{VI_f}\left(\frac{\mathrm{t}}{\mathrm{D^2}}\right), \tag{2}$$

where E is the incident energy (cal/cm^2), t is the arcing time (s), x is the distance factor, C_f is the calculation factor, V is the system voltage (V), D is the distance from possible arc point to person (mm), E_n is the normalised incident energy (cal/cm^2), and I_f is the three-phase bolted fault current (A).

As can be seen in the two equations above, the incident energy is dependent on the system voltage, fault current and the amount of time the fault remains on the electrical network.

2.1.3 Limiting or reducing arc energy

Limiting arc energy under fault conditions can be done in a number of ways. The most practical ways are to reduce the fault current magnitude, or to reduce the amount of time the arc remains on the electrical network during fault conditions.

The earth fault current in a MV electrical network can be limited by installing a neutral earthing compensator with a neutral earthing resistor. Currently in Eskom, neutral earthing compensators and resistors are installed on the MV side of distribution transformers. The NECR limits the earth fault current to a maximum of approximately 360 A. The installation of a NECR allows for the detection of earth faults by creating an earth point in the delta configured MV network, as shown in Figure 2-1.

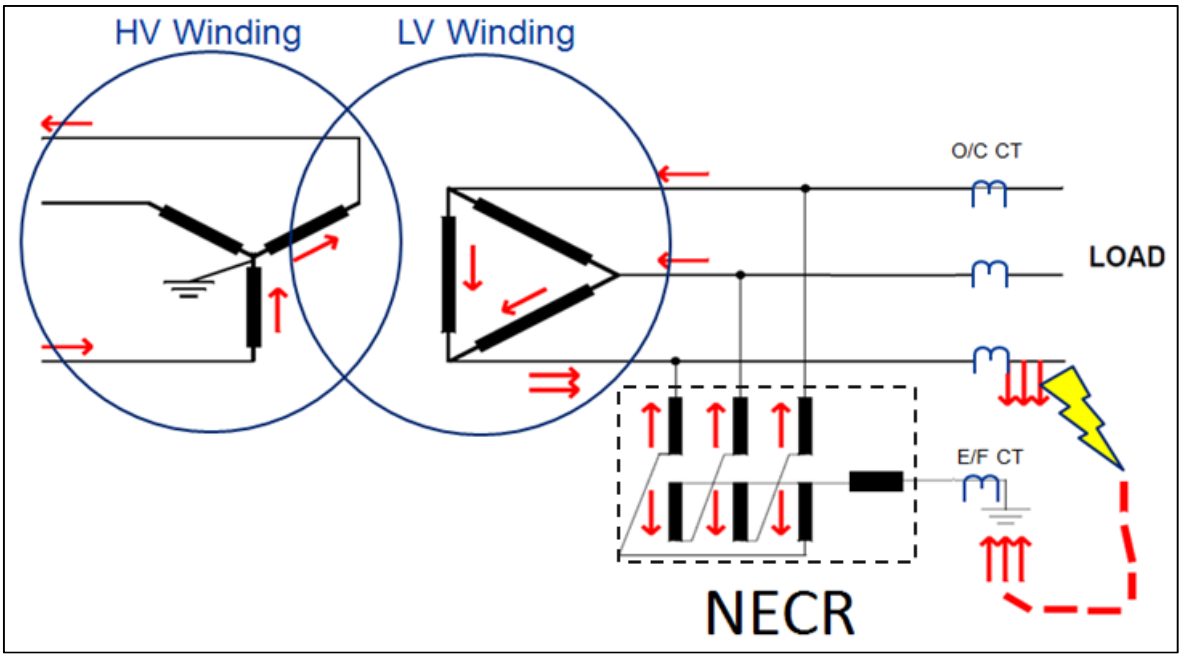

Figure 2-1 Earth fault current flow in a network grounded by means of a NECR [22]

Another way of limiting earth fault current is by installing Peterson coils. The tuning of such coils can prove to be challenging [5]. In some countries the magnitude of earth faults are limited by operating the overhead electrical network in an ungrounded configuration. The magnitude of earth fault currents is mostly dependent on the phase-to-earth capacitive coupling of the feeder as shown in Figure 2-2 [5].

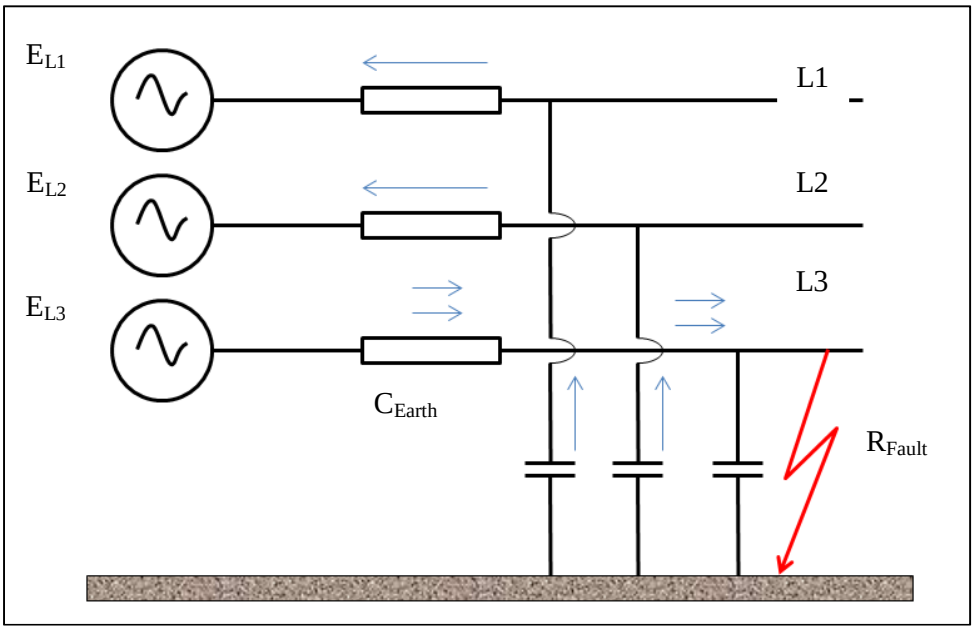

Figure 2-2 Capacitive currents flowing in an unearth network under fault conditions

The installation of NECRs and Peterson coils reduces the phase-to-earth fault levels in a network. The reduction of phase-to-phase fault levels can be accomplished by means of current limiting fuses or current limiting reactors [23], [24]. One disadvantage of a current limiting reactor is that it introduces additional impedance into the electrical network, which results in additional voltage drops. It can also introduce harmonics into the electrical network due to the additional inductance altering the parallel resonating point of the network, especially if there are shunt capacitors installed downstream on radial MV networks [25]. The reduction of the phase-to-phase fault level of a network negatively affects the network stability. Starting of large motors might cause voltage dips and have longer starting times.

With reference to equation (1) and (2) the electrical arc energy is directly proportional to the arcing time. The arcing time can be defined as the total amount of time it takes to clear a fault from the electrical network - which is usually achieved by the tripping of a circuit breaker. The total fault-clearing time is the summation of the protection relay operating time, which depends on the type of protection philosophy that is implemented, plus the breaker opening time. Typical breaker mechanism opening times can range from 30 ms to 80 ms with regards to MV breakers and cannot be influenced. The protection relay operating time can, however, be modified by changing the protection settings philosophy on the relay [26].

2.1.4 Arc quenching

Electrical arcs can be quenched in a number of different ways. The most common way of quenching an arc is to remove the source of current feeding into the fault by means of a breaker operation. The electrical arc is quenched inside the breaker poles by an insulation medium (oil, vacuum or SF_6) as the breaker contacts move apart from each other [27]. An arc on an overhead line can also self-extinguish due to the rising of the hot ionised air that increases the electrical arc resistance up to a point where the arc quenches, as illustrated in Figure 2-3.

Figure 2-3 Arc quenching due to heat rise [7]

The presence of strong winds can also increase the electrical arc resistance to a point where the arc quenches, as illustrated in Figure 2-4.

Figure 2-4 Arc quenching due to an increase in arc resistance [7]

Studies conducted in Finland regarding ungrounded 20 kV networks [5] have concluded that if the fault current in an overhead electrical network can be reduced to a point below 35 A, the electrical arc should quench. Other research has shown that an electrical arc cannot sustain itself if the AC voltage drops below 120 V [6].

In the case of an earth fault, limiting the fault current below 35 A is possible by temporarily unearthing the MV network. By unearthing the network, the return path of the fault current back to the substation is removed. The earth fault should quench, provided that the fault is of a temporary nature and capacitive coupling of the ungrounded MV network is less than 35 A [5].

In the case of a phase-to-phase fault, it is quite difficult to limit the high fault currents to a point below 35 A in order to ensure successful arc quenching. It has been recorded that a number of phase-to-phase faults, which were initiated by lightning, successfully quenched on their own without any breaker operation [28]. Figure 2-5 below shows an example of natural quenching without a breaker operation.

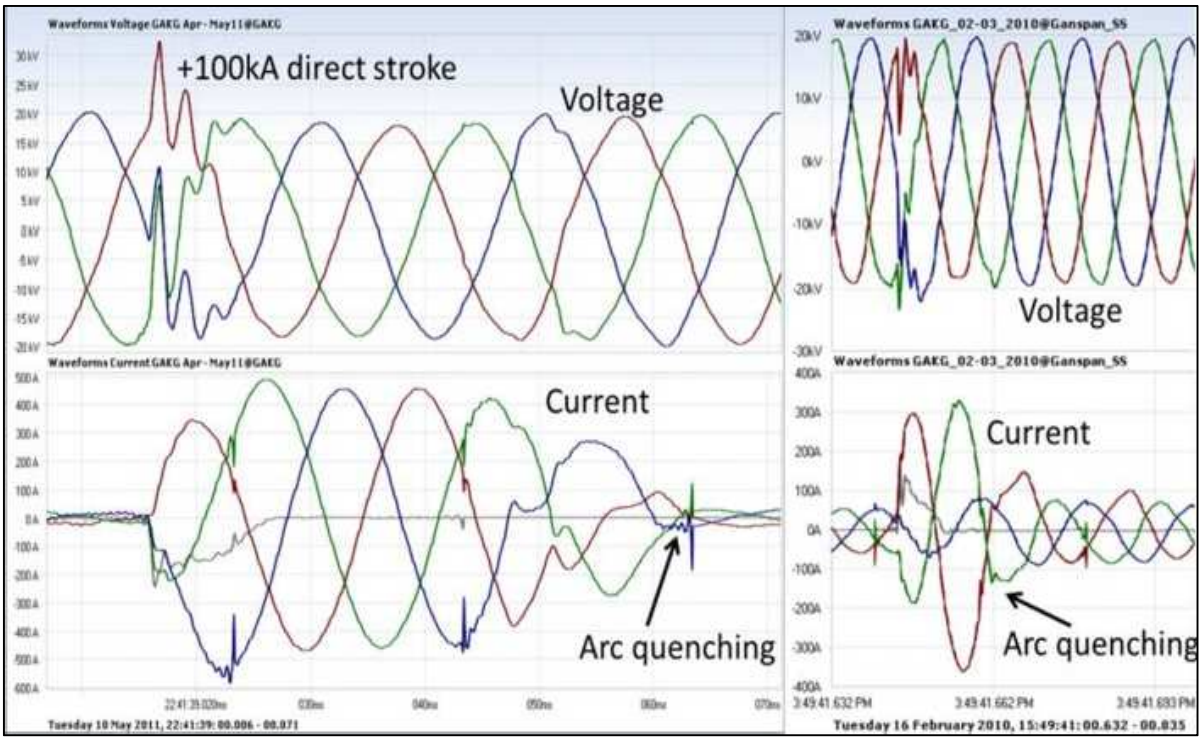

Figure 2-5 Example of arc quenching [28]

2.2 Electrical faults

An electrical fault is initiated by insulation breakdown between a live electrical conductor and earth, or between two live conductors with different potentials. Electrical faults within an electrical network can be permanent or temporary in nature. Permanent faults, also referred to as sustained faults, require the tripping of an upstream breaker in order to isolate the faulty section of the line. Temporary faults, which are also referred to as transient faults, also require the tripping of an upstream breaker in order to clear the fault from the network. Self-quenching of temporary faults has been recorded without the tripping of an upstream breaker [28].

2.2.1 Permanent faults

Sustained faults can be defined as faults that are of a permanent nature and result in circuit breakers running through their auto-reclose sequence until the breaker ultimately locks out in the open position. This requires that the fault be located and repaired before the electrical network can be successfully re-energised. The following faults are categorised as sustained faults:

- Failure of primary plant equipment
- Failure of structures
- Failure of conductors or cables
- Failure of line hardware.

Failure of line hardware includes equipment like insulators, transformers, isolators and fuses. If a fault remains across the sheds of an insulator for a prolonged period of time, it can lead to the failure of the insulator as shown in Figure 2-6.

Figure 2-6 Insulator failure on the FJM 22 kV line due to sustained fault across insulator sheds

Repeated flashovers across the sheds of an insulator will lead to the degrading of the insulator material over time. When an insulator is not properly designed, the electric field along the surface of the insulator can become too high. This results in the air along the surface of the insulator breaking down, causing partial discharges on the surface of the dielectric. Partial discharges damage the carbon bonds in some polymers, which causes carbon tracking to become visible on the surface of the insulator, as shown in Figure 2-7 [2]. Tracking will continue until a flashover occurs.

Figure 2-7 Tracking across sheds of insulator [2]

2.2.2 Transient faults

Transient faults can be defined as faults that remain on an electrical network and typically require a circuit breaker operation to quench. In most cases, as soon as the circuit breaker closes, the object responsible for causing the temporary fault would not be part of the electrical circuit anymore. During the fault condition, damage can be caused to insulators, conductors, line hardware and other electrical equipment due to the heat and mechanical energy associated with an electrical arc. Transient faults also negatively impact power quality in terms of voltage dips and momentary interruptions. Although air in a non-confined space is a self-restoring insulation medium, if the voltage across it exceeds 3kV/mm a flashover will occur and be sustained [2]. Scenarios that could cause transient faults where air is the main insulation medium are:

- Wind
- Lightning strokes
- Animals
- Vegetation.

Conductor clashing occurs when overhead conductors clash against each other and result in a phase-to-phase fault. This usually occurs during thunderstorms where strong gusts of wind are present. Conductor clashing occurs on MV lines due to the incorrect tensioning of overhead conductors and where conductor spans are too long. Incorrect tensioning causes excessive conductor sagging, especially where long span lengths are encountered [29].

Most lines in central South Africa are susceptible to lightning activity [30]. It has been reported that up to 78% of all MV equipment failures were caused by lightning [28]. Lightning can be defined as the phenomenon of a large electric discharge from a charged cloud, in the form of a spark or flash [31], [32].

HV lines are usually equipped with shielding wires and the tower footing resistances are relatively low - typically less than 20 Ω. MV lines, on the other hand, are generally unshielded and the footing resistance of these structures can be well in excess of 20 Ω. The basic insulation level of HV and EHV insulators are also a factor of three to six times higher than the 150 kV BIL of MV insulators. Therefore, MV lines are more prone to lightning flashovers and back flashovers, especially for high amplitude lightning strokes [33]. Although little can be done to prevent lightning from terminating on an MV overhead line, an attempt can be made to minimise the extent of the damage by clearing the fault as quickly as possible.

2.3 Single-phase tripping of circuit breakers

Any fault condition within an electrical network requires a breaker trip in order to clear the fault. The fault-clearing time influences the amount of energy which equipment on the network is subjected to under fault conditions. The time it takes for a breaker to trip will determine the amount of ionised air and plasma that is formed under a fault condition.

2.3.1 Single-phase tripping in HV and EHV networks

Single-phase tripping is utilised within HV and EHV networks where the majority of the faults are earth faults. Single-phase tripping refers to the tripping of only the faulty phase as compared to a full three-phase interruption. In order of frequency of occurrence, earth faults occurs the most, followed by phase-to-phase, phase-to-phase-to-earth and three-phase faults [18]. As was pointed out earlier, current literature suggests that the percentage of earth faults on HV and EHV networks account for approximately 70% and 90% of all faults respectively [19].

The single-phase auto reclosing philosophy on EHV lines is configured in such a way that only the single-phase breaker connected to the faulty phase trips. The tripped breaker remains in the open position for a short period of time to allow for the fault to quench whereafter the breaker recloses. If the fault has successfully quenched, the breaker will remain in the closed position. However, if the breaker recloses onto the fault, all three single-phase breakers will trip and remain in the open position.

Literature indicates the following advantages when single-phase auto-reclosing schemes are utilised in HV and EHV networks [20]:

- Improvement in system reliability and availability
- Improvement in the transient state stability of the electrical network
- Decrease in overvoltage's caused by switching.

One problem that is encountered in the single-phase auto-reclosing philosophy is the phenomenon of the secondary arc current. The secondary arc current can be defined as the current that continues to flow in the arc after the tripping of the single-phase breaker. The primary fault current (I_A) and secondary arc current (I_{sec}) for a single-phase to earth fault is graphically illustrated in Figure 2-8 [21].

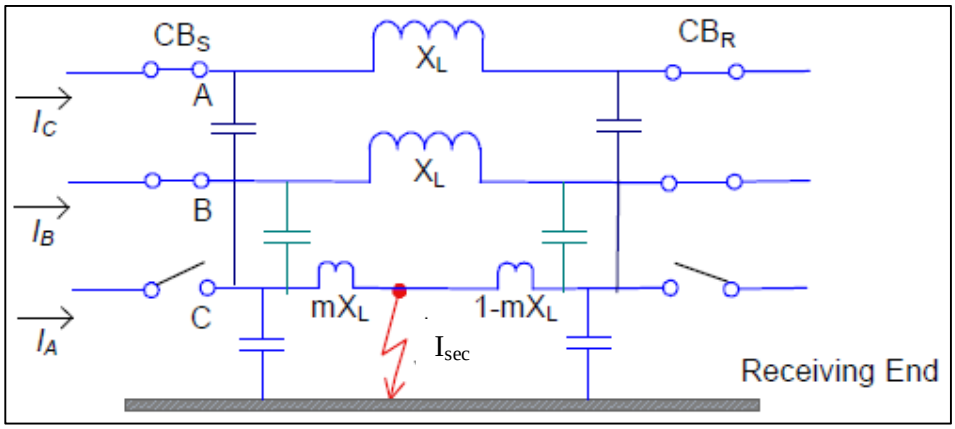

Figure 2-8 Single line diagram depicting phase-to-earth fault

The secondary arc current is the sum of the electromagnetic and electrostatic currents assuming a fully transposed, symmetrical transmission line and can be expressed as [20]:

$$I_{sec} = I_{sm} + I_{sc}, \tag{3}$$

where I_{sec} is the secondary arc current, I_{sm} is the electromagnetic coupling current, and I_{sc} is the electrostatic coupling current.

If the capacitive and inductive coupling between the two healthy phases and the faulty phase is strong enough, the arc will be sustained by the secondary arc current. When the arc does not successfully quench, a three-phase trip will be initiated once the single pole breaker recloses. [34]. It can also be noted that the inductive coupling contributes much less towards the secondary arc current compared to the capacitive coupling component [21].

Zevallos and Tavares [35] mention that in the case of a transmission line with a length of 100 km, the secondary arc current can be in the range of 10 A to 100 A, due to capacitive and inductive coupling.

Literature states that the initial arc (primary arc) proves to have a much greater deterministic behaviour than the secondary arc, when observed during field- and laboratory testing. The arcing channel of the secondary arc can be severely influenced by a number of external conditions, which include factors like wind and the surrounding ionised air [19]. Literature has shown that the secondary arc in air can be expressed by means of a differential equation with regards to the arc conductance, as [19], [36], [21]:

$$\frac{dg}{dt} = \frac{1}{\tau}(G - g), \tag{4}$$

where G is the stationary arc conductance, τ is the arc time constant, and g is the instantaneous arc conductance.

The stationary arc conductance (*G*) can be expressed as [19], [36], [21]:

$$G = \frac{|i_{arc}|}{u_{st}}, \tag{5}$$

where i_{arc} is the instantaneous arc current and u_{st} is the stationary arc voltage. The stationary arc voltage is given by [19], [36], [21]:

$$u_{st} = (u'_0 + r'_0|i_{arc}|) \times l_{arc}(t), \tag{6}$$

where u'_0 is the characteristic arc voltage per length, l_{arc} is the instantaneous arc length and r'_0 is the characteristic arc resistance per length.

The magnitude of the secondary arc current and recovery voltage, which are present across the secondary arc path, is essential as it will determine whether the arc extinguishes. The secondary arc directly influences the success rate with regards to the quenching of electrical faults [20].

2.3.2 Single-phase tripping in MV networks

A number of sources have indicated that the majority of faults within MV networks are single-phase faults [3], [4], [5], [37]. Furthermore, it has also been documented that a large percentage of these faults are transient in nature [14], [16].

The following negative effects can be associated with single-phase tripping [25], [38]:

- It can lead to ferroresonance in transformers
- Will create a single phasing condition for three-phase motors
- Fault may not clear due to the two healthy phases back-feeding into the faulty phase
- Possible mal-operation of earth relays in double circuit lines due to the flow of zero sequence currents.

Ferroresonance is a term that refers to the oscillating phenomenon that occurs between a capacitor and a non-linear inductor [39]. During ferroresonance conditions, high overvoltages and distorted overcurrent conditions may be encountered [40].

Figure 2-9 below shows an unbalanced three-phase electrical diagram where the phase-A of the supply voltage is opened, similar to a fuse failure condition or a single-phase breaker operation. One should note that the transformer primary winding is connected in delta configuration.

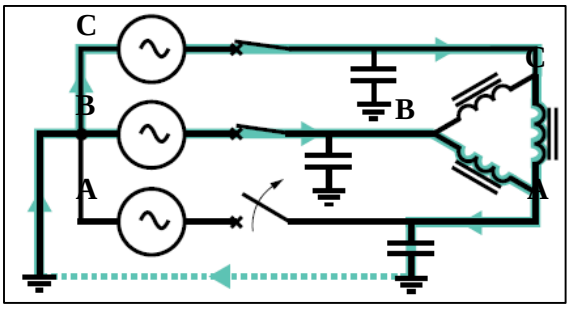

Figure 2-9 Loss-of-phase condition in an grounded electrical network [25]

During a loss-of-phase condition on a lightly loaded transformer with a delta or ungrounded wye primary winding configuration, ferroresonance can occur. The core of the transformer acts as the non-linear inductance. The capacitance consists of:

- Coupling between the different phases of the overhead line
- Coupling between phases and earth of the overhead line.

Symptoms of ferroresonance include [25], [40], [41]:

- Overvoltage and overcurrent
- Audible noise
- Insulation breakdown
- Sustained levels of distortion
- Overheating of equipment

Another challenge encountered with a single-phase tripping philosophy in MV networks is that heat is generated in three-phase motors during a voltage-unbalance event.

The main hurdle to overcome in order to implement single-phase tripping on MV lines successfully is the secondary arc phenomenon. Secondary arc currents are normally encountered in single-phase auto-reclosing schemes on HV and EHV lines. This is due to the capacitive and inductive coupling, which the two healthy phases have on the faulty phase - thereby inducing the flow of a secondary arc current. It is important that, when implementing single-phase auto-reclosing philosophy, that the faulty phase must be de-energised long enough for the secondary arc to quench.

The majority of MV lines within the Eskom network are supplied form a Ynd substation transformer with a Δ secondary winding configuration. The pole mounted transformers that supplies customers on radial MV lines have a Δ load side and a Y supply side configuration (Dyn). In the event of a phase-A to earth fault on the delta configured MV line, the phase-A breaker will trip. This is graphically illustrated in Figure 2-10:

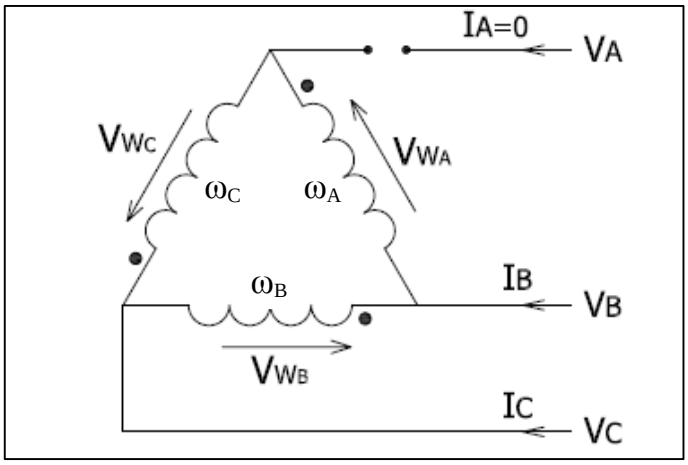

Figure 2-10 Transformer Δ primary winding with phase-A breaker open [42]

With the phase-A breaker open, the voltage across the ω_B transformer winding remains unchanged at nominal system voltage ($V_{B\text{-}C}$). Transformer windings ω_A and ω_C will both maintain only half of their original voltages as shown in Figure 2-10. The following equations are applicable according to Norouzi [42]:

$$V\omega_B = V_{B\text{-}C,} \tag{7}$$

$$V\omega_C = V\omega_A = -\frac{1}{2}V_{B\text{-}C}, \tag{8}$$

$$I_A = 0, \tag{9}$$

$$I_C = -I_{B.} \tag{10}$$

Sutherland performed similar tests by creating an open phase condition on a Δ/Y configured transformer. He observed the following voltages being present on the secondary side of the transformer [38]:

Table 2-1 Voltages present on secondary side of Δ/Y transformer under loss-of-phase condition (phase-A)

Transformer configuration	*Primary* side of transformer: phase-to-earth per unit voltages			*Secondary* side of transformer: phase-to-earth per unit voltages		
Δ / Y	$V_{A\text{-}E}$	$V_{B\text{-}E}$	$V_{C\text{-}E}$	$V_{a\text{-}e}$	$V_{b\text{-}e}$	$V_{c\text{-}e}$
	0	1	1	0.58	1	0.58

The single-phase tripping of breakers could yield the following advantages [38], [43]:

- Possibility of voltage dip ride through for plant equipment
- Reduces the impact of voltage dips that propagate onto adjacent MV lines if breakers are set to trip instantaneously for fault conditions
- Customers with single-phase loads, which are connected to the non-faulty phases will not experience a power interruption
- If there are only single-phase customers on the MV line, and provided that customers are equally split between phases, it will result in a significant decrease with regards to the average number of customers being interrupted during an earth fault.

2.4 Capacitive coupling

Capacitive coupling is caused by the induction of an alternating charge onto another electrical object, because of the presence of a voltage on an overhead power line. This is due to the distributed capacitance between the overhead line and the object, as well as the distributed capacitance between the object and ground [44]. For the most basic single-phase case, the capacitive coupling is illustrated in Figure 2-11.

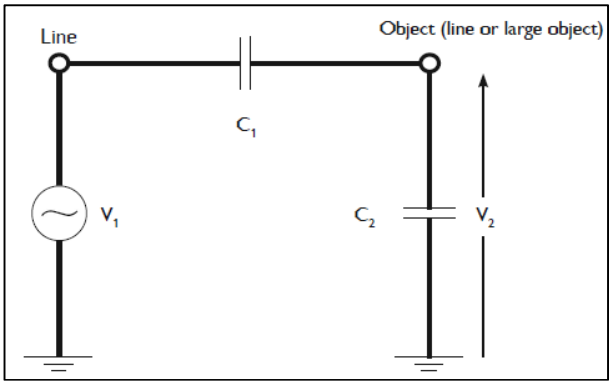

Figure 2-11 Capacitive coupling between overhead line and adjacent object [44]

The relationship between the induced voltage (V_2) and the system voltage of the overhead line to earth (V_1) is given by

$$V_2 = V_1 \frac{C_1}{C_1 + C_2}, \tag{11}$$

where C_1 is the distributed capacitance between the overhead line and the object, and C_2 is the distributed capacitance between the object and earth.

From the equation given above, it is evident that [44]:

- Theoretically, V_2 can be as high as V_1 if $C_1 = C_2$. This suggests that high voltages could be induced by means of capacitive coupling
- If V_2 is short circuited (earth fault condition), the resultant current flowing through C_1 is proportional to the length of the parallel exposure between the overhead line and object
- Magnitude of the capacitive coupling is dependent on the system voltage of the overhead line
- Magnitude of the capacitive coupling is independent of the system phase currents of the overhead line.

The total capacitive coupling of a MV overhead line under normal operating conditions is negligible due to the presence of all three phases, which cancel each other out [45]. However, during an earth fault condition in an ungrounded network, the picture changes quite drastically. This is especially true in the case of long rural lines which are supplied from the same substation. The majority of the capacitive coupling occurs between the two healthy phases and earth as well as the coupling between the healthy phases and the affected phase, as shown graphically in Figure 2-12.

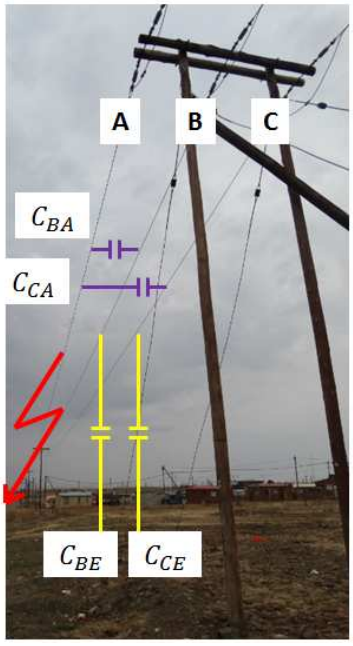

Figure 2-12 Capacitive coupling between phases and phase-to-earth in an ungrounded network

A single line diagram depicting only the phase-to-earth capacitive coupling during an earth fault is shown in Figure 2-13. One should note that $I_{B\text{-}E}$ and $I_{C\text{-}E}$ are the phase-to-earth capacitive currents, and I_{Cap} is the total phase-to-earth capacitive current.

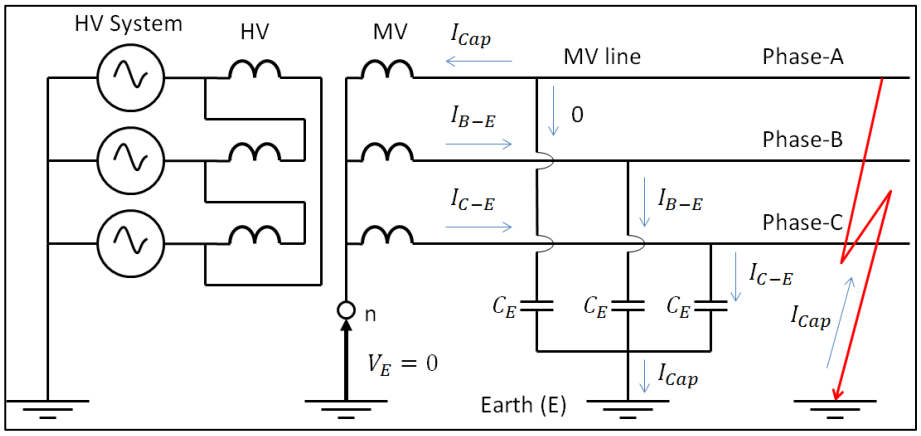

Figure 2-13 Flow of capacitive currents between phases and earth during an earth fault in an ungrounded network [4]

When an electrical network is ungrounded under fault conditions, the network voltage neutral reference point shifts from its normal fixed point to the affected phase - thereby resulting in full phase-to-phase system voltages being present across phase-to-earth terminals [4], [46], as is illustrated in Figure 2-14.

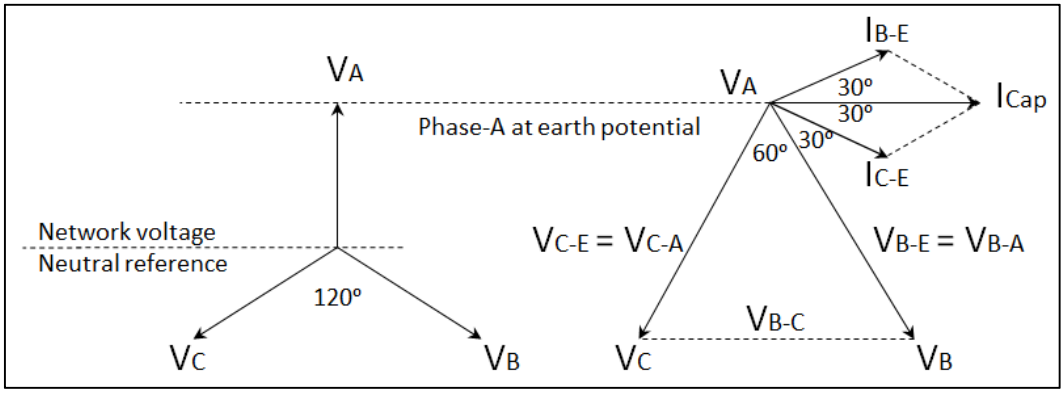

Figure 2-14 Three-phase phasor diagram before and after the unearthing of an electrical network under earth fault conditions [4]

The secondary voltages of a Δ/Y stepdown transformer will not change when the network is ungrounded because there is still nominal phase-to-phase voltages present across the transformer MV windings.

From Figure 2-13 and Figure 2-14, one can deduce that the total phase-to-earth capacitive current between the healthy phases and earth ($I_{Total\ phase-to-earth\ capacitive\ current}$), can be expressed as the sum of the current vectors:

$$I_{\text{Total phase-to-earth capacitive current}} = |\bar{I}_{B-E} + \bar{I}_{C-E}|, \quad (12)$$

or alternatively,

$$I_{\text{Total phase-to-earth capacitive current}} = I_{B-E}\cos(30^{o}) + I_{C-E}\cos(30^{\circ}), \quad (13)$$

where $I_{B\text{-}E}$ is the capacitive current flowing to earth from phase-B, and $I_{C\text{-}E}$ is the capacitive current flowing to earth from phase-C.

The capacitive current between the healthy phases and the faulty phase ($I_{Total\ phase-to-phase\ capacitive\ current}$), shown in Figure 2-12, can be expressed as the sum of the current vectors:

$$I_{\text{Total phase-to-phase capacitive current}} = |\bar{I}_{B-A} + \bar{I}_{C-A}|, \quad (14)$$

or alternatively,

$$I_{\text{Total phase-to-phase capacitive current}} = I_{B\text{-}A}\cos(30^{o)} + I_{C\text{-}A}\cos(30^{\circ}), \quad (15)$$

where $I_{B\text{-}A}$ is the capacitive current flowing from phase-B to phase-A, and $I_{C\text{-}A}$ is the capacitive current flowing from phase-C to phase-A.

Theoretically the total capacitive current can be written as (assuming delta overhead line configuration):

$$I_{\text{Capacitive total}} = I_{\text{Total phase-to-phase capacitive current}} + I_{\text{Total phase-to-earth capacitive current}},$$

which can also be expressed in terms of system voltages and capacitance as

$$I_{\text{Capacitive total}} = \frac{2\pi f C_{coupling} V_{pp}}{\sqrt{3}}, \quad (16)$$

where f is the power system frequency, V_{pp} is the system phase-to-phase voltage, and $C_{coupling}$ is the sum of the phase-to-phase and phase-to-earth capacitance.

Määttä [47] has indicated that overhead lines in a 20 kV system could have a capacitance of 6 nF/km per phase with an earth fault current of 0.067 A/km. This does correlate with other measurements that have been conducted where a capacitive current as high as 34 A was observed. The 34 A was measured under an earth fault condition in an ungrounded 22 kV system, which had a combined overhead line length of approximately 600 km [7].

Määttä [47] further indicated that cables could produce earth fault currents of up to 4 A/km, which is significantly higher as compared to overhead lines.

For a three-phase system, the capacitance per phase between the overhead conductor and earth can be expressed as [48]:

$$C_{\text{phase-to-earth}} = \frac{2\pi\varepsilon_0}{\operatorname{arcosh}\left(\frac{d}{r}\right)}, \tag{17}$$

$$= \frac{2\pi\varepsilon_0}{\ln\left(\frac{d}{r} + \sqrt{\frac{d^2}{r^2} - 1}\right)} \text{ F/m}, \tag{18}$$

where r is the radius of conductors (m), ε_0 is the permittivity constant which is 8.85×10^{-12}, and d is the distance between centre of the conductor and earth (m).

For a three-phase system, the capacitance between two conductors can be expressed as [48]:

$$C_{\text{phase-to-phase}} = \frac{\pi\varepsilon_0}{\operatorname{arcosh}\left(\frac{d}{2r}\right)}, \tag{19}$$

$$= \frac{\pi\varepsilon_0}{\ln\left(\frac{d}{2r} + \sqrt{\frac{d^2}{4r^2} - 1}\right)} \text{ F/m}, \tag{20}$$

where r is the radius of conductors (m), ε_0 is the permittivity constant which is 8.85×10^{-12}, and d is the distance between centres of both conductors (m).

From the equations above, it can be concluded that the magnitude of the capacitive current is dependent on the following factors:

- Length of the conductor
- Size of the conductor (thickness)
- Operating voltage of the electrical network
- Distance between the conductors.

Another factor that also influences the magnitude of the capacitive current, but to a lesser extent, is the distance between the conductors and earth [49].

2.5 Power quality

The National Energy Regulator of South Africa, in accordance with its directive on power quality, has developed a number of standards that assists with the managing of power quality by licensees in South Africa. One such standard is the NRS 048 standard [12], which focusses on the quality of supply.

Power quality, also known as voltage quality, covers quite a number of disturbances within an electrical network [50]. The power quality of an electrical network with regards to voltage can be grouped into three sections, namely voltage waveform quality, voltage disturbances and voltage continuity.

The main factors influencing the voltage waveform quality are:

- Voltage frequency
- Voltage harmonics
- Voltage magnitude
- Voltage flicker
- Voltage unbalance.

The main events, which cause voltage disturbances on electrical networks are:

- Impulses/spikes
- Dips
- Swells
- Transients.

The voltage continuity of an electrical network is influenced by the number of interruptions that occur. These interruptions can be divided into two categories, namely momentary and sustained interruptions.

When transient faults on MV networks are cleared without causing a power interruption to customers, it improves the power quality of that network with regards to voltage continuity (interruptions). By reducing the time that the fault remains on the network, one can improve the power quality of that network with regards to voltage disturbances (voltage dips).

2.5.1 Voltage dips

Voltage dips represent a very important aspect of power quality due to the severe effect it can have on plant operations [9]. Voltage dips can be defined as a reduction in system voltage for a period of less than three seconds. Voltage dips are usually caused by equipment failures, conductor clashing or lightning strokes within the electrical network. A voltage dip can also occur due to starting of large motors [13]. Voltage dips encountered due to electrical faults are more severe than voltage dips caused by the starting up of a motor [10].

Voltage dips are characterised by the dip depth, which is the difference between the actual voltage and declared system voltage, and the dip duration. Figure 2-15 shows a window of how voltage dips are currently classified in the NRS 048-2 standard with Z2 class dips being the most severe in terms of dip depth and dip duration.

<table>
<tr><th rowspan="2">Range of dip depth
ΔU
(expressed as a percentage of declared voltage U_d)</th><th rowspan="2">Range of residual voltage
U_r
(expressed as a percentage of declared voltage U_d)</th><th colspan="3">Duration
t</th></tr>
<tr><th>20 < t ≤ 150 ms</th><th>150 < t ≤ 600 ms</th><th>0,6 < t ≤ 3 s</th></tr>
<tr><td>10 < ΔU ≤ 15</td><td>90 > U_r ≥ 85</td><td rowspan="3"></td><td colspan="2" rowspan="2">Y</td></tr>
<tr><td>15 < ΔU ≤ 20</td><td>85 > U_r ≥ 80</td><td rowspan="2">Z1</td></tr>
<tr><td>20 < ΔU ≤ 30</td><td>80 > U_r ≥ 70</td><td rowspan="3">S</td></tr>
<tr><td>30 < ΔU ≤ 40</td><td>70 > U_r ≥ 60</td><td>X1[a]</td><td rowspan="3">Z2</td></tr>
<tr><td>40 < ΔU ≤ 60</td><td>60 > U_r ≥ 40</td><td>X2</td></tr>
<tr><td>60 < ΔU ≤ 100</td><td>40 > U_r ≥ 0</td><td colspan="2">T</td></tr>
</table>

Figure 2-15 Voltage dip window [12]

By adjusting the fault-clearing times of protection equipment within an MV network, it is possible to reduce the duration of voltage dips [10]. The dip depth is a function of the fault level of the electrical network and cannot be altered by adjusting the fault-clearing times of protection equipment and can be written as [26]:

$$V_{\text{dip expected}} = \frac{I_{\text{fault current}}}{I_{\text{fault level}}} \times 100\% \,, \tag{21}$$

where $V_{dip\ expected}$ is the voltage dip that can be expected at the source, $I_{fault\ current}$ is the current flowing under fault conditions, and $I_{fault\ level}$ is the maximum current that can flow under fault conditions at the source.

This formula can also be expressed in terms of network impedances. The voltage that can be expected at the point of common coupling during a three-phase fault is:

$$V_{res} = \frac{Z_f}{Z_s + Z_f}, \tag{22}$$

where Z_f is the impedance of the line, Z_s is the impedance of the source, and V_{res} is the voltage expected at the point of common coupling.

From the equations above, it is evident that a voltage dip is more severe if the fault is located closer to the source. The network impedance directly influences the depth of voltage dip that can be expected [13].

Voltage dips are not only confined to the line on which the fault occurs. Voltage dips can propagate to all lines that are connected to the same source. If the depth of a voltage dip is severe and remains on the network for a prolonged period of time, it causes sensitive plant equipment of customers to trip. This will have a negative financial impact on all customers who are supplied from the same source. Some plant equipment might be able to successfully ride through voltage dips that are short in duration and small in magnitude. Research done with regards to the dip ride through capabilities of programmable logic controllers shows that the odds of such a controller riding through a voltage dip reduces quite drastically as the dip duration increases [11].

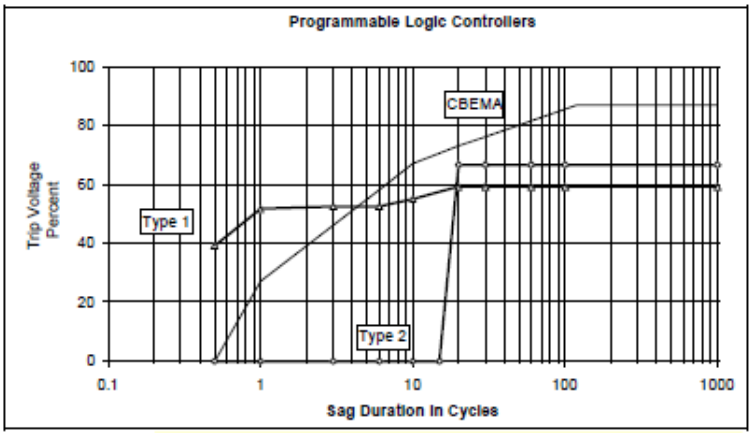

Figure 2-16 Dip ride through capabilities of two different programmable logic controllers [11]

The South African grid connection code for renewable power plants connected to the transmission system or the distribution system, gives guidelines for the expected dip ride through capabilities of a renewable power plant [51]. During the dip ride through process, the renewable power plant must not disconnect form the electrical network (area A and B) as shown in Figure 2-17.

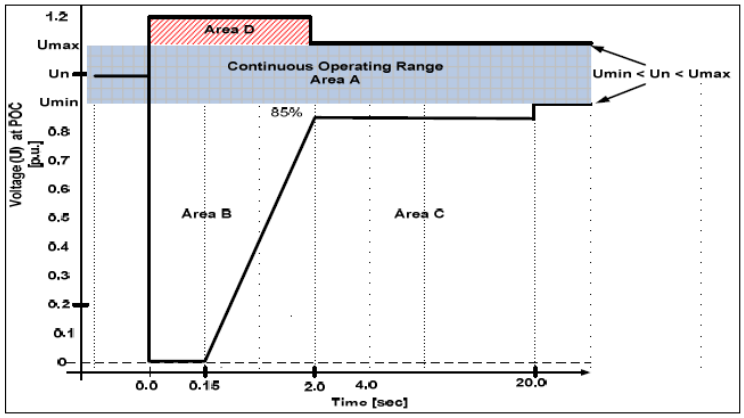

Figure 2-17 Voltage ride through capability for some categories of renewable power plants [51]

Voltage dips caused by faults on a HV network will propagate to the connected MV networks. Faults on a radial MV line might also propagate to parallel MV lines depending on the system fault levels and fault location. Research has indicated that sensitive production equipment of industries can operate incorrectly during voltage dip conditions [52]. Figure 2-18 shows a summary of fault types that caused the incorrect operation of sensitive production equipment.

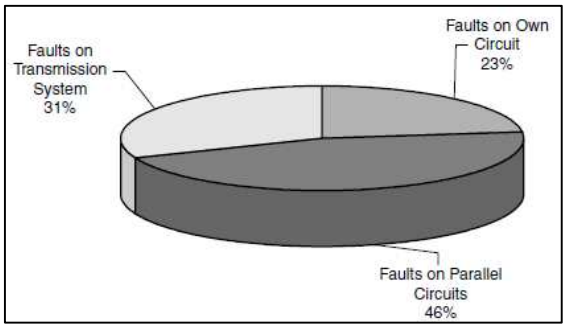

Figure 2-18 Distribution of fault types, which resulted in the incorrect operation of sensitive production equipment [52]

It is, therefore, important to clear any fault on an electrical network as fast as possible in order to reduce the duration of the voltage dip that can be propagated onto parallel lines.

2.5.2 Voltage continuity

The term voltage continuity refers to the ability of the power utility to provide an uninterrupted power to customers [12]. The term voltage interruption can be defined as an event where the supply voltage falls to zero for more than three-seconds [52]. A voltage interruption can be seen as a planned or unplanned event that results in the disconnection of one or more phases of the electrical network, which supplies a customer [12]. Voltage interruptions can be divided into two categories, namely:

- Momentary interruptions
- Sustained interruptions.

An interruption occurs when the only remaining circuit to a point of supply is disconnected due to:

- Permanent faults
- Transient faults
- Mal-operation of switchgear
- Emergency switching operations.

For an electrical fault within MV distribution networks, a breaker will open all three its poles, regardless of whether the fault is a multi-phase fault or earth fault. This causes motors to come to a stop as motor contactors will drop out as soon as there is a power interruption. This results in an interruption in plant production, even though the three-phase breaker may have successfully reclosed after the temporary fault is cleared from the network.

NERSA defines a momentary interruption within the NRS 048-2 standard as [12]:

- An unplanned or planned event
- Disconnection of one or more phases of the electrical network
- Event which is prevalent for a period of three-seconds to five minutes for MV and LV networks, whereafter full three-phase supply must be restored
- Event which is prevalent for a period of three-seconds to one minute for HV and EHV networks, whereafter full three-phase supply must be restored.

The NRS 048-2 standard specifies the allowable amount of sustained interruptions per year, as shown in Figure 2-19.

1	2	3
Network category	**Unplanned interruptions, number**	**Planned interruptions, number**
A	3 (6)	< 1 (3)
B	18 (75)	4 (11)

NOTE 1 The values for 50 % of customers reflect the number of events per annum that are generally not exceeded in the case of 50 % of customers in South Africa.

NOTE 2 The values for 95 % of customers reflect the number of events per annum that are generally not exceeded in the case of 95 % of customers in South Africa.

NOTE 3 Characteristic values for category C networks will generally be between those of category A and category B networks.

Figure 2-19 Allowable sustained interruptions per year stated within the NRS 048-2 standard [12]

2.6 Critical literature review

All types of electrical faults put strain on electrical equipment. In order to reduce the damage caused by electrical faults, it is important to reduce the arc energy of the fault. Methods of reducing the arc energy is to limit the fault current magnitudes by using current limiting reactors or Peterson coils [4], [5], [23], [24]. A more effective method to influence the arc energy is to reduce the time the fault remains on the electrical network. Practically, it is quite difficult to substantially reduce phase-to-phase fault currents in an MV network. Reducing the fault level of a network can limit the phase-to-phase fault currents; however, the starting of large motors might introduce voltage dips and have longer starting times. The fault-clearing times can easily be reduced by implementing an instantaneous tripping philosophy. It is therefore proposed to reduce the arc energy by means of the neutral breaker -and single-phase breaker schemes.

Research has indicated that most faults, which result in breaker operations within MV networks, are temporary in nature [14], [15]. These findings do seem to correlate with the number of transient faults that equated to approximately 61% on Eskom MV networks within the FSOU during 2014/2015 and 2015/2016 financial years. All transient faults have a negative impact on power quality with regards to voltage dips and voltage interruptions. When transient faults are not cleared fast enough, it causes damage to equipment, which may lead to a permanent fault occurring. Sources have also indicated that approximately 30% of permanent faults started as a transient fault [16].

Faults in MV networks are generally cleared by means of three-phase breaker trips, which result in a voltage interruption to customers. In EHV and HV networks, single-phase tripping is utilised. In order to reduce the number of earth faults encountered in MV networks, some countries operate parts of their networks in an ungrounded configuration. When the fault current is limited below 35 A in an ungrounded network or 60 A in a compensated network, faults should successfully self-extinguish [5], [4]. Other sources have indicated that phase-to-phase faults have self-extinguished even though the fault current magnitude was much higher than 60 A in a compensated network [28], [53]. Although it has been recorded that faults could self-extinguish at high fault currents, a more conservative secondary arc current limit of 20 A is recommended. This is to ensure that the fault-clearing conditions are optimal for any transient fault event.

Capacitive current forms an important component of the secondary arc current. Some of the literature that was reviewed varied with regards to how much capacitive current could be expected in ungrounded systems. In one case, an average capacitive current of 0.35 A/km is

calculated in an ungrounded 11 kV system [4]. This equates to 0.7 A/km for an ungrounded 22 kV system, which is relatively high. Another source indicates that the capacitive current in an ungrounded 20 kV system is in the range of 0.067 A/km [47]. Other work performed indicates that an average of 0.06 A/km was measured on an ungrounded 22 kV system [7]. When comparing these findings, two of the results correlate well with each other and will be used as a guideline [7], [47]. Capacitive current is dependent on a number of variables, which include the system voltage, conductor type and structure dimensions [49]. Therefore, the capacitive current needs to be calculated from first principles for each unique scenario in order to obtain accurate results.

It is well known that if an induction motor operates in a voltage unbalance condition, it results in the derating of the motor [54], [55], [56]. This is due to the additional heat that is generated within the windings of the motor during a voltage unbalance condition. This again is due to the heat build-up being influenced by the stator and rotor resistance [55]. It does seem that the derating of the motors in literature is only applicable to motors that operate in a voltage unbalance scenario for an extended period of time. Mention is made that a 10 $^{\circ}$C increase in winding temperature will half the life expectancy of a three-phase induction motor [56]. No mention is made as to what the effects are with regards to life expectancy of motors when a voltage unbalance scenario is encountered for only a few seconds. According to the author of this dissertation, if a voltage unbalance scenario was to be encountered for a few seconds, it is not likely that a 10 $^{\circ}$C increase in motor winding temperature will occur.

2.7 Summary

In order to clear a transient earth fault, the return path of the current needs to be removed. This can be done by installing a breaker between the NECR and earth, which will trip instantaneously for an earth fault condition. Instantaneous tripping reduces the arc energy of an earth fault quite substantially when compared to the IDMT E/F protection philosophy of a normal MV feeder breaker. There will be no supply interruption to customers when the delta configured MV network is ungrounded temporarily.

In order to clear transient phase-to-phase faults on MV networks, it is proposed to only trip one of the two affected phases instantaneously. Instantaneous tripping reduces the arc energy of the phase-to-phase fault quite substantially when compared to the IDMT O/C protection philosophy of a normal MV feeder breaker. Although the customer will experience a reduction in voltage in some phases, it will not result in a three-second supply interruption. Implementing single-phase tripping on a MV feeder creates the possibility of voltage dip ride through for plant equipment.

--- Chapter 3 ---

Protection philosophies

In order to support the exploration of the issues described in Chapter one, this chapter elaborates more on the functioning of the neutral breaker and single-phase breaker schemes. In this chapter, a unique protection philosophy is developed for the neutral breaker and single-phase breaker schemes. The protection philosophies must be developed such that they will integrate with existing protection philosophies currently implemented in distribution networks.

3.1 Clearing of transient faults

In order to attempt to clear any electrical fault, the secondary arc current, which is the sum total of the electrostatic and electromagnetic coupling current, must be limited to a value below 35 A [5], [20]. The clearing of transient phase-to-earth faults can be achieved by temporarily unearthing the network for a certain time period.

For phase-to-phase faults in MV networks, the clearing of transient faults is achieved by issuing a three-phase trip, which results in a supply interruption to customers. However, if the fault path of the two affected phases could be interrupted by the operation of only one single-phase breaker, the fault should quench - provided that it is temporary in nature. This will not result in a full three-phase supply interruption to customers.

3.2 Neutral tripping protection philosophy

3.2.1 Proposed neutral breaker scheme philosophy

In order to temporarily unearth the MV electrical network, it is proposed that a circuit breaker be installed between the NECR neutral and the substation earth mat. Upon detecting any earth fault condition, the proposed neutral breaker trips instantaneously in order to temporarily unearth the network, as shown in Figure 3-1. This operation reduces the earth fault current to only the capacitive current component - thereby allowing the arc to quench as illustrated in Figure 3-2. The capacitive current path is depicted by the dotted line in Figure 3-1 and Figure 3-2. One should note that as soon as the MV network is ungrounded, the capacitive current increases substantially due to the voltage rise on the healthy phases.

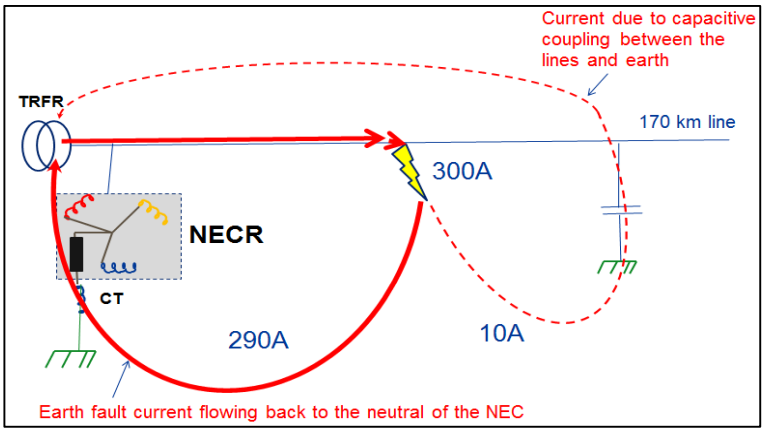

Figure 3-1 A simple illustration that shows the current paths for a 300 A transient earth fault condition with neutral breaker in closed position (grounded MV network)

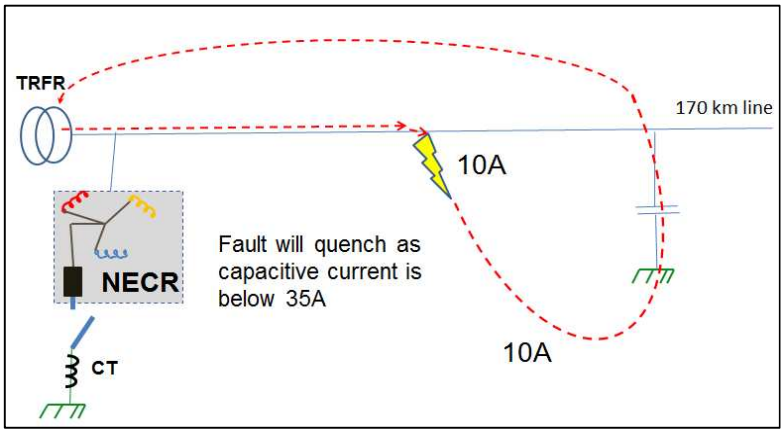

Figure 3-2 A simple illustration neutral breaker in the open position (ungrounded MV network)

Where only one NECR is present at a substation as shown in Figure 3-3, one pole of the three-phase circuit breaker is used to connect the NECR neutral with the substation earth mat. For safety purposes, it is recommended that the other two breaker poles are connected to earth.

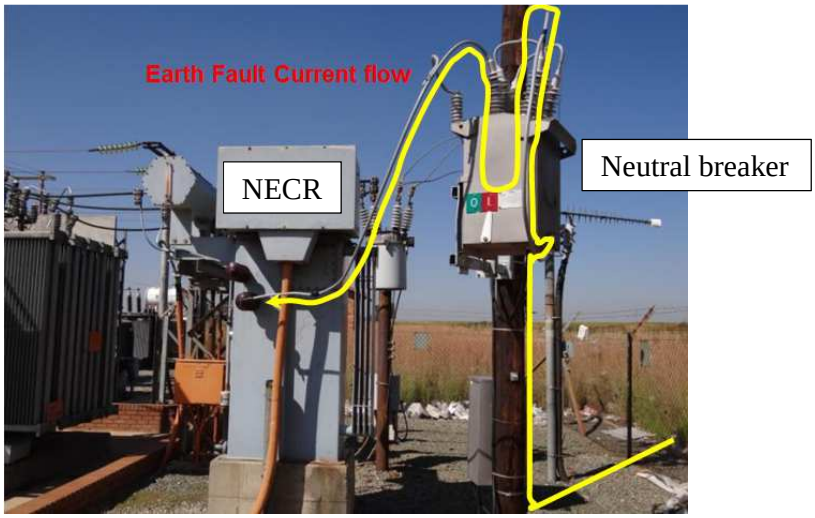

Figure 3-3 Physical installation of the neutral breaker scheme

The neutral breaker remains in the closed position until a fault current starts passing through the NECR. The overcurrent protection functionality of the neutral breaker is used to issue a trip signal to the breaker under fault conditions. The overcurrent pickup setting will be set to 10 A, which is higher than the maximum pickup recommended for sensitive earth fault protection in MV networks, in order to avoid any nuisance tripping [26]. The 10 A setting ensures that the neutral breaker will not trip for any earth leakage currents that could be generated by insulators and surge arrestors. In the event where the neutral breaker trips for a fault condition, it remains in the open position for a few seconds to allow for the successful quenching of the arc before it automatically closes.

During the period where the MV network is temporarily ungrounded, the primary arc bypasses the capacitive coupling of the faulty phase-to-earth until the arc is quenched [47], [57]. This is illustrated in Figure 3-4 with the equivalent sequence diagram shown in Figure 3-5, where C_E is the total phase-to-earth capacitance of the network.

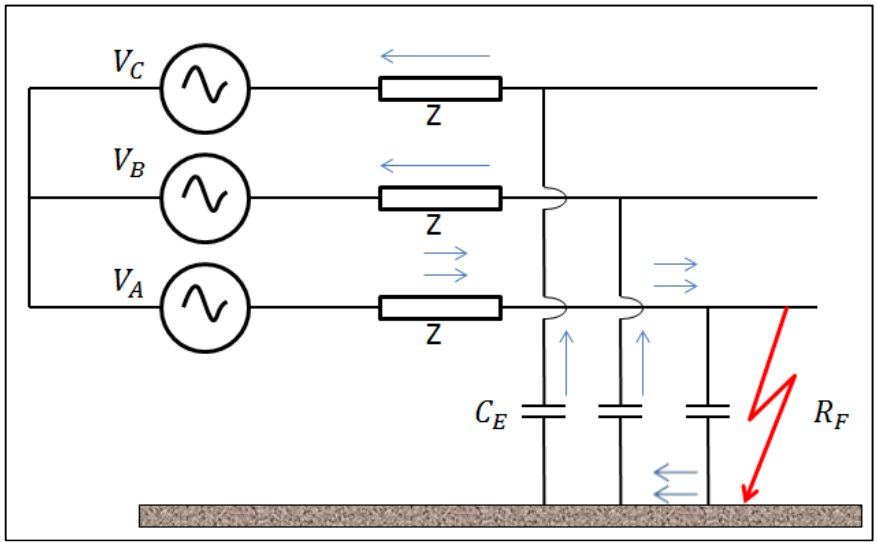

Figure 3-4 Earth fault in an ungrounded electrical network [47]

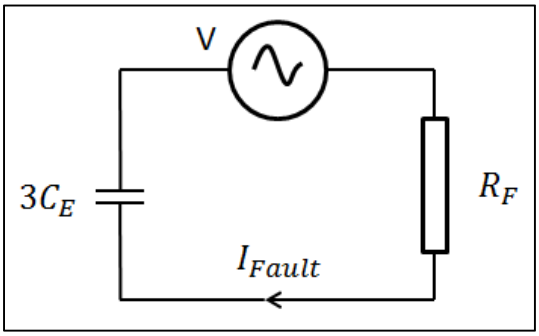

Figure 3-5 Equivalent circuit for an earth fault in an ungrounded electrical network [5], [47], [57]

In the case where the fault resistance is zero (R_F = 0), the fault current (I_{Fault}) can be expressed as [5], [57]:

$$\mathrm{I_{Fault}} = 3\mathrm{C_e}\omega\mathrm{V}, \tag{23}$$

where the angular frequency of the electrical network is

$$\omega = 2\pi f. \tag{24}$$

The fault current is dependent on the operating voltage of the network and the length of the overhead line which influences the coupling capacitance [49]. For a fault resistance greater than zero, the fault current ($I_{E/F}$) can be expressed as [5], [57]:

$$\mathrm{I_{E/F}} = \frac{\mathrm{I_F}}{\sqrt{1+\left(\frac{\mathrm{I_F}}{\mathrm{V}}\mathrm{R_F}\right)^2}}. \tag{25}$$

The zero sequence current present at the substation consists of the capacitive currents of the healthy parallel lines, which are connected to the same NECR [5]. The zero sequence voltage (V_0), also termed the neutral point displacement voltage, is dependent on the fault current that flows due to capacitive coupling and is shown in equation (26):

$$\mathrm{V_0} = \frac{1}{3\omega\mathrm{C_E}}\mathrm{I_{E/F}}. \tag{26}$$

In the case of a solidly grounded network, the zero sequence voltage is equal to the pre-fault phase-to-earth voltage of the faulty phase. The phase-to-earth voltages of the healthy phases under fault conditions (V_A = 0) will not drastically increase due to the network voltage neutral reference point remaining at ground potential. However, as soon as the system is ungrounded under fault conditions, the network voltage neutral reference point shifts. This results in full phase-to-phase system voltages, being present across the Δ-configured MV overhead line phase-to-earth terminals as shown in Figure 3-6 [4], [46], [58].

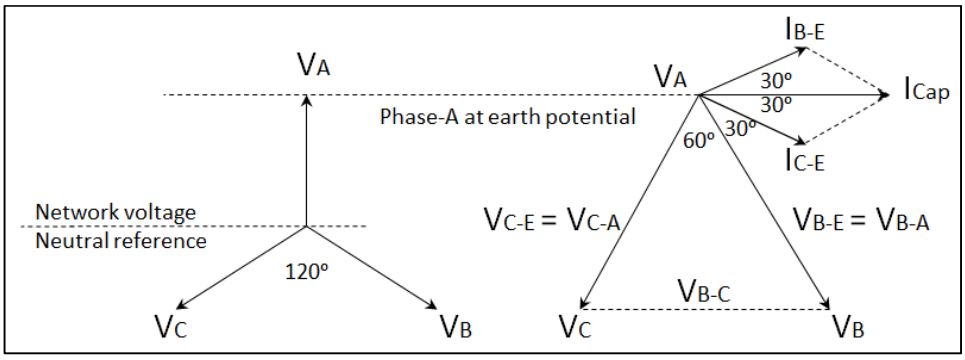

Figure 3-6 Capacitive current and system voltage vectors of an ungrounded MV network during an earth fault condition [4]

Due to the increase in phase-to-earth voltages on the two healthy phases, the MV neutral bushings of all substation transformers are required to be fully insulated [59]. It is also important to ensure that the rest of the electrical network is insulated for full phase-to-phase voltages across phase and earth terminals. In the case of Eskom MV networks, all equipment is rated to withstand phase-to-phase voltages across phase-to-earth terminals.

When the neutral breaker has closed, irrespective of whether the fault has cleared or is still prevalent on the network, the breaker remains in the closed position for a set time. This setting allows the relevant network breaker the opportunity to isolate the permanent fault from the MV network.

3.2.2 Operating philosophy of neutral breaker

In order to decide on how long the electrical network needs to be ungrounded, the following factors need to be taken into account:

- Sensitive earth fault protection philosophy
- Earth fault protection philosophy
- Time it takes for the secondary arc to quench.

Public fatalities and injuries are some of the biggest risks that power utilities face. Contact incidents might occur due to energised power lines laying on the ground. A contact incident may also occur in the case of low-hanging conductors that are within arm's reach, especially if such a low-hanging conductor is in the vicinity of a human settlement. The main challenge encountered with a contact incident is that the fault current could be lower than the pickup current setting of normal earth fault protection schemes [60]. The low fault current experienced during a contact incident could be due to a combination of:

- Network impedance
- High soil resistivity that results in a high earthing resistance
- Fault impedance.

Although the fault current that passes through a person might be relatively low due to high fault impedance, ventricular contraction of the heart is possible. If sustained, ventricular contraction could lead to death [49]. Therefore, sensitive earth fault protection is vital for any power utility as it could be the only protection that might pick up a high impedance fault condition. It is recommended that the pickup current setting of sensitive earth fault protection must not be set lower than 3 A to avoid nuisance tripping of a breaker due to leakage currents in an electrical network. It is also recommended that the pickup current setting of sensitive earth fault protection

must not be set higher than 9 A due to E/F protection settings on a substation NECR being set at 10 A. For an 11 kV overhead line with a current pickup setting of 6 A the maximum loop impedance coverage (sum of the zero, positive and negative sequence impedances) equates to approximately 3000 Ω at 11 kV and 6000 Ω at 22 kV for overhead lines [26].

For an earth fault or sensitive earth fault scenario within the Free State operating unit, the relevant MV breaker trips and remains open for three-seconds before reclosing. During the three-seconds in which the breaker is in the open position, the arc would have had ample time to quench. If the arc has not quenched within the three-second period, it can be due to the fault being permanent in nature.

3.2.3 Factors influencing the success rate of the neutral breaker scheme

An important factor which influences the success rate of the neutral breaker scheme is the quenching of the secondary arc. The secondary arc current is primarily dependent on the capacitive coupling between:

- Remaining healthy two phases and earth
- Remaining healthy phases and the affected phase.

The magnitude of the capacitive current can be expressed in terms of system voltages and capacitance as [4]:

$$I_{\text{capacitive total}} = \frac{2\pi f C_{\text{coupling}} V_{\text{pp}}}{\sqrt{3}}, \qquad (27)$$

where f is the power system frequency, V_{pp} is the system phase-to-phase voltage, and $C_{coupling}$ is the sum between the phase-to-phase and phase-to-earth capacitance.

The magnitude of the capacitive current is dependent on the operating voltage of the electrical network and the combined length of all the lines (A, B, C and D) connected to the same NECR. This is shown graphically in Figure 3-7.

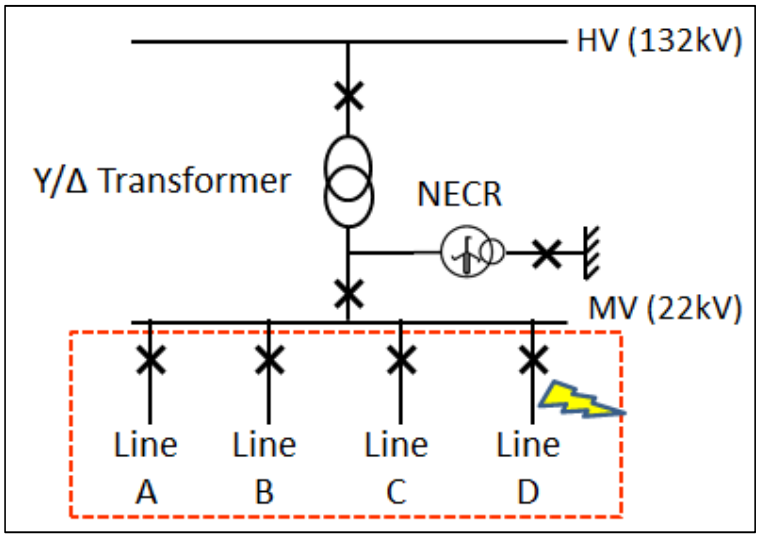

Figure 3-7 Single line diagram of substation

Ferroresonance should not be a factor when ungrounding the network, since there is no single phasing event present on the primary or secondary side of the transformer.

3.3 Single-phase tripping protection philosophy

3.3.1 Proposed single-phase breaker scheme philosophy

This dissertation aims to implement single-phase tripping on radial MV overhead lines. The network diagram in Figure 3-8 illustrates that three single-phase breakers are installed after the substation line breaker, one per phase. The aim is that for a phase-to-phase fault occurring on the network, only one of the two affected single-phase breakers trips instantaneously and stays open for a set time before it automatically recloses.

Referring to Figure 3-8 below as an example, if there is a phase-A to phase-B fault between Breaker 2 and Breaker 3, only the phase-A single-phase breaker trips whilst the other two single-phase breakers remain in the closed position. The phase-A single-phase breaker remains in the open position for one-second, to allow the secondary arc to quench, and then recloses. In the event of a transient phase-A to phase-B fault, no other breaker on the line trips after the phase-A single-phase breaker quenches the arc successfully. In the event of a permanent phase-A to phase-B fault, the normal system protection isolates the fault after the phase-A single-phase breaker recloses.

The implementation of this philosophy enables the quenching of transient phase-to-phase faults without causing a three-phase supply interruption to any of the customers on the line. The arc energy is also limited, which reduces the damage caused by the electrical arc.

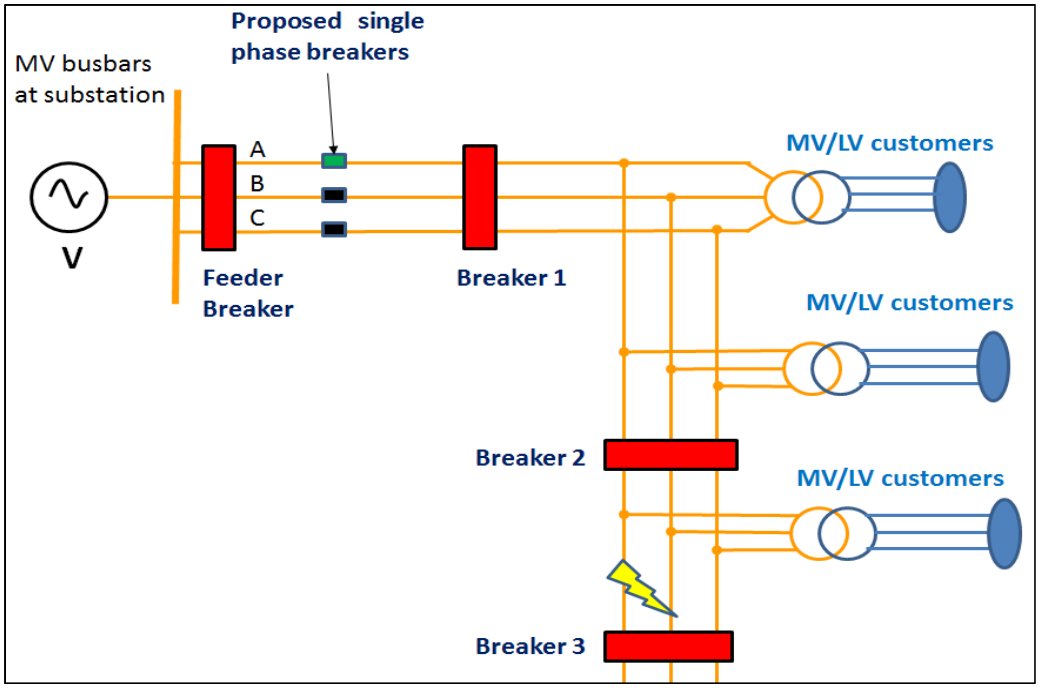

Figure 3-8 Illustration of a MV line with a phase-to-phase fault

The auto-reclose time of the single-phase breakers is set to one-second because it:

- Ensures that there is sufficient time for transient faults to quench
- Limits the length of the single-phase momentary interruption to which customers are subjected
- Limits the extent of voltage dip propagation on neighbouring lines.

When the single pole breaker recloses after a fault-clearing attempt, it remains in the closed position for one minute to allow normal system protection to operate in the event of a permanent fault.

In order to avoid nuisance tripping of downstream breakers during the operation of the single-phase breaker scheme, the loss-of-phase protection on all the breakers must be set to operate only after ten-seconds.

During the period in which one of the single-phase breakers are in the open position, the sequence diagram in Figure 3-9 is applicable [61].

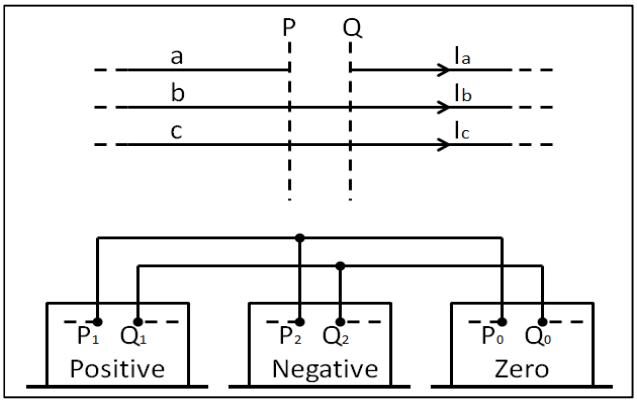

Figure 3-9 Sequence diagram for a single-phase open circuit condition – reproduced from [61]

It can be seen from Figure 3-9 that the following equations hold,

$$(V_A)_{PQ} \neq 0, \tag{28}$$

$$(V_B)_{PQ} = (V_C)_{PQ} = 0, \tag{29}$$

$$I_A = 0, \tag{30}$$

$$I_B = I_C \neq 0. \tag{31}$$

Keeping in mind that $I_A = 0$, the phase sequence components of the current can be expressed as [61]:

$$I_1 = \frac{1}{3}(aI_b + a^2I_c), \quad (32)$$

$$I_2 = \frac{1}{3}(a^2I_b + aI_c), \quad (33)$$

$$I_0 = \frac{1}{3}(I_b + I_c). \quad (34)$$

The advantage of implementing instantaneous tripping, in the range of 30 ms, is that the incident arc energy will be limited quite significantly. The available incident energy of an electrical arc can be expressed as [8]:

$$E = 5.12x10^5 VI_f\left(\frac{t}{D^2}\right), \quad (35)$$

where E is the incident energy (cal/cm^2), t is the arcing time (s), V is the system phase-to-phase voltage (V), D is the distance from possible arc point to person (mm), and I_f is the three-phase bolted fault current (A).

As can be seen in equation (35), the amount of arc energy is dependent on the system voltage, fault current and the amount of time the fault remains on the electrical network. By implementing the single-phase breaker scheme, the faults on the line can be cleared up to 40 times faster, from a worst case trip time of 1.2 s to 30 ms.

3.3.2 Operating philosophy of single-phase breaker

The main concerns with regards to single-phase tripping are the secondary arc current and the risks which are associated with single phasing conditions and ferroresonance [38].

The secondary arc current is the sum of the capacitive coupling- and inductive coupling current. The capacitive current of the single-phase breaker scheme is much less when compared to the proposed neutral breaker scheme. Reason being, for a phase-to-phase fault condition the capacitive coupling between the phases and earth is negligible [49]. The conductor length influencing the capacitive coupling is limited to the length of the affected line only, and not all the lines connected to the substation NECR, as is the case with the neutral breaker scheme.

During a prolonged single phasing condition, the windings of a three-phase motor will heat up, especially if the motor is operating under heavy loading conditions [38]. However, little heat is generated within the windings of motors under a single phasing condition if the event is only prevalent for a second. During the one-second period, the electrical arc would have had enough

time to quench. This is due to the instantaneous single-phase breaker trip time of 30 ms, which reduces the amount of ionised air forming during a fault condition.

During lightning storms, MV fuses of transformers are prone to failure if they are not protected by a parallel path surge arrestor [28], [62], [63]. If a fuse failure occurs on a three-phase transformer, the customer usually has to report it to the contact call centre of the power utility. After the reporting of the single-phase event, it could take up to a few hours to restore three-phase supply to a customer, due to various reasons. According to literature, a prolonged single phasing condition on a lightly loaded transformer could cause damage to the insulation of the transformer due to ferroresonance. This leads to an overvoltage and overcurrent scenario [25], [40], [41]. However, most of the time after an operator has replaced a failed fuse, the three-phase Δ/Y transformer is returned back into service without any problems.

This does pose the question: How much detrimental damage will occur within the one-second during which a transformer might be subjected to a ferroresonance state? A reasonable deduction can therefore be made that if most transformers are able to withstand an extended time in a single phasing condition, and still be operational, the chances are high that when a transformer is subjected to the same conditions, for only one-second, it will not cause the unit to fail.

Lastly, the single pole breakers are configured to trip on O/C protection with a definite trip time. Therefore, the O/C pickup setting is set higher than the maximum load current of the line and lower than the maximum continuous current rating of the breaker (100 A). A pickup of 80 A will ensure that the breaker is still able to detect an E/F close to the end of the MV line. The phase-B breaker, which is normally the centre phase of an overhead MV line, is set to trip instantaneously for a fault current above 80 A. The outer phase-A and phase-C single-phase breakers have a slight delay of 100 ms before tripping. This is to ensure that only one of the single-phase breakers trip for a phase-to-phase fault. The single pole breaker scheme is not able to detect an earth fault or with a magnitude lower than the current pickup setting of 80 A.

3.3.3 Factors influencing the success rate of the single-phase tripping scheme

An important factor, which influences the success rate of the scheme, is the magnitude of the secondary arc current. The magnitude is dependent on the capacitive coupling of the electrical network and the inductive coupling due to the possible back feeding through Δ/Y transformers. If the sum of both these currents can be limited to a value below 35 A, it will greatly assist with the effectiveness of the proposed scheme [5]. The capacitive coupling component can be influenced by implementing this scheme on lines which operate at a lower voltage or have a shorter line length [44], [49].

The time it takes for the arc to quench can be decreased by reducing the amount of ionised air and plasma that is created during an electrical arc [19]. If there are excessive amounts of ionised air, plasma and carbon formed during fault conditions, it might lead to the unsuccessful quenching of the fault, resulting in a supply interruption.

3.4 Summary - Protection philosophies

Both the neutral breaker scheme and single pole breaker scheme are designed to encourage the quenching of transient faults on MV lines. The efficiency with which the schemes clear faults can result in improved system reliability and power quality. Each scheme does, however, have its own advantages and limitations; therefore, each scheme will have different criteria for choosing where they should be implemented.

The neutral breaker scheme caters primarily for transient phase-to-earth faults, although the scheme might assist in clearing phase-to-phase-to-earth faults. The scheme attempts to reduce the earth fault current to a value below 35 A. As soon as an earth fault of 10 A or higher is detected, the neutral breaker will trip within 60 ms. This ensures that a transient earth fault is cleared from the MV network as quickly as possible, to limit damage to the electrical network, humans and animals during a contact incident. The protection philosophy of the neutral breaker scheme is designed in such a way that it will not interfere with any breakers currently installed within the same MV network. The success rate of the neutral breaker scheme depends primarily on the magnitude of the capacitive current. The magnitude of the capacitive current is influenced by the combined lengths of all lines connected to the same NECR as well as the voltage level of the applicable MV network.

Due to the high risk of an electrical contact incident (broken or low-hanging conductor) within a dense populated area, it is imperative to clear the earth fault as quickly as possible. A fast fault-clearing time will reduce electrical burn wounds substantially during such a contact incident. It is therefore proposed that the neutral breaker be installed in densely populated areas where line lengths are short.

The single-phase breaker scheme is able to clear earth faults and phase-to-phase faults. As soon as an earth fault or phase-to-phase fault is detected, the single pole breaker will trip within 30 ms. This ensures that transient faults are cleared from an MV network as quickly as possible. During a phase-to-phase fault condition, only one of the two single-phase breakers trips. This results in a customer only experiencing a loss-of-phase condition for one-second as compared to a three-phase momentary power interruption. The protection philosophy of the single pole

breaker scheme is designed in such a way that it will not interfere with any breakers currently installed within the same MV network.

Although this scheme can be implemented on short or long MV lines, it is recommended that this scheme be implemented on long, rural MV lines. In the case of a rural MV line, which has a length of at least 200 km, it is more likely that the line is exposed to a high number of transient fault conditions.

--- Chapter 4 ---

Line model verification

As mentioned by Hänninen [5], electrical arcs are likely to quench if the current can be reduced to a magnitude below 35 A. It is important to verify the accuracy of the line model and the parameters used in the simulations. The line parameters have a significant influence on the magnitude of the capacitive current during fault conditions. In order to verify the line model, mathematical calculations are compared to line model simulation results. The line model was also validated by means of a field test where actual measurements were compared to the simulation results of the line model.

4.1 Capacitive coupling in grounded networks

Figure 4-1 shows an earth fault condition within a dual phase grounded electrical network. Note that the phase-A breaker has tripped for the fault condition.

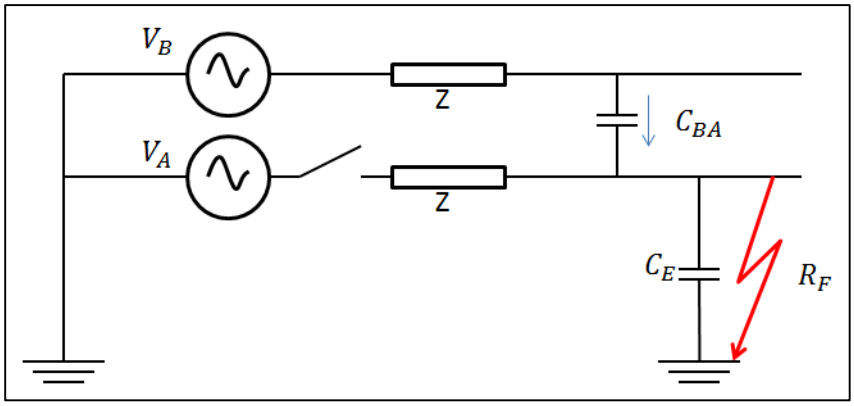

Figure 4-1 Single line diagram of dual phase grounded network under an earth fault condition

The equivalent sequence diagram of Figure 4-1 is shown in Figure 4-2.

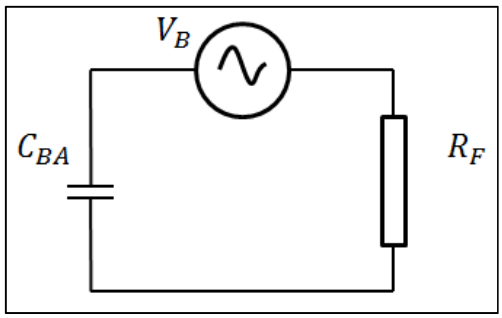

Figure 4-2 Equivalent circuit diagram of a dual phase grounded network under an earth fault condition

The majority of the capacitive coupling occurs between the healthy phase and the faulty phase. While the phase-A breaker is in the open position, the phase-to-earth capacitive coupling can be neglected. The capacitive current is calculated based on the following assumptions:

- Arc resistance is neglected
- The faulty phase is at earth potential
- Phase-A breaker is in the open position.

4.1.1 Calculations – Dual phase grounded system

During an earth fault condition, with the phase-A breaker in the open position, the voltage between phase A and B (V_{BA}) reduces by a factor of $\sqrt{3}$ (phase-to-earth voltage). Therefore, the total capacitive current between the healthy phase and the faulty phase can be expressed as:

$$I_{\text{capacitive current}} = 2\pi f C_{\text{phase-to-phase}} V_{BA},$$

where f is the power system frequency, V_{BA} is the system phase-to-phase voltage, and $C_{phase\text{-}to\text{-}phase}$ is the phase-to-phase capacitance (F/m). The capacitance between two phase conductors can be expressed as [18], [48], [64]:

$$C_{\text{phase-to-phase}} = \frac{\pi\varepsilon_0}{\operatorname{arcosh}\left(\frac{d}{2r}\right)},$$

$$= \frac{\pi\varepsilon_0}{\ln\left(\frac{d}{2r} + \sqrt{\frac{d^2}{4r^2} - 1}\right)},$$

where, r is the radius of conductors (m), ε_0 is the permittivity constant which is 8.85×10^{-12}, and d is the distance between the centre of both conductor (m).

Consider a 22 kV overhead line with a length of 232 km, which is strung with ASCR Fox conductor, that has a radius of 0.415 cm. If the configuration of the dual phase structure is such that the faulty and healthy phases are 9 m and 9.9 m above ground level respectively, with a distance of 1.309 m between the two phases, the capacitive current can be calculated as follows:

$$C_{\text{phase-to-phase}} = \frac{\pi\varepsilon_0}{\ln\left(\frac{d}{2r} + \sqrt{\frac{d^2}{4r^2} - 1}\right)}$$

$$= \frac{\pi\varepsilon_0}{\ln\left(\frac{1.309}{2r} + \sqrt{\frac{1.309^2}{4r^2} - 1}\right)}$$

$$= 4.842 \text{ pF/m}$$

$$I_{\text{capacitive current}} = 2\pi f C_{\text{phase-to-phase}} V_{BA} \times \text{lenght}$$

$$= 2\pi(50)(4.842 \times 10^{-12})(12760)(232000)$$

$$= 4.488 \text{ A}$$

4.1.2 Simulations – Dual phase grounded system

Figure 4-3 shows the model created in the electrical simulation software package ATPdraw.

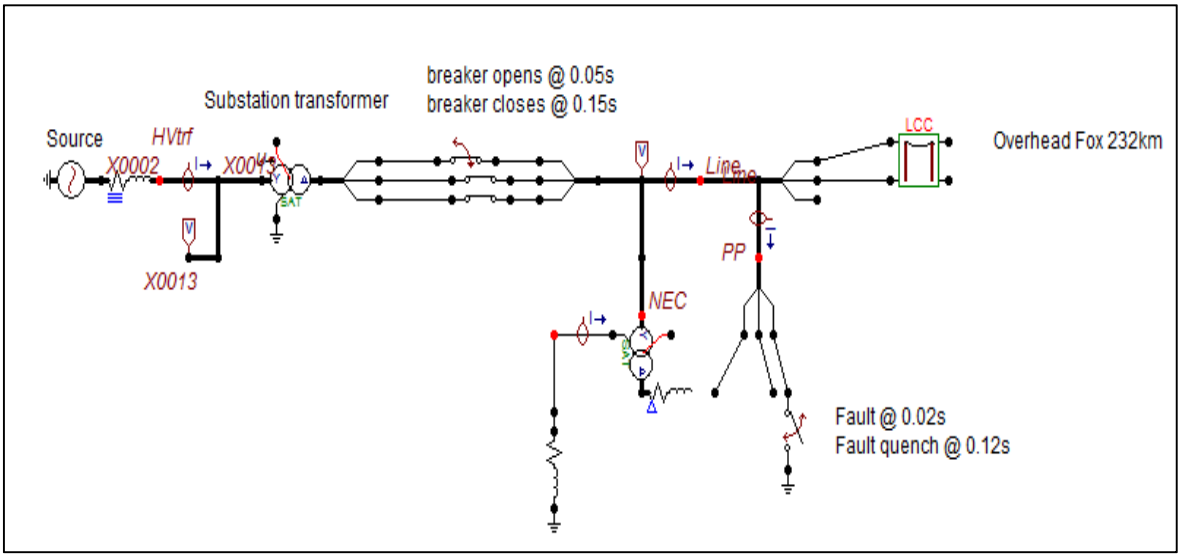

Figure 4-3 Grounded dual phase network model

Table 4-1 displays the conductor specifications used in the line model.

Table 4-1 Conductor specifications

ASCR conductor	Reactance (Ω/km)	Resistance (Ω/km)	Radius of conductor (cm)
Fox	0.45	0.86	0.4185

The physical dimensions of the T-Frame structure used in the line model, including the mid-span sagging of the conductors is given in Table 4-2.

Table 4-2 Physical dimensions of dual phase structure model in ATPdraw

Phase conductor	Phase-A	Phase-B
Horisontal dimension (m)	0	0.95
Height of conductors at T-frame structure (m)	9	9.9
Height of conductors at mid-span (m)	8	8.9

The simulated capacitive current was found to be 4.44 A (rms) as shown in Figure 4-4. This correlates well with the calculated result of 4.488 A.

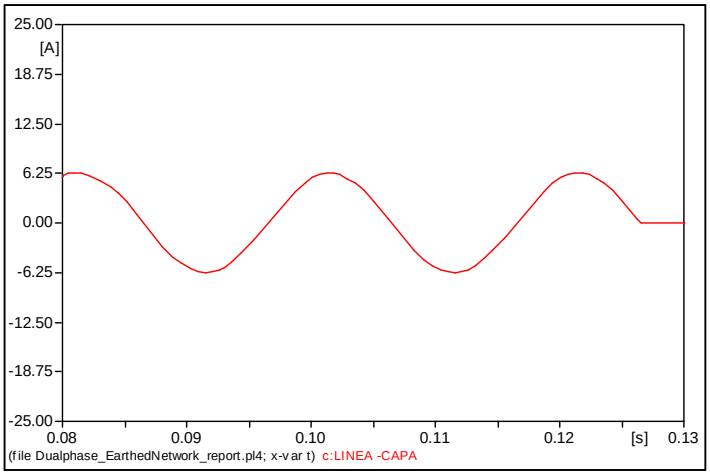

Figure 4-4 Simulated capacitive current of dual phase grounded network

4.2 Capacitive coupling in ungrounded networks

Figure 4-5 shows an earth fault condition within a dual phase electrical network. Note that the neutral breaker has tripped for the fault condition, causing the system to become temporarily ungrounded.

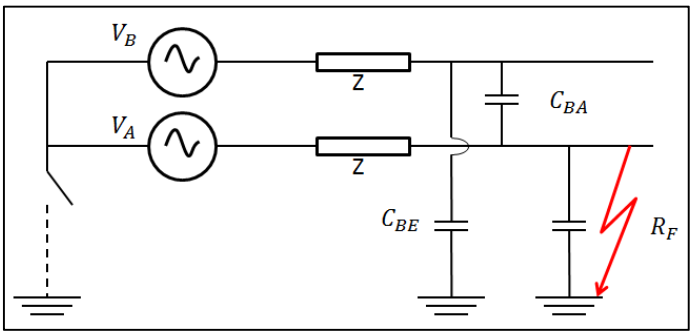

Figure 4-5 Single line diagram of dual phase ungrounded network under an earth fault condition

The equivalent sequence diagram of Figure 4-5 is shown in Figure 4-6.

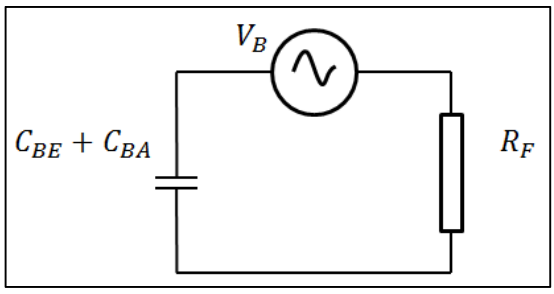

Figure 4-6 Equivalent circuit diagram of dual phase ungrounded network under an earth fault condition

The capacitive current is the sum of the coupling between the healthy phase and faulty phase, and the coupling between healthy phase and earth. The capacitive current is calculated based on the following assumptions:

- Arc resistance is neglected
- The faulty phase is at earth potential
- Neutral breaker is in the open position.

4.2.1 Calculations – Dual phase ungrounded system

During an earth fault condition, with the neutral breaker in the open position, the total capacitive current can be expressed as:

$$I_{\text{Capacitive total}} = I_{\text{Total phase-to-phase capacitive current}} + I_{\text{Total phase-to-earth capacitive current}}.$$

The capacitive current can be expressed in terms of system voltage and capacitance as:

$$I_{\text{Total phase-to-phase capacitive current}} = \frac{2\pi f C_{\text{phase-to-phase}} V_{\text{p-p}}}{\sqrt{3}},$$

$$I_{\text{Total phase-to-earth capacitive current}} = \frac{2\pi f C_{\text{phase-to-earth}} V_{\text{p-e}}}{\sqrt{3}},$$

where f is the power system frequency, V_{pp} is the system phase-to-phase voltage, V_{pe} is the system phase-to-earth voltage, $C_{phase\text{-}to\text{-}phase}$ is the phase-to-phase capacitance (F/m), and $C_{phase\text{-}to\text{-}earth}$ is the phase-to-earth capacitance (F/m).

The capacitance between the healthy conductor and earth can be expressed as [18], [48], [64]:

$$C_{\text{phase-to-earth}} = \frac{2\pi\varepsilon_0}{\operatorname{arcosh}\left(\frac{d}{r}\right)},$$

$$= \frac{2\pi\varepsilon_0}{\ln\left(\frac{d}{r} + \sqrt{\frac{d^2}{r^2} - 1}\right)},$$

where r is the radius of conductors (m), ε_0 is the permittivity constant which is 8.85×10^{-12}, and d is the distance between the centre of the conductor and earth (m).

The capacitance between the healthy conductor and faulty phase conductor at earth potential can be expressed as [18], [48], [64]:

$$C_{\text{phase-to-phase}} = \frac{\pi\varepsilon_0}{\operatorname{arcosh}\left(\frac{d}{2r}\right)},$$

$$= \frac{\pi\varepsilon_0}{\ln\left(\frac{d}{2r} + \sqrt{\frac{d^2}{4r^2} - 1}\right)},$$

where r is the radius of conductors (m), ε_0 is the permittivity constant which is $8.85\text{x}10^{-12}$, and d is the distance between the centres of both conductors (m).

Consider a 22 kV overhead network with a length of 232 km, which is strung with ASCR Fox conductor, that has a radius of 0.415 cm. If the configuration of the dual phase structure is such that the faulty and healthy phases are 9 m and 9.9 m above ground level respectively, with a distance of 1.309 m between the two phases, the capacitive current can be calculated as follows:

$$C_{\text{phase-to-phase}} = \frac{\pi\varepsilon_0}{\ln\left(\frac{d}{2r} + \sqrt{\frac{d^2}{4r^2} - 1}\right)}$$

$$= \frac{\pi\varepsilon_0}{\ln\left(\frac{1.309}{2\times 0.00415} + \sqrt{\frac{1.309^2}{4(0.00415)^2} - 1}\right)}$$

$$= 4.842 \text{ pF/m}$$

$$C_{\text{phase-to-earth}} = \frac{2\pi\varepsilon_0}{\ln\left(\frac{d}{r} + \sqrt{\frac{d^2}{r^2} - 1}\right)}$$

$$= \frac{2\pi\varepsilon_0}{\ln\left(\frac{9.9}{0.00415} + \sqrt{\frac{9.9^2}{0.00415^2} - 1}\right)}$$

$$= 3.522 \text{ pF/m}$$

$$I_{\text{Total phase-to-phase capacitive current}} = \frac{2\pi f C_{\text{phase-to-phase}} V_{p-p}}{\sqrt{3}}$$

$$= 4.488 \text{ A}$$

$$I_{\text{phase-to-earth capacitive current}} = \frac{2\pi f C_{\text{phase-to-earth}} V_{p-e}}{\sqrt{3}}$$

$$= 3.522 \text{ A}$$

$$\therefore I_{\text{Capacitive total}} \cong 8.01 \text{ A.}$$

4.2.2 Simulations – Dual phase ungrounded system

Figure 4-7 shows the line model created in ATPdraw.

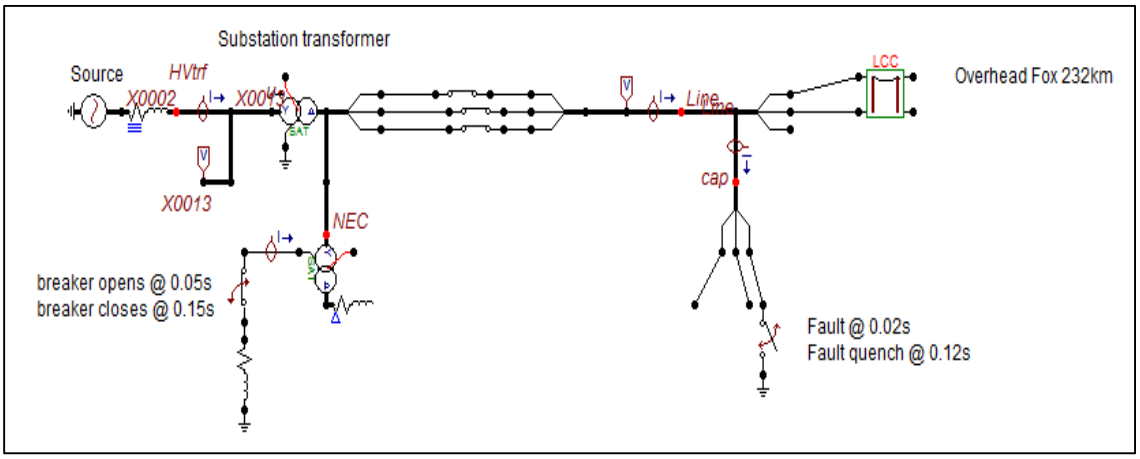

Figure 4-7 Ungrounded dual phase network model

Line models strung with ACSR Fox conductor were used. The line length was set to be 232 km. The physical dimensions of the T-Frame structures used in the line model, including the mid-span sagging of the conductors, are given in Table 4-3.

Table 4-3 Physical dimensions of dual phase structure model in ATPdraw

Phase conductor	Phase-A	Phase-B
Horisontal dimension (m)	0	0.95
Height of conductors at T-frame structure (m)	9	9.9
Height of conductors at mid-span (m)	8	8.9

The simulated capacitive current was found to be 8.31 A (rms) as shown in Figure 4-8. This correlates well with the calculated result of 8.01 A. The slight difference in current can be ascribed to the fact that during the simulation, conductor sagging is taken into account.

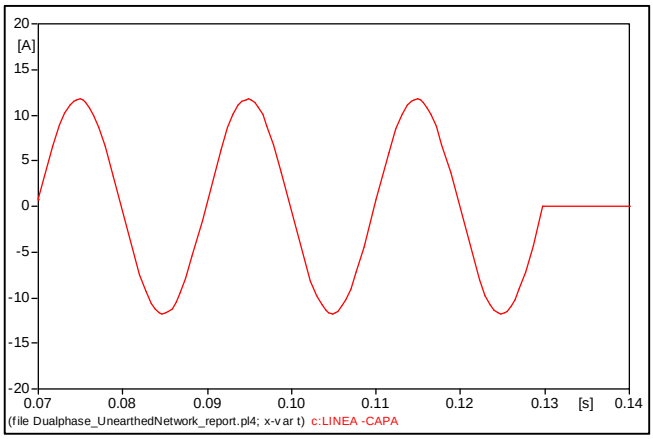

Figure 4-8 Simulated capacitive current of dual phase ungrounded network

4.3 Capacitive coupling in three-phase grounded networks

Figure 4-9 shows an earth fault condition within a grounded three-phase electrical network. Also note that the phase-A breaker is in the open position.

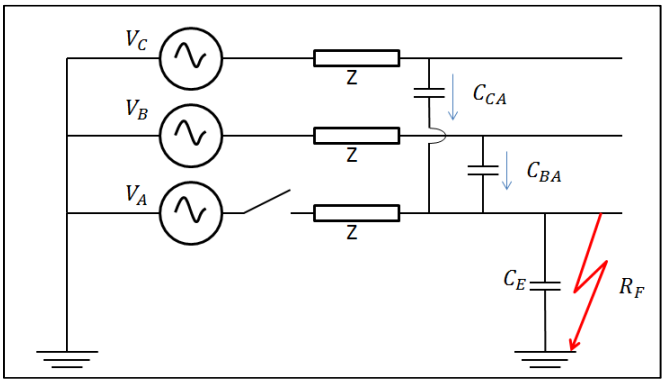

Figure 4-9 Single line diagram of three-phase grounded network under an earth fault condition

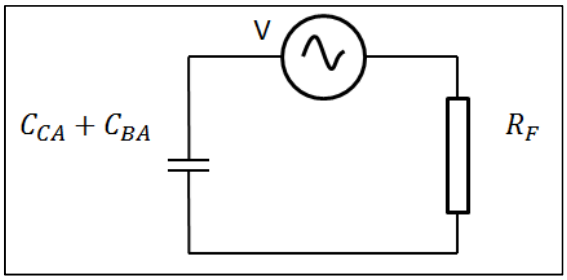

Figure 4-10 Equivalent circuit diagram of three-phase grounded network under an earth fault condition

The majority of the capacitive coupling is between the two healthy phases and the faulty phase. With the phase-A breaker in the open position, the capacitive coupling between the healthy phases and earth can be neglected.

The capacitive current is calculated based on the following assumptions:

- Arc resistance is neglected
- The faulty phase is at earth potential
- Phase-A breaker is in the open position.

4.3.1 Calculations – Three-phase grounded system

During an earth fault condition with the phase-A breaker in the open position, the three-phase phasor diagram changes as shown in Figure 4-11. Phase-to-phase voltages under normal system conditions reduce to phase-to-earth values. The 120° phase difference between V_{AB} and V_{AC} influences the sum total of the capacitive current due to V_A being zero after the opening of the phase-A breaker shown in Figure 4-11.

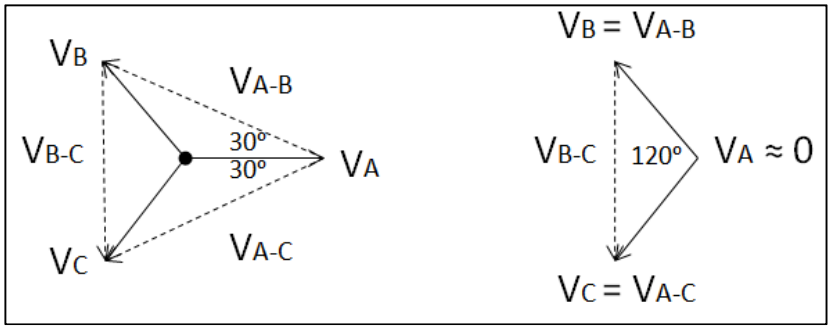

Figure 4-11 Phasor diagram of grounded system before and after a single-phase breaker operation

Therefore, the total capacitive current between the healthy phases and the faulty phase can be expressed as:

$$I_{\text{Total phase-to-phase capacitive current}} = I_{B-A}\cos 60° + I_{C-A}\cos 60°,$$

where $I_{B\text{-}A}$ is the capacitive current flowing from phase-B to phase-A, $I_{C\text{-}A}$ is the capacitive current flowing from phase-C to phase-A, and $I_{capacitive\ current}$ is the total phase-to-phase capacitive current. The capacitive current can be expressed in terms of system voltage and capacitance as:

$$I_{\text{Total phase-to-phase capacitive current}} = \frac{2\pi f C_{\text{phase-to-phase}} V_{p-p}}{\sqrt{3}},$$

where f is the power system frequency, V_{pp} is the system phase-to-phase voltage (which is equivalent to phase-to-earth voltage), and $C_{phase\text{-}to\text{-}phase}$ is the phase-to-phase capacitance (F/m). The capacitance between two healthy phases and the faulty phase can be expressed as [64]:

$$C_{\text{phase-to-phase}} = \frac{\pi \varepsilon_0}{\ln\left(\frac{d\sqrt{3}}{r}\right)},$$

where r is the radius of conductors (m), ε_0 is the permittivity constant which is 8.85×10^{-12}, and d is the distance between the centres of both conductors (m).

Consider a 22 kV overhead network with a length of 232 km, which is strung with ASCR Fox conductor, that has a radius of 0.415 cm. When the three overhead conductors are equally spaced with a distance of 1m between two phases, the capacitive current can be calculated as follows:

$$C_{\text{phase-to-phase}} = \frac{\pi\varepsilon_0}{\ln\left(\frac{d\sqrt{3}}{r}\right)}$$

$$= \frac{\pi\varepsilon_0}{\ln\left(\frac{1\sqrt{3}}{0.00415}\right)}$$

$$= 3.0785 \text{ nF/m}.$$

Due to the equally spaced line, C_{BA} is equal to C_{CA}. The capacitive current is calculated as:

$$I_{\text{Total phase-to-phase capacitive current}} = \frac{2\pi f C_{\text{phase-to-phase}} V_{p-p}}{\sqrt{3}} \times 2 \times \cos(60°) \text{ A}$$

$$= 1.649 \text{ A}.$$

4.3.2 Simulations – Three-phase grounded system

Figure 4-12 shows the three-phase line model created in ATPdraw.

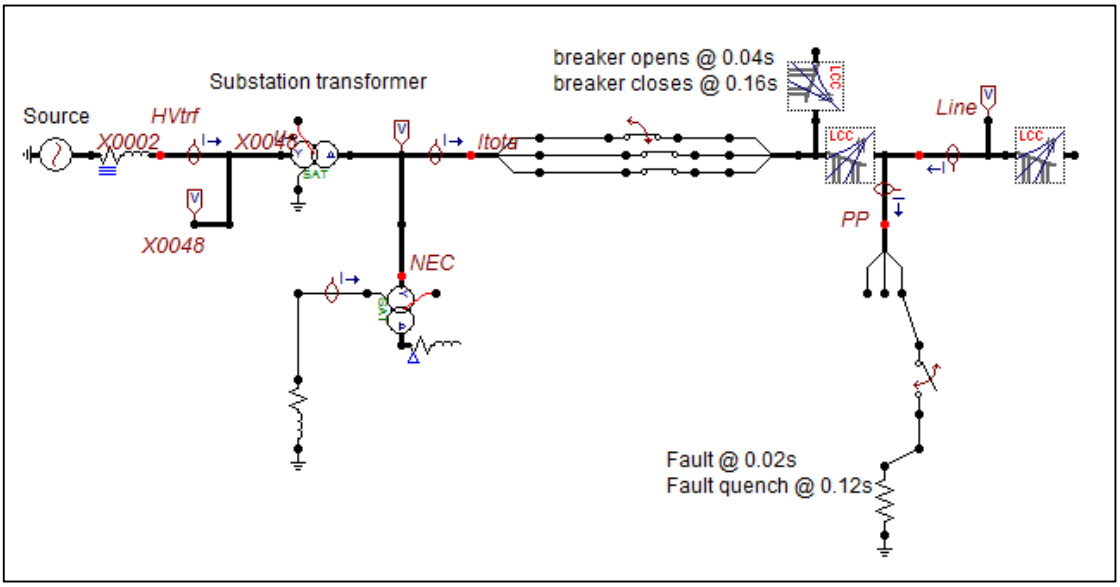

Figure 4-12 Grounded three-phase network model

The same overhead line length and conductor type used in the calculations, are used in the simulation. The physical dimensions of the T-Frame structures as well as the conductor specifications are given in Table 4-4.

Table 4-4 Physical dimensions of three-phase structure model in ATPdraw

	Ph.no.	React	Rout	Resis	Horiz	Vtower	Vmid
#		[ohm/km AC]	[cm]	[ohm/km AC]	[m]	[m]	[m]
1	1	0.45	0.4185	0.86	0	8	8
2	2	0.45	0.4185	0.86	0.5	8.866	8.866
3	3	0.45	0.4185	0.86	1	8	8

The simulated capacitive current was found to be 1.66 A (rms) as shown in Figure 4-13. This correlates well with the calculated result of 1.65 A.

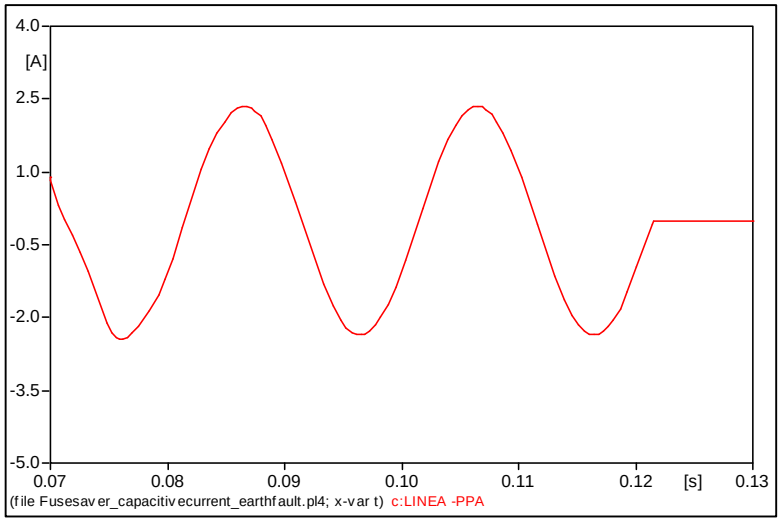

Figure 4-13 Simulated capacitive current of three-phase grounded network

4.4 Capacitive coupling in three-phase ungrounded networks

Figure 4-14 shows an earth fault condition within an ungrounded three-phase electrical network.

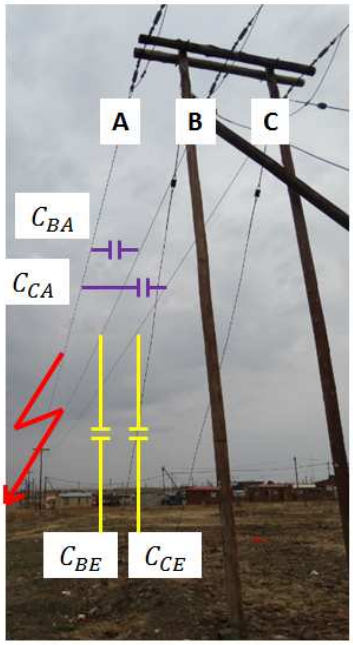

Figure 4-14 Phase-A to earth fault

The majority of the capacitive coupling in an unearth network is between:

- The healthy phases and the faulty phase
- The healthy phases and earth.

The capacitive current is calculated based on the following assumptions:

- Arc resistance is neglected
- Faulty phase is at earth potential
- Earth resistance back to the substation is negligible.

4.4.1 Calculations – Three-phase ungrounded network

Figure 4-15 shows the three-phase phasor diagram before and after the network is ungrounded, while there is a phase-A to earth fault present on the network. While the network is temporarily ungrounded during an earth fault condition, the phase-to-earth voltages can increase to phase-to-phase values. The 60° phase difference between V_{AB} and V_{AC} influences the capacitive current as depicted in Figure 4-15.

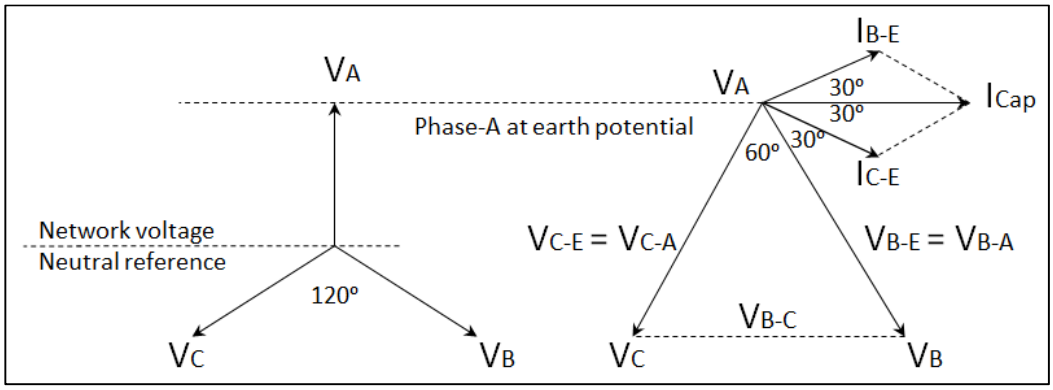

Figure 4-15 Three-phase phasor diagram before and after the unearthing of a system under an earth fault condition [3]

The phase-to-earth capacitive current between the healthy phases and earth can be expressed as:

$$I_{\text{Total phase-to-earth capacitive current}} = I_{B-E}\cos 30^{o} + I_{C-E}\cos 30^{\circ},$$

where $I_{B\text{-}E}$ is the capacitive current flowing to earth from phase B, $I_{C\text{-}E}$ is the capacitive current flowing to earth from phase C, and $I_{Total\ phase-to-earth\ capacitive\ current}$ is the total phase-to-earth capacitive current.

The capacitive current between the healthy phases and the faulty phase can be expressed as:

$$I_{\text{Total phase-to-phase capacitive current}} = I_{B-A}\cos 30^{o} + I_{C-A}\cos 30^{\circ},$$

where $I_{B\text{-}A}$ is the capacitive current flowing from phase-B to phase-A, $I_{C\text{-}A}$ is the capacitive current flowing from phase-C to phase-A, and $I_{Total\ phase-to-phase\ capacitive\ current}$ is the total phase-to-phase capacitive current.

Theoretically, the total capacitive current can be written as (assuming delta overhead line configuration):

$$I_{\text{Capacitive total}} = I_{\text{Total phase-to-phase capacitive current}} + I_{\text{Total phase-to-earth capacitive current}}.$$

The capacitive current can also be expressed in terms of system voltage and capacitance as:

$$I_{\text{Total phase-to-phase capacitive current}} = \frac{2\pi f C_{\text{phase-to-phase}} V_{\text{p-p}}}{\sqrt{3}},$$

$$I_{\text{Total phase-to-earth capacitive current}} = \frac{2\pi f C_{\text{phase-to-earth}} V_{\text{p-e}}}{\sqrt{3}},$$

where f is the power system frequency, V_{pp} is the system phase-to-phase voltage, V_{pe} is the system phase-to-earth voltage, $C_{phase\text{-}to\text{-}phase}$ is the phase-to-phase capacitance (F/m), and $C_{phase\text{-}to\text{-}earth}$ is the phase-to-earth capacitance (F/m). For a three-phase system, the capacitance per phase between the healthy and faulty phase conductors can be expressed as [18], [48], [64]:

$$C_{\text{phase-to-earth}} = \frac{2\pi\varepsilon_0}{\operatorname{arcosh}\left(\frac{d}{r}\right)},$$

$$= \frac{2\pi\varepsilon_0}{\ln\left(\frac{d}{r} + \sqrt{\frac{d^2}{r^2} - 1}\right)},$$

where r is the radius of the conductors (m), ε_0 is the permittivity constant which is 8.85×10^{-12}, and d is the distance between the centre of the conductor and earth (m). For a three-phase system the capacitance between two conductors can be expressed as [18], [48], [64]:

$$C_{\text{phase-to-phase}} = \frac{\pi\varepsilon_0}{\operatorname{arcosh}\left(\frac{d}{2r}\right)},$$

$$= \frac{\pi\varepsilon_0}{\ln\left(\frac{d}{2r} + \sqrt{\frac{d^2}{4r^2} - 1}\right)},$$

where r is the radius of the conductors (m), ε_0 is the permittivity constant which is 8.85×10^{-12}, and d is the distance between the centres of both conductors (m).

As mentioned by Hänninen [5], electrical arcs are likely to quench if the current can be reduced to a magnitude below 35 A. Therefore, in order to make sure that the electrical arc quenches, a more conservative current of 20 A is chosen to be the limiting factor. For a capacitive current of 20 A the calculated allowable distances for various system voltages and conductor sizes are given in Table 4-5 for T-frame structures. Figure 4-16 shows the physical dimensions of the T-frame structures. The capacitive coupling calculations were done assuming that the MV network is ungrounded.

Table 4-5 Maximum allowable line length for T-frame structures

System voltage (kV)	ACSR Conductor radius	C_{B-E} (F/m)	C_{C-E} (F/m)	C_{B-A} (F/m)	C_{B-C} (F/m)	Maximum combined line length
11	Fox – 0.0042 m	$6.61x10^{-12}$	$6.574x10^{-12}$	$5.36x10^{-12}$	$5.18x10^{-12}$	678 km
11	Mink – 0.0055 m	$6.83x10^{-12}$	$6.79x10^{-12}$	$5.66x10^{-12}$	$5.45x10^{-12}$	652 km
11	Hare – 0.0071 m	$7.05x10^{-12}$	$7.01x10^{-12}$	$5.97x10^{-12}$	$5.74x10^{-12}$	626 km
22	Fox – 0.0042 m	$6.61x10^{-12}$	$6.574x10^{-12}$	$5.36x10^{-12}$	$5.18x10^{-12}$	339 km
22	Mink – 0.0055 m	$6.83x10^{-12}$	$6.79x10^{-12}$	$5.66x10^{-12}$	$5.45x10^{-12}$	325 km
22	Hare – 0.0071 m	$7.05x10^{-12}$	$7.01x10^{-12}$	$5.97x10^{-12}$	$5.74x10^{-12}$	313 km

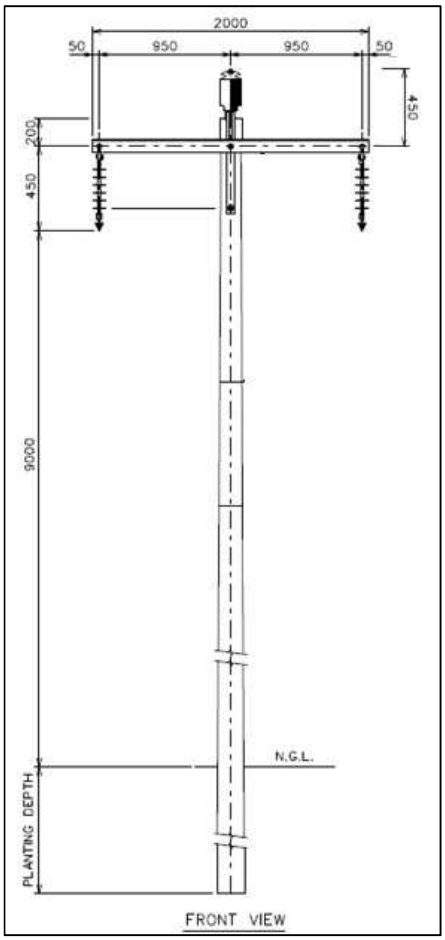

Figure 4-16 Physical dimensions of T-frame structure

4.4.2 ATP draw simulations

The capacitive coupling calculations, for a phase-A to earth fault condition in an ungrounded network, are verified with the line model created in ATPdraw. The calculated maximum allowable line lengths in Table 4-5 are used as inputs to the line models. A capacitive current of approximately 20 A must be obtained for each case, in order to verify the accuracy of the three-phase line model.

Figure 4-17 shows the ATPdraw line model for an ungrounded three-phase network and the conductor specifications used in the line model is given in Table 4-6.

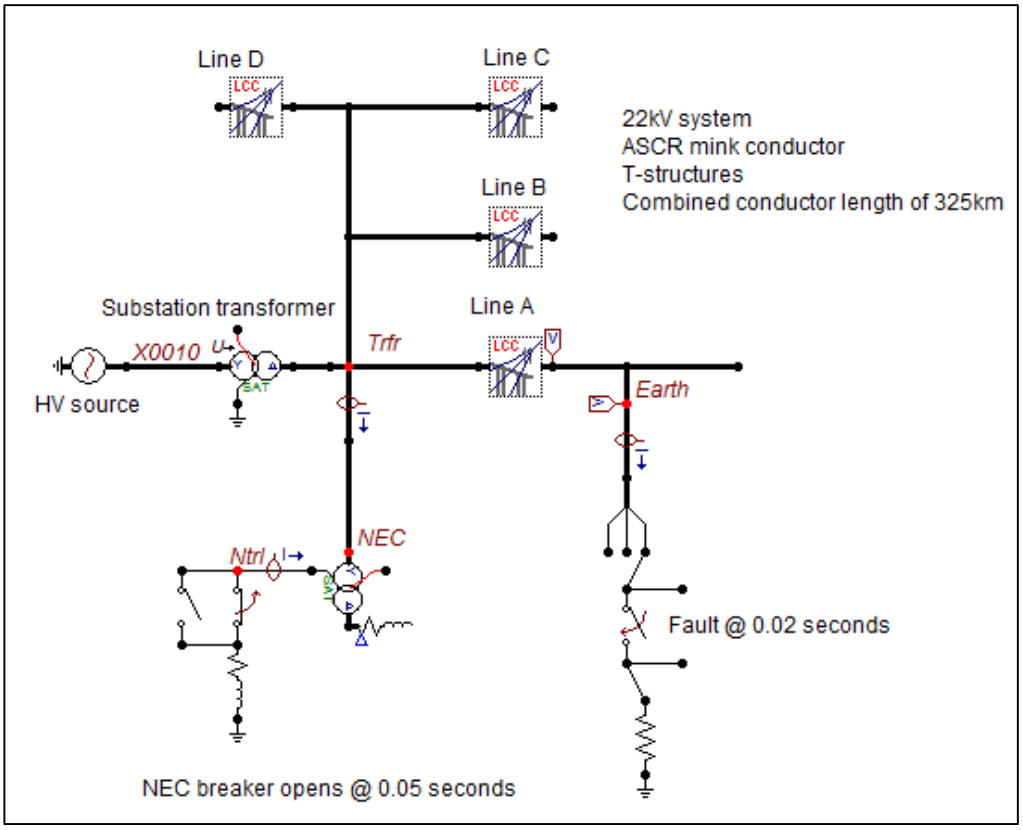

Figure 4-17 ATPdraw capacitive coupling model

Table 4-6 Conductor specifications

ASCR conductor	Reactance (Ω/km)	Resistance (Ω/km)	Radius of conductor (cm)
Fox	0.45	0.86	0.4185
Mink	0.44	0.5	0.55
Hare	0.41	0.32	0.708

The physical dimensions of the T-Frame structure used in the line model, including the mid-span sagging of the conductors are given in Table 4-7.

Table 4-7 Physical dimensions of T-frame structure model in ATPdraw

Phase conductor	Horisontal dimension (m)	Height of conductors at T-frame structure (m)	Height of conductors at mid-span (m)
Phase-A	0	9	8
Phase-B	0.95	9.9	8.9
Phase-C	1.9	9	8

The magnitude of the capacitive current obtained from the line model simulations are given in Table 4-8.

Table 4-8 Simulated maximum allowable line length for T-frame structures

System voltage (kV)	ACSR Conductor radius	Line length	Simulated capacitive coupling rms current (A)
11	Fox	678 km	20.4 A
11	Mink	652 km	19.7 A
11	Hare	626 km	19.2 A
22	Fox	339 km	20.2 A
22	Mink	325 km	19.93 A
22	Hare	313 km	19.4 A

The simulated and calculated results correlate well with each other. The slight difference with regards to the magnitude of the capacitive current can be ascribed to conductor sagging and voltage drops - which ATPdraw takes into consideration. Calculations were also performed on the assumption that the faulty phase is at ground potential. ATPdraw takes the actual voltage at the fault location into account.

The maximum allowable overhead line lengths calculated in Table 4-5 will be used as a guideline for selecting appropriate locations to implement the neutral breaker and single-phase breaker schemes.

4.5 Validation of capacitive coupling simulations

In order to verify the accuracy and validity of the capacitive current simulation results, two field tests were performed. Both tests were done on three-phase networks where the MV network was temporarily ungrounded during a permanent earth fault condition. The two test sites that were used for the testing was Ganspan - and Thabong East substations.

4.5.1 Ganspan substation

At Ganspan substation, no underground MV cables are utilised, only MV overhead lines. Table 4-9 gives a brief overview of the test site.

Table 4-9 Ganspan substation details

Number of MV lines	4
Operating voltage	22 kV
Conductor types	Combination of Fox, Mink and Hare
Structure types	Majority T-frame structures
Combined length of overhead lines	560 km

For calculation and simulation purposes, Mink conductor was used. The majority of the structures on the four MV lines are of a T-frame configuration and is therefore used in the capacitive current calculations. The physical dimensions of the T-frame structures used in the calculations and simulations are displayed in Table 4-10.

Table 4-10 Mink conductor and T-frame structure properties

	Ph.no.	React	Rout	Resis	Horiz	Vtower	Vmid
#		[ohm/km AC]	[cm]	[ohm/km AC]	[m]	[m]	[m]
1	1	0.44	0.55	0.5	0	9	7.5
2	2	0.44	0.55	0.5	0.95	9.9	8.4
3	3	0.44	0.55	0.5	1.9	9	7.5

By applying the formulas listed in section 4.4.1 of this dissertation, for a phase-A earth fault, the following results were obtained:

$$C_{B-E} = 6.79 \times 10^{-12}\ \mathrm{F/m},$$
$$C_{C-E} = 6.87 \times 10^{-12}\ \mathrm{F/m},$$
$$C_{B-A} = 5.08 \times 10^{-12}\ \mathrm{F/m},$$
$$C_{C-A} = 4.76 \times 10^{-12}\ \mathrm{F/m}.$$

The capacitive currents of both healthy phases to earth can be calculated as:

$$I_{B-E} = 8.78\ \mathrm{A},$$
$$I_{C-E} = 8.89\ \mathrm{A}.$$

With the total phase-to-earth capacitive current being,

$$I_{\text{Total phase-to-earth capacitive current}} = I_{be}\cos 30^{o} + I_{ce}\cos 30^{\circ},$$
$$= 15.3\ \mathrm{A}.$$

The capacitive currents of both healthy phases to the faulty phase can be calculated as:

$$I_{B-A} = 11.37\ \mathrm{A},$$
$$I_{C-A} = 10.64\ \mathrm{A}.$$

With the total phase-to-phase capacitive currents being,

$$I_{\text{Total phase-to-phase capacitive current}} = I_{ba}\cos 30^{o} + I_{ca}\cos 30^{\circ},$$
$$= 19.06\ \mathrm{A}.$$

The total capacitive current is therefore:

$$I_{\text{Capacitive total}} = I_{\text{Total phase-to-phase capacitive current}} + I_{\text{Total phase-to-earth capacitive current}},$$
$$= 34.36\ \mathrm{A}.$$

An overview of the ATPdraw model created to replicate Ganspan substation is shown in Figure 4-19.

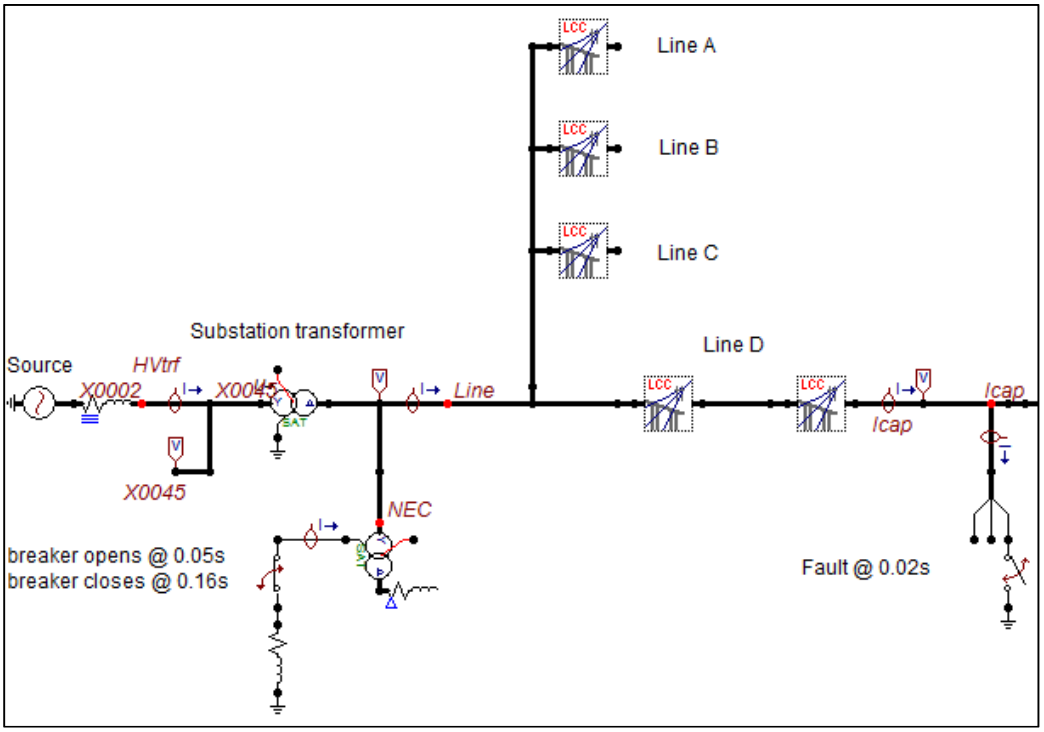

Figure 4-18 Ganspan substation ATPdraw model

The simulated capacitive current during the unearthing of the electrical network under an earth fault condition was found to be 35.5 A (rms). This correlates well with the calculated capacitive current of 34.36 A.

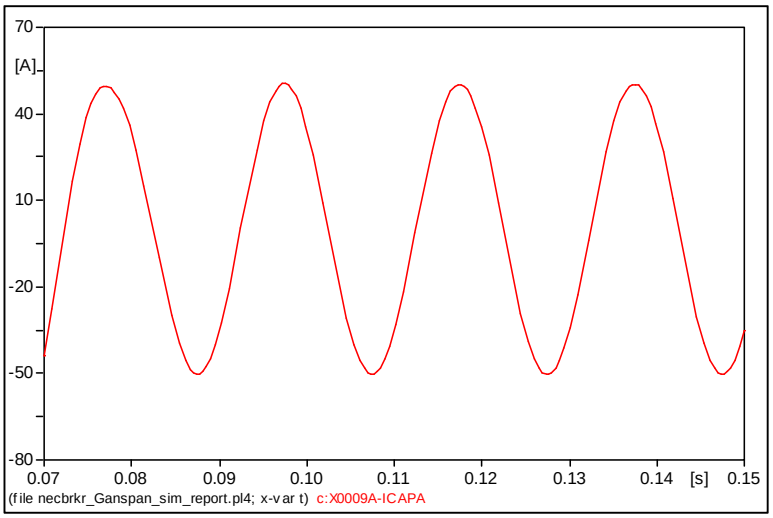

Figure 4-19 Simulated capacitive current (35.5 A)

A permanent earth fault was created on the 22 kV GAKG overhead line, which is supplied from Ganspan substation, during a field test. The MV network was temporarily ungrounded for a short

period to allow for the measurement of the capacitive current. The capacitive current was measured to be approximately 34 A (rms) as shown in Figure 4-20. During the period in which the MV network was temporarily ungrounded, the phase-to-earth voltages increased.

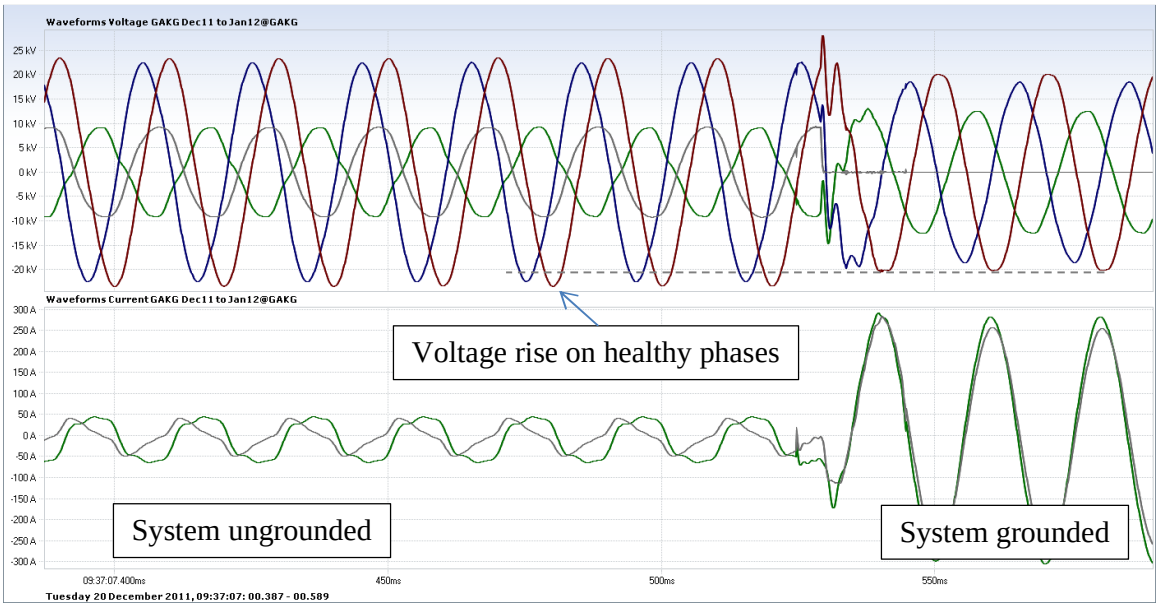

Figure 4-20 Measured capacitive current on GAKG line (34 A) while MV network was temporarily ungrounded

The measured, simulated and calculated capacitive current results correlates with each other. It can therefore be said that the line models used in the ATPdraw simulation is now verified to be accurate.

4.5.2 Thabong East substation

At Thabong East substation the majority of the MV network consists of overhead lines although there is a small section of underground cable also present. Table 4-11 gives a brief overview of the test site.

Table 4-11 Thabong East substation specifics

Number of MV lines	8
Operating voltage	11 kV
Structure types	T-frame structures
Combined length of overhead lines	195 km
Conductor used	Majority Mink conductor with sections of Fox conductor
Combined length of MV cable	5.7 km
Underground cable used	95 mm^2 XLPE cable

For calculation and simulation purposes, Mink conductor was used. The physical dimensions of the T-frame structures used in the calculations and simulations are displayed in Table 4-12.

Table 4-12 Mink conductor and T-frame structure properties

	Ph.no.	React	Rout	Resis	Horiz	Vtower	Vmid
#		[ohm/km AC]	[cm]	[ohm/km AC]	[m]	[m]	[m]
1	1	0.44	0.55	0.5	0	9	7.5
2	2	0.44	0.55	0.5	0.95	9.9	8.4
3	3	0.44	0.55	0.5	1.9	9	7.5

The XLPE cable specifications used in the calculations and simulations are displayed in Table 4-13.

Table 4-13 XLPE cable (95mm^2) specifications

DATA	UNIT	VALUE
R	Ohm/m	0.000247
X	Ohm/m	0.0001
C	µF/m	0.000303

By applying the formulas listed in section 4.4.1 of this dissertation for a phase-A earth fault, the following results were obtained with regards to the capacitance of only the overhead lines:

$$C_{B-E} = 6.97 \times 10^{-12}\ \mathrm{F/m},$$

$$C_{C-E} = 7.09 \times 10^{-12}\ \mathrm{F/m},$$

$$C_{B-A} = 5.08 \times 10^{-12}\ \mathrm{F/m},$$

$$C_{C-A} = 4.76 \times 10^{-12}\ \mathrm{F/m}.$$

The capacitance of the XLPE 95 mm^2 cable is:

$$C_{C-E} = C_{B-A} = C_{C-A} = C_{B-E} = 1.727 \times 10^{-6}\ \mathrm{F/m}\ .$$

The sum of the phase-to-earth capacitive currents of the overhead line and MV cable are:

$$I_{B-E} = 3.56\ \mathrm{A},$$

$$I_{C-E} = 3.59\ \mathrm{A}.$$

With the total phase-to-earth capacitive current calculated as:

$$I_{\text{Total phase-to-earth capacitive current}} = I_{B-E}\cos 30^{o} + I_{C-E}\cos 30^{\circ},$$

$$= 6.2\ \mathrm{A}.$$

The sum of the phase-to-phase capacitive currents of the overhead line and MV cable are:

$$I_{B-A} = 5.43 \text{ A},$$

$$I_{C-A} = 5.3 \text{ A}.$$

With the total phase-to-phase capacitive current calculated as:

$$I_{\text{Total phase-to-phase capacitive current}} = I_{B-A}\cos 30° + I_{C-A}\cos 30°,$$

$$= 9.29 \text{ A}.$$

The total capacitive current is therefore:

$$I_{\text{Capacitive total}} = I_{\text{Total phase-to-phase capacitive current}} + I_{\text{Total phase-to-earth capacitive current}},$$

$$= 15.5 \text{ A}.$$

An overview of the ATPdraw model created to replicate Thabong East substation is shown in Figure 4-21.

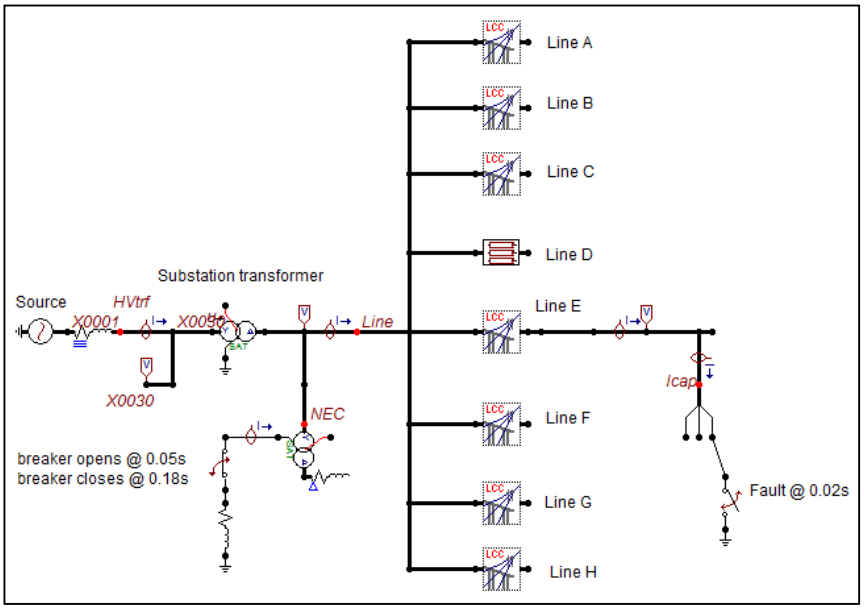

Figure 4-21 Thabong East substation ATPdraw model

The simulated capacitive current, shown in Figure 4-22, during the unearthing of the electrical network under an earth fault condition, was found to be 15.1 A (rms). This correlates well with the calculated capacitive current result of 15.5 A.

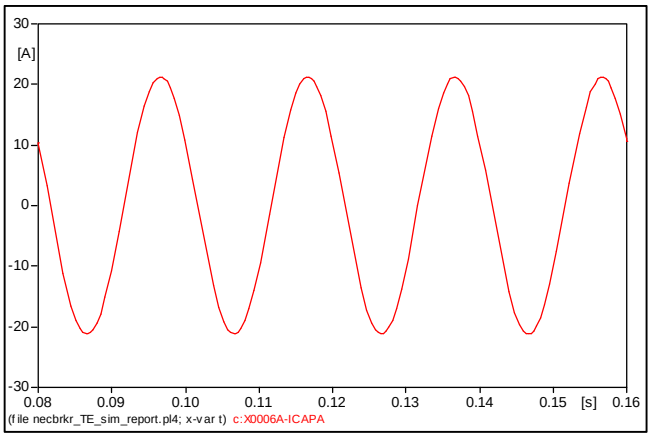

Figure 4-22 Simulated capacitive current (15.1 A)

A permanent earth fault was created on the 11 kV TEG overhead line, which is supplied from Thabong East substation. The MV network was ungrounded for a short period to allow for the measurement of the capacitive current. The capacitive current was measured to be approximately 15.9 A (rms), as shown in Figure 4-23.

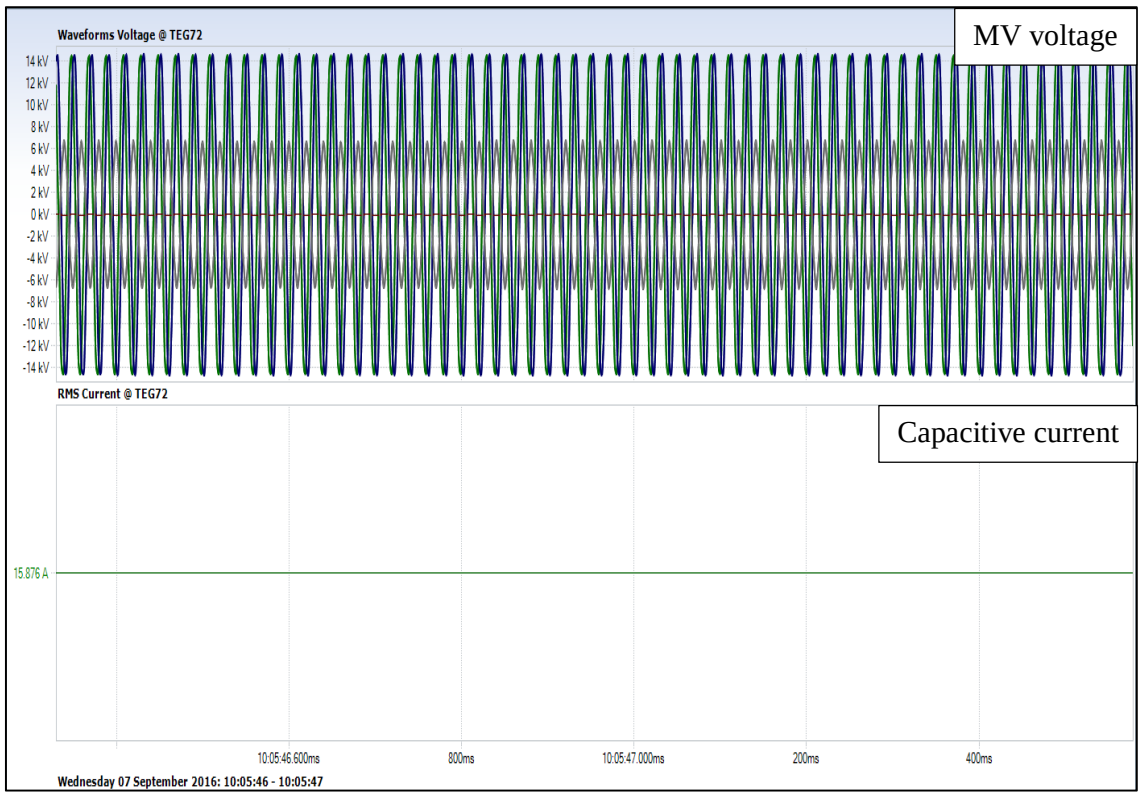

Figure 4-23 Measured capacitive current on TEG line (approximately 15.9 A) while network was temporarily ungrounded

The measured, simulated and calculated capacitive current results correlates with each other. It can, therefore, be said that the line and cable models used in the ATPdraw simulation is now verified to be accurate.

4.6 Summary – Line model

For electrical arcs to quench in an ungrounded network, the secondary arc current needs to be below 35 A [4], [5]. One of the contributing factors towards the secondary arc current is the capacitive coupling current. From the calculations and simulation results, it is clear that the capacitive current is dependent on the following factors:

- Length of the overhead line
- Size of the conductor
- Operating voltage of the electrical network
- Distance between the conductors
- Distance between conductors and earth.

When comparing the calculated capacitive current results of the various overhead line configurations with the corresponding simulation line models, the results correlates as shown in Table 4-14.

Table 4-14 Comparison between the calculated and simulated capacitive current results, for different overhead line configurations

Overhead line configuration	Calculated results	Simulated results
Dual phase grounded network	4.488 A	4.44 A
Dual phase ungrounded network	8.01 A	8.31 A
Three-phase grounded network	1.65 A	1.66 A

The slight difference between the calculated and simulated results can be ascribed to conductor sagging and voltage drop that ATPdraw takes into consideration. Capacitive current calculations were also performed on the assumption that the faulty phase is at ground potential. ATPdraw takes the actual voltage at the fault location into consideration, which is dependent on factors like the arc and earth impedance.

The calculated and simulated results shown in Table 4-15 of an ungrounded three-phase MV network correlated well with the measured results obtained from the two field tests. The line models can therefore be seen as being accurate and will be used in the integrated models of the neutral breaker and single-phase breaker schemes in Chapter 6.

Table 4-15 Comparison between the calculated, simulated and measured capacitive current results on an ungrounded three-phase network during an earth fault condition

Test location	Calculated result	Simulated result	Measured result
Ganspan substation (22 kV, 560 km overhead line)	34.36 A	35.5 A	34 A
Thabong East substation (11 kV, 195 km overhead line, 5.7 km underground cable)	15.5 A	15.1 A	15.9 A

Underground cables have a much larger influence on the magnitude of the capacitive current compared to overhead lines, as shown in the Thabong East measurements. When the conductor size and length of a MV cable increases in the network, it results in the increase of the capacitive current. It is therefore recommended that the neutral breaker and single-phase breaker schemes not be implemented in MV networks that utilise underground cables that exceed 15 km in length and have a nominal cross section area larger than 95 mm^2.

--- Chapter 5 ---

Transformer model verification

In this chapter, a transformer model is created in ATPdrawin order to simulate the transformer's response under a loss-of-phase condition. The transformer model will be verified by means of a field test, to ensure that the feedback current of the transformer model is accurate. The magnitude of the feedback current influences the arc quenching ability of the single-phase breaker scheme. Consider the earth fault condition located on the primary side of a Δ/Y transformer, which is shown graphically in Figure 5-1. Even after the phase-A breaker trips for an earth fault on the line, current will still be back fed into the earth fault through the primary windings of the Δ/Y transformers. The feedback current magnitude I_A, is dependent on the load current of the transformer [38].

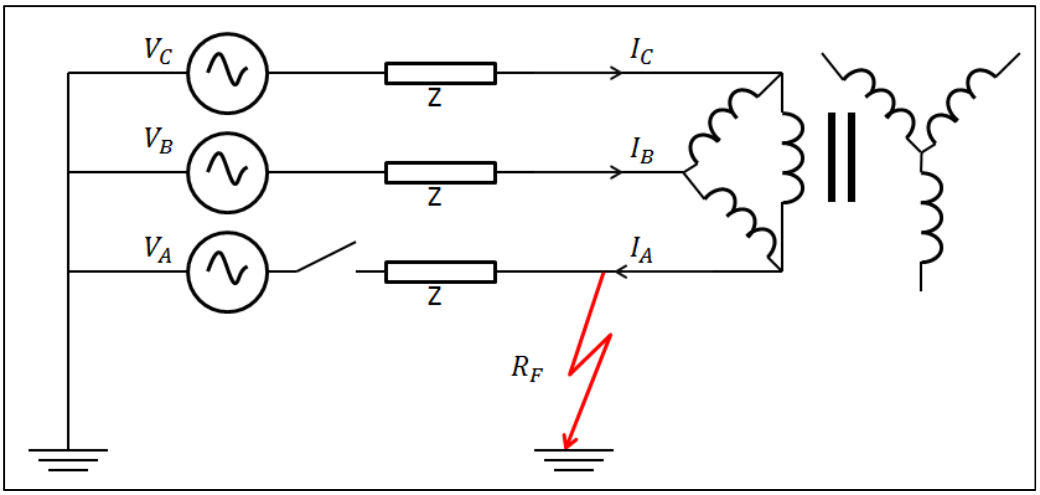

Figure 5-1 Feedback current through Δ/Y transformer during an earth fault, under a loss-of-phase condition

5.1 Transformer model

5.1.1 Transformer parameters

The majority of pole mounted transformers installed on MV rural lines within the Free State range from 25 kVA to 100 kVA in size. The following transformer parameters were used in order to populate the 50 kVA transformer model in ATPdraw:

Table 5-1 Transformer parameters

Parameter	Value
Primary voltage (phase-to-phase)	22 kV
Secondary voltage (phase-to-phase)	440 V
Winding ratio at nominal tap	95
Primary winding resistance (@ 20 ^{0}C)	85.48 Ω
Primary winding inductance	461.62 mH
Secondary winding resistance (@ 20 ^{0}C)	0.0274 Ω
Secondary winding inductance	89.43 µH
Excitation current	1.85 A
Equivalent iron loss resistance	1.98 MΩ
Average flux density	1.778 T
Vector group	Dyn11
Core type	Three leg core

5.1.2 Feedback current

Sutherland [38] performed tests by creating a loss-of-phase condition on a Δ/Y configured transformer. He observed the following voltages on the secondary side of the transformer:

Table 5-2 Voltages present on secondary side of Δ/Y transformer under a loss-of-phase condition (phase-A) [38]

Transformer configuration	*Primary* side of transformer: phase-to-earth per unit voltages			*Secondary* side of transformer: phase-to-earth per unit voltages		
Δ / Y	V_{A-E}	V_{B-E}	V_{C-E}	V_{a-e}	V_{b-e}	V_{c-e}
	0	1	1	0.58	1	0.58

Even though there is no voltage present on the phase-A primary side of the transformer, 58% of the LV nominal voltage is still measured on the secondary side of the transformer.

5.1.3 Transformer model simulation

The ATPdraw model used to simulate the transformer feedback current during an earth fault condition is shown in Figure 5-2. A 4.6 kVA single-phase load is connected to the phase-c secondary side of the transformer. An earth fault is created on the phase-C conductor 20 ms into the simulation.

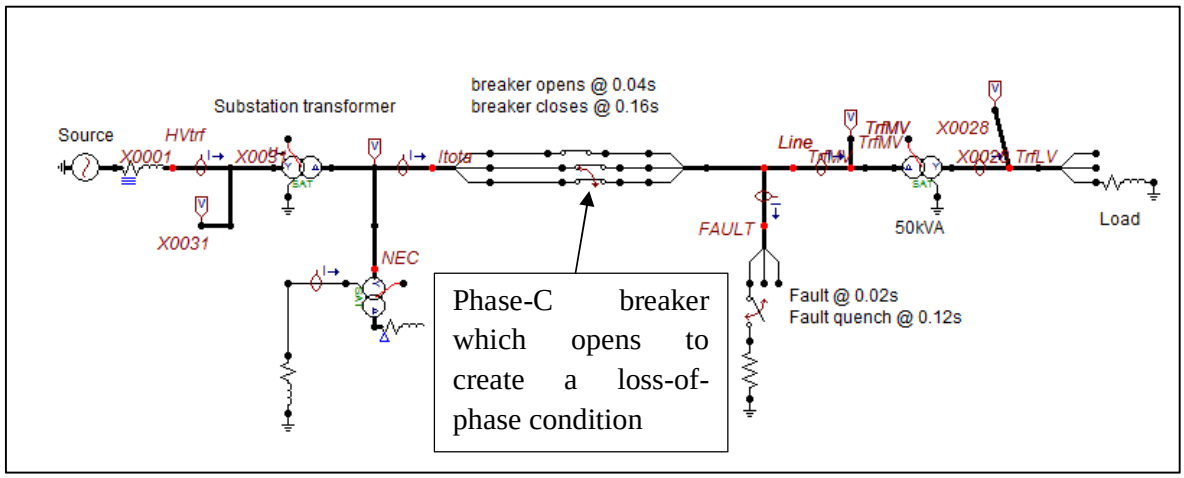

Figure 5-2 ATPdraw model - loss-of-phase condition

The earth fault condition causes an increase in the phase-to-earth voltages of the healthy phases, which continues until the phase-C breaker opens. After the phase-C breaker opens, the transformer is energised by only two phases. The simulated MV voltage waveforms are shown in Figure 5-3.

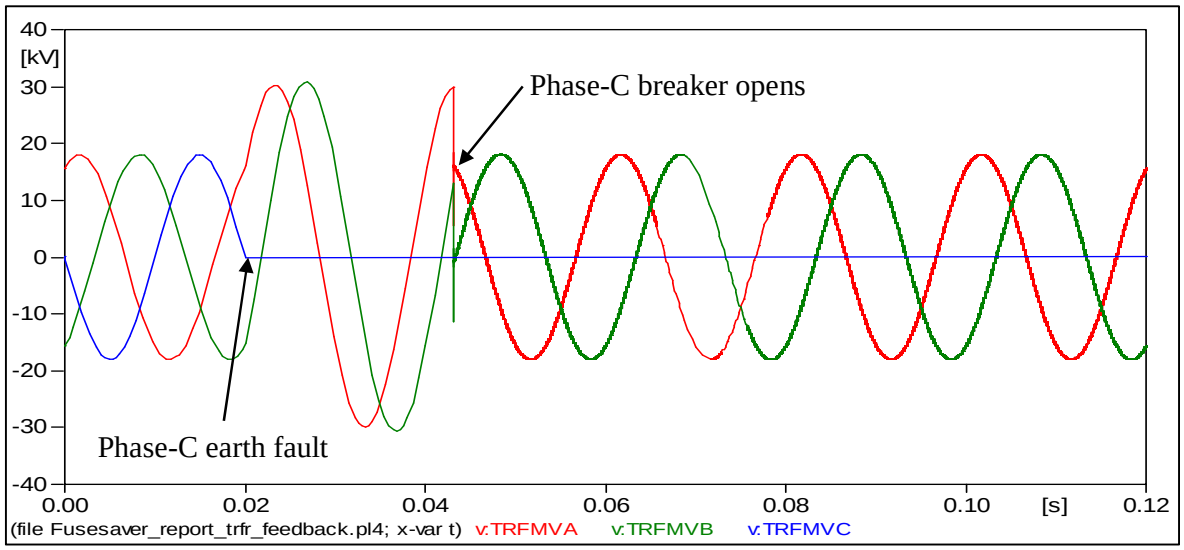

Figure 5-3 Simulated MV voltage waveforms

It can be seen from Figure 5-4 that two of the phase-to-earth voltages on the secondary side of the Δ/Y transformer decrease to approximately 58%, when the phase-C breaker is open.

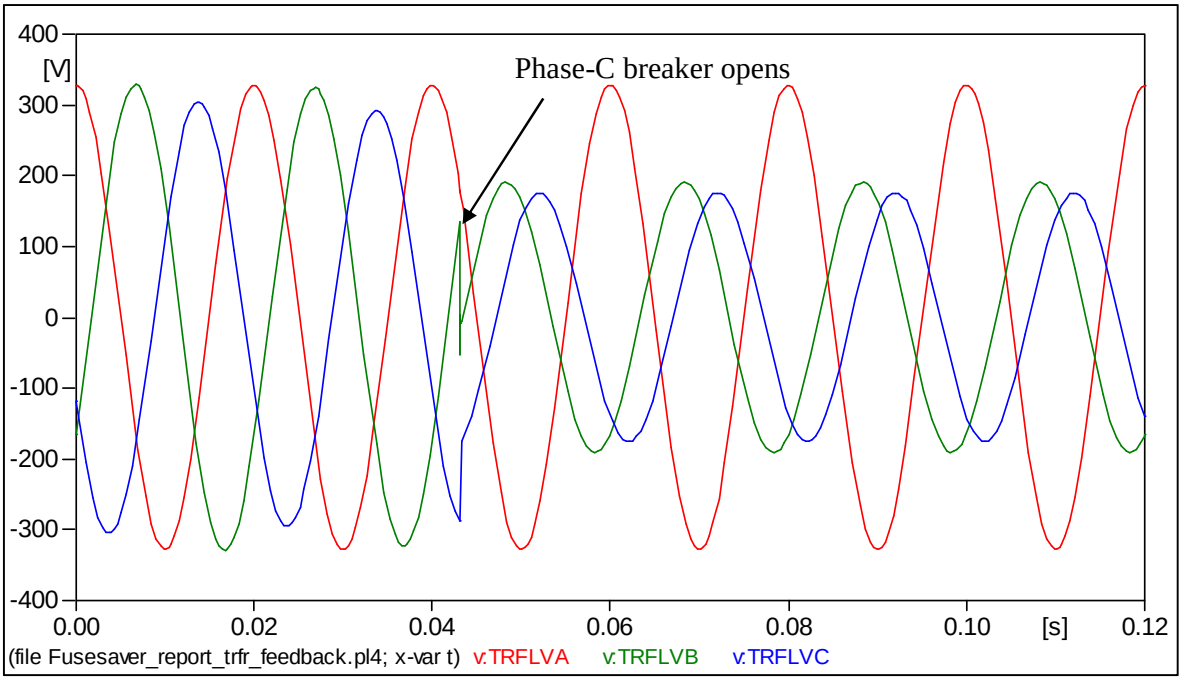

Figure 5-4 LV voltage waveforms

Figure 5-5 shows the current waveform on the secondary side (phase-c) of the Δ/Y transformer.

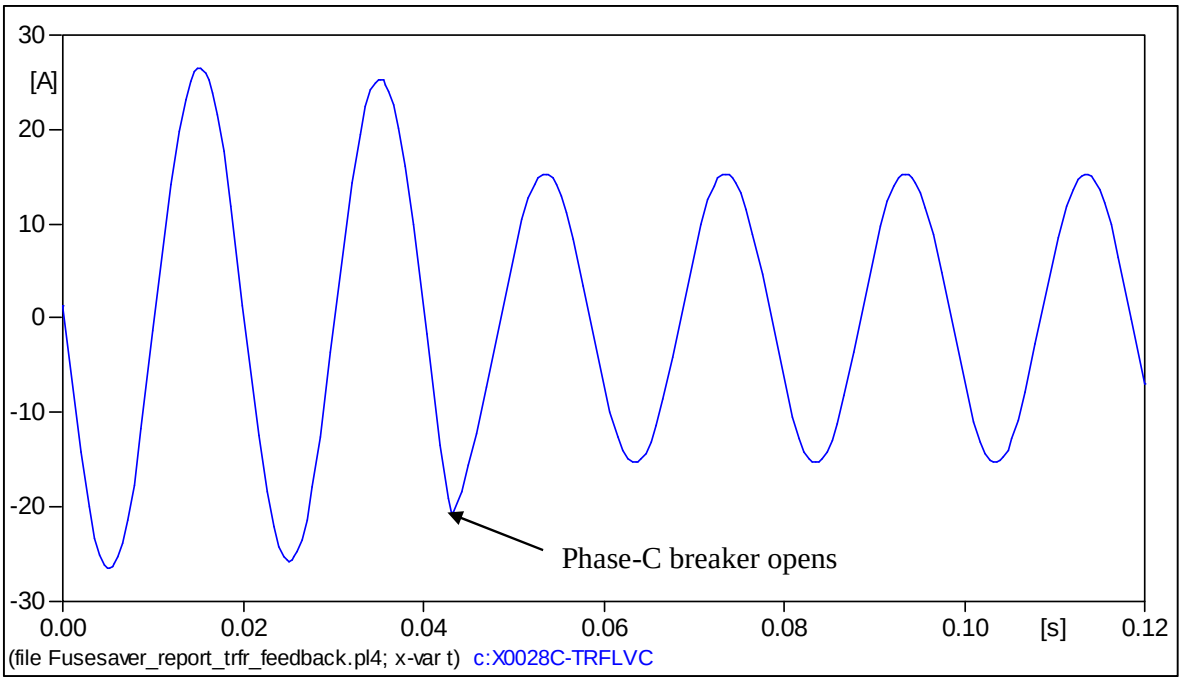

Figure 5-5 Phase-c current waveform (secondary side of transformer)

Figure 5-6 shows the feedback current on the primary side of the transformer, during the loss-of-phase condition. One should note that the transformer is feeding approximately 120 mA (rms) back into the earth fault.

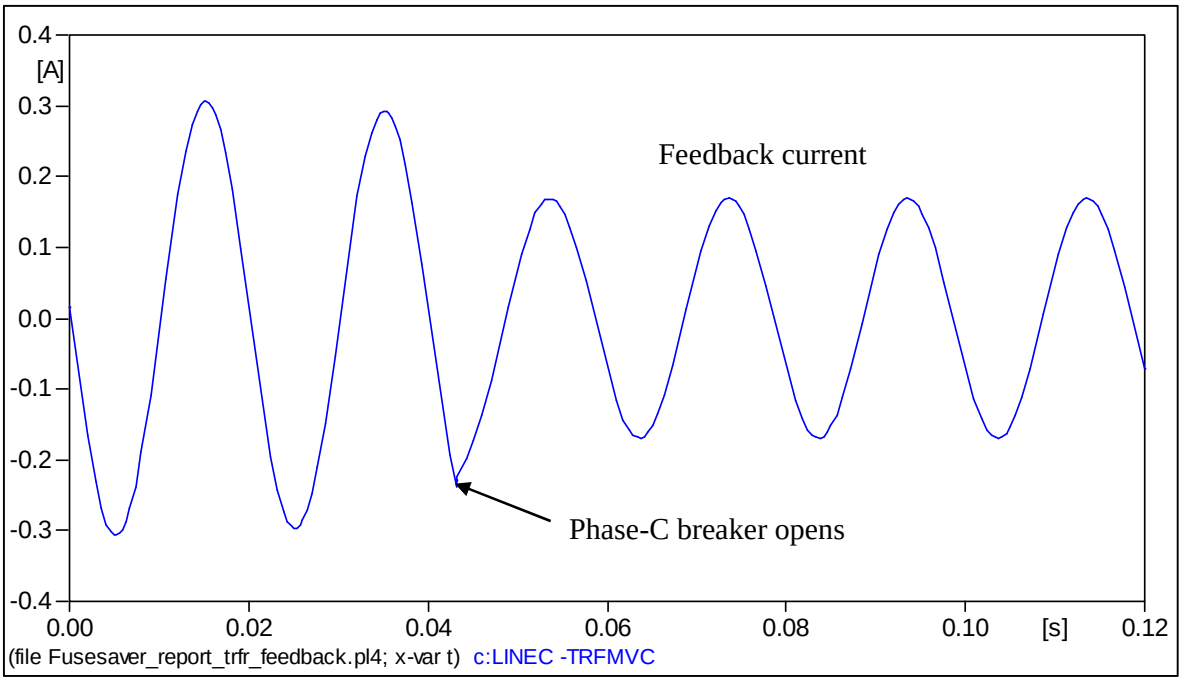

Figure 5-6 MV feedback current (120 mA rms)

5.1.4 Transformer model verification

In an attempt to verify the transformer model, a similar scenario was created on a 50 kVA transformer. The phase-C isolator of the transformer was removed to create a loss-of-phase condition. To simulate an earth fault condition the phase-C transformer MV bushing was earthed. Figure 5-7 shows the field test setup.

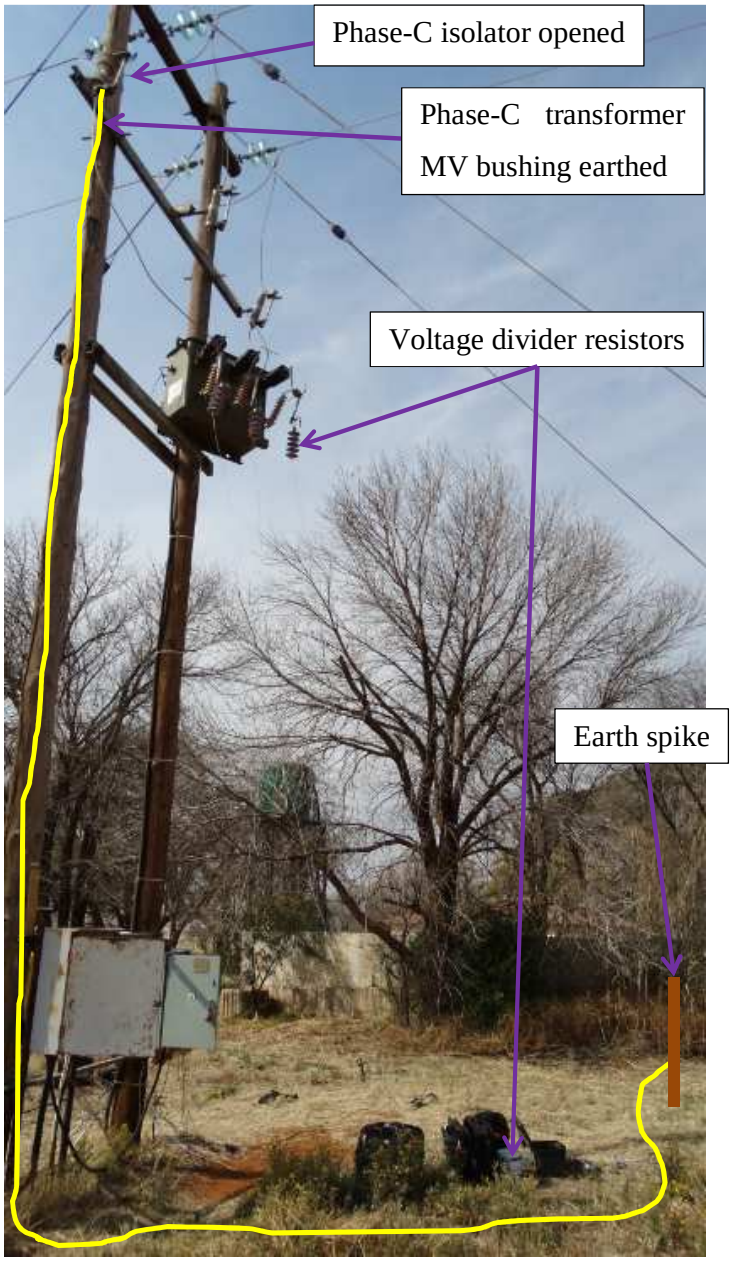

Figure 5-7 Transformer feedback current test setup

The MV voltages are measured by means of a resistor divider circuit. The phase-C feedback current is measured by means of a Rogowski coil. The LV voltage and currents are also measured during the course of the test. The overall measurement taken during the field test is

shown in Figure 5-8; note that the 50 kVA Δ/Y transformer was energised by only two phases during the course of the field test.

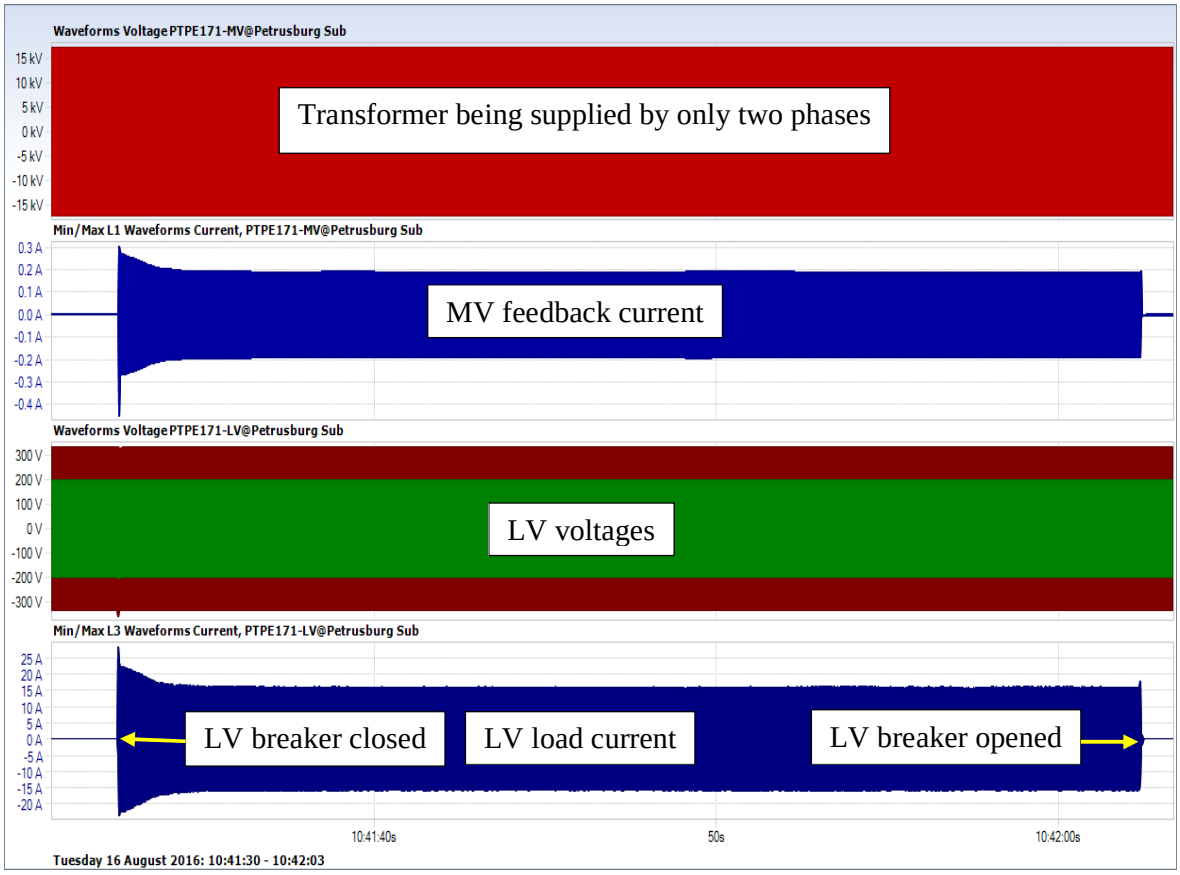

Figure 5-8 MV and LV voltage and current waveforms

With no load connected to the Δ/Y transformer, the feedback current is dependent only on the transformer excitation currents, which was in the range of 10 mA. As soon as the single-phase load was added to the transformer, the feedback current flowing into the fault increased to approximately 132 mA (rms). A detailed measurement of the MV and LV voltages and currents are shown in Figure 5-9.

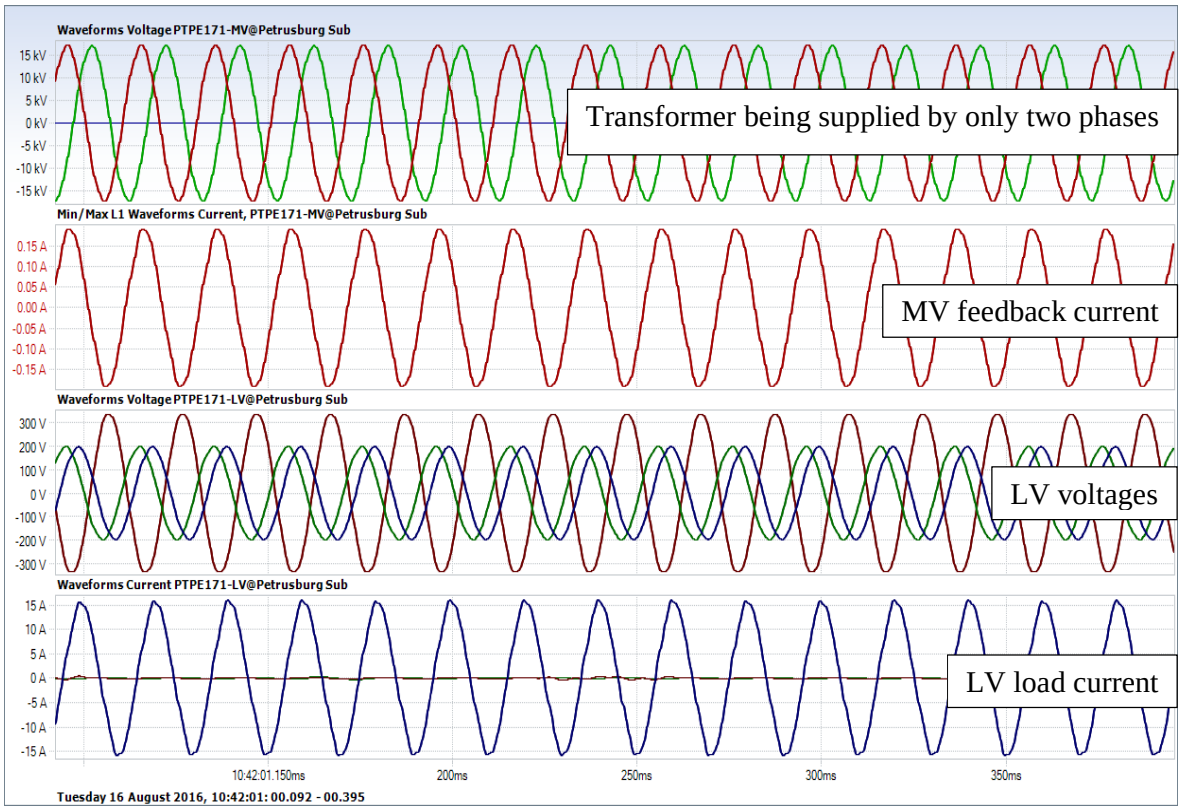

Figure 5-9 Detailed waveforms - Feedback current approximately 132 mA (rms)

The measured result of the feedback current shown in Figure 5-9 correlates well with the simulated feedback current of 120 mA (rms). The voltage waveforms of both the simulated and measured results also align when compared with each other. The transformer model created in ATPdraw is now validated to be accurate.

5.2 Feedback current vs transformer loading

To determine what the feedback current response of a transformer is under a loss-of-phase condition when the load is varied, a simulation needed to be performed. Four transformers were used in the simulation, with loads ranging from 1.95 kVA to 7.61 kVA. Figure 5-10 shows a graph of the feedback current plotted against the transformer load, during an earth fault, under loss-of-phase condition.

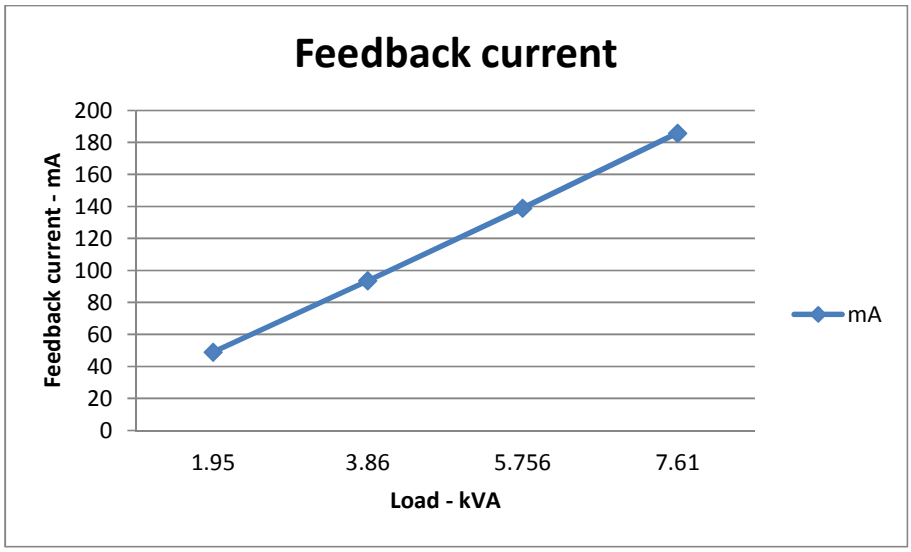

Figure 5-10 Feedback current plotted against transformer load

From the results it is evident that the feedback current linearly increases as the transformer loading increases. In order to validate these findings, a similar field test was performed. The overview of the field test results are given in Figure 5-11. The field test results also indicate that the feedback current of the transformer increases linearly as the transformer loading increased.

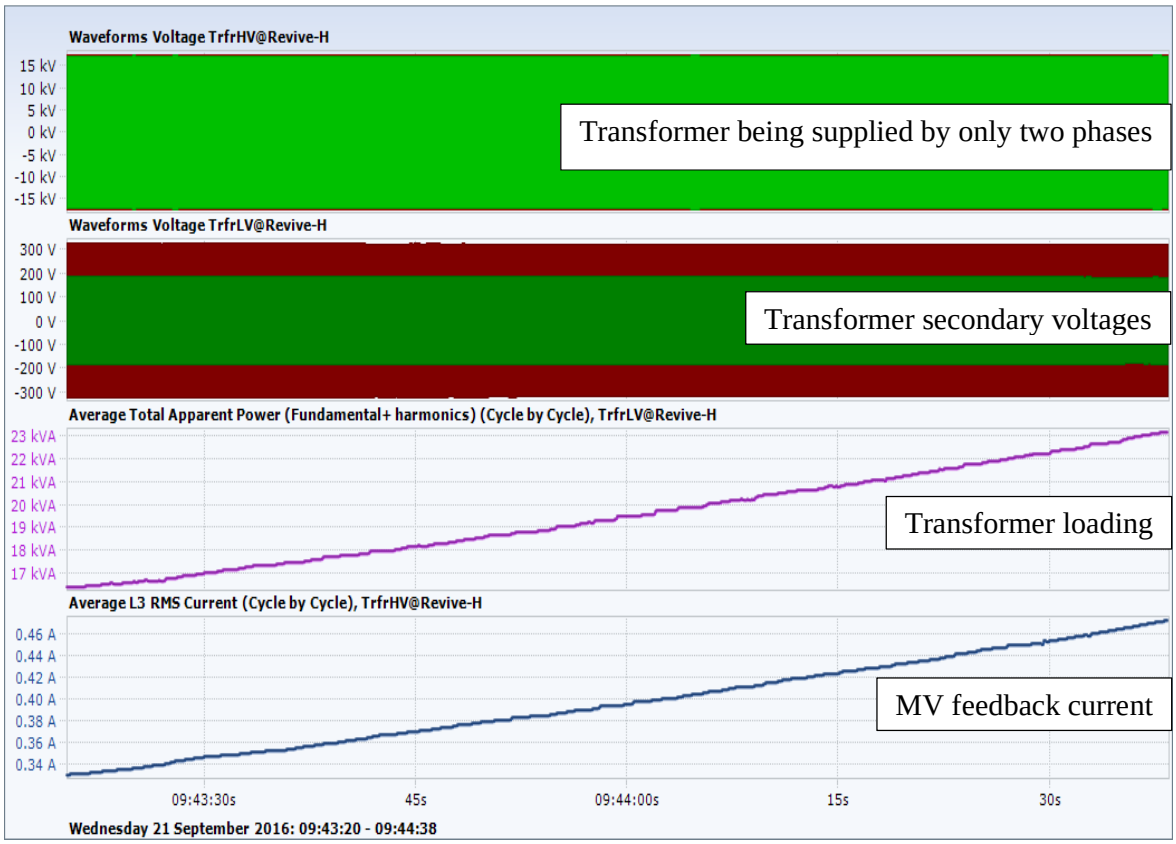

Figure 5-11 Measured results of feedback current increasing linearly as transformer loading increases

5.3 Summary – Transformer model

For electrical arcs to quench in an ungrounded network, the secondary arc current needs to be limited below 35 A [4], [5]. One of the contributing factors towards the secondary arc current is the transformer feedback current, which is present when a loss-of-phase occurs during a fault condition.

When comparing the simulated results of the Δ/Y transformer model with the measured results, the feedback current magnitude correlates well with each other as shown in Table 5-3.

Table 5-3 Feedback current of Δ/Y transformer with 4.6 kVA connected load

	Feedback current magnitude
Simulated result	120 mA
Measured result	132 mA

The slight difference between the simulated and measured results, shown in Table 5-3, can be due to measurement errors of the current transformers used during the field test. The tap position of the transformer will also influence the magnitude of the feedback current. The voltage waveforms of the simulated and measured results also aligned with each other.

From the simulation and measured results in Section 5.2, it is evident that the magnitude of the feedback current is linearly dependent on the loading of the Δ/Y transformer. Similar findings were obtained when tests were performed on a Δ/Y transformer in a 12.7 kV network [38].

The transformer model and parameters can be seen as being accurate. The validated transformer model will be used in the integrated models of the neutral breaker and single-phase breaker schemes in Chapter 6.

--- Chapter 6 ---

Site selection and Integrated models

In Chapter 6, trial sites are identified for the neutral breaker and single-phase breaker schemes. Suitable trail sites are selected based on:

- Findings regarding capacitive coupling discussed in Chapter 4
- Historical fault data of proposed locations
- Lightning density analyses of proposed locations.

The validated line model in Chapters 4 and the validated transformer model in Chapters 5 are combined to develop integrated models in ATPdraw. Separate integrated models are created for the neutral breaker and single-phase breaker schemes in Chapter 6, which are used for simulation purposes.

6.1 Identification of trial sites

6.1.1 Background for choosing trial sites for neutral breaker scheme

The neutral breaker scheme aims to clear transient earth faults without causing a supply interruption to customers. The scheme might also aid in the clearing of phase-to-phase-to-earth faults, by eliminating the earth fault current component.

The combined length of all lines that are connected to the same NECR, where the neutral breaker scheme is implemented, contributes to the magnitude of the capacitive coupling current. It is recommended that this scheme be implemented in high-density populated areas where line lengths are relatively short. Currently, within the Eskom FSOU, the protection philosophy with regards to urban lines are summarised in Table 6-1 [26]:

Table 6-1 ARC philosophy for urban MV overhead lines

Fault condition	Number of ARCs allowed
O/C	1
E/F	1
Sensitive E/F	0

If any of the line breakers within an urban MV overhead network trips on sensitive E/F protection, the breaker will lock-out. When a breaker lock-out occurs, the Eskom operator first needs to inspect the MV line before he is allowed to close the line breaker, even though there is a high probability that the fault was temporary in nature. In some cases, the switchgear and protection panels are old and do not allow separate auto reclose settings of normal E/F and sensitive E/F protection. This causes a breaker to trip and lockout for an E/F condition as well. If a breaker trips and locks out on an urban line, which normally supplies a large amount of customers, it negatively impacts SAIDI and SAIFI values.

It is recommended that the neutral breaker scheme not be implemented in areas where MV cables are in excess of 15 km in length. This is due to the significant contribution that cables have on the capacitive coupling of the electrical network, as discussed in Chapter 4.

6.1.2 Background for choosing trial sites for single-phase breaker

The single-phase breaker scheme aims to clear transient earth faults as well as phase-to-phase faults by means of single-phase tripping. The scheme aids in reducing the amount of arc energy which electrical equipment is exposed to during transient fault conditions.

The capacitive coupling during a fault condition is limited only to the length of the MV line on which the single-phase breakers are installed. It is proposed that this scheme be implemented on long rural lines (> 200 km), with a history of numerous transient faults events. The Eskom FSOU protection philosophy for rural MV lines is summarised in Table 6-2 [26]:

Table 6-2 ARC philosophy for rural MV overhead lines

Fault condition	Number of ARCs allowed
O/C	2
E/F	2
Sensitive E/F	0

6.2 Neutral breaker proposed sites

The substations listed in Table 6-3 were selected for the implementation of the neutral breaker scheme. A large number of customers are currently supplied by these substations. The MV lines supplied from these substations have experienced numerous transient fault events over a two-year period. Based on the findings in Chapter 4, all substations listed in Table 6-3 will have a capacitive current of less than 20 A.

By implementing the neutral breaker scheme at the selected substations, approximately 23% of the current customer base of 232953 within the Eskom FSOU will be included.

Table 6-3 Proposed sites to implement neutral breaker scheme

Substation name	MV line voltage	Combined length of MV lines	Number of customers supplied	Historic transient faults
Thabong Bulk 132/11 kV	11 kV	36.6 km	6524	32.3%
Thabong East 132/11 kV	11 kV	200.7 km	14382	40.59%
Meloding 132/11 kV	11 kV	148.5 km	10730	47.45%
Theunissen Munic 88/11 kV	11 kV	252.5 km	5668	62.74%
Kutlwanong 132/11 kV	11 kV	50.5 km	11934	37.2%

Two years of historical data obtained from Eskom's NEPS database was used to produce the information listed in Table 6-3. For more detailed information on the types of faults experienced at the substations refer to Appendix A. Transient faults mostly fall into the following root cause categories:

- Overhead line problem
- Fault not found
- Conductor problem
- Adverse weather
- Lightning.

A gridded exposure lightning analysis was performed for all MV lines connected to the selected substations. The Eskom fault analysis and lightning locating system (FALLS) was used to perform the gridded exposure analysis over a five-year period, to obtain the average lightning ground stroke density maps. Some areas of the MV lines indicate an average ground stroke density as high as 30 strokes per year. Refer to Appendix B for the detailed lightning study per substation.

6.3 Single-phase breaker proposed sites

The Petrusburg East (PTPE) and Diepfontein (PTDI) 22 kV overhead lines, which are supplied from Petrusburg substation, were selected to implement the single-phase breaker tripping philosophy. The Petrusburg East overhead line supplies 124 customers and has a length of 233 km. The line has a total of 153 pole-mounted transformers installed, with a combined installed capacity of 7.5 MVA. The Diepfontein overhead line supplies 2140 customers and has a length of 18 km. The line has a total of 34 pole-mounted transformers installed, with a combined installed capacity of 2.5 MVA. The Diepfontein overhead line also supplies the Petrusburg municipality. The loading of both lines rarely exceeded 2.5 MVA over a 18-month period, as shown in Figure 6-1.

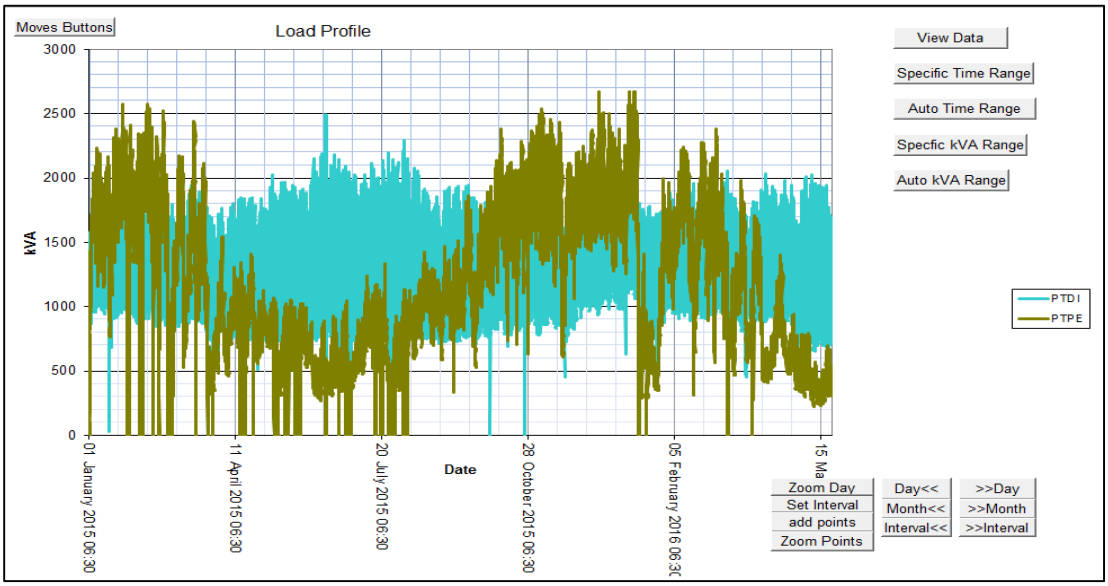

Figure 6-1 Load profiles of PTPE and PTDI over an 18 month period

A gridded exposure lightning analysis was performed on the Petrusburg East and Diepfontien MV lines by using the FALLS system. The gridded exposure analysis in Figure 6-2 and Figure 6-3 show the lightning ground stroke density with an applied 2 km x 2 km grid. The analysis was performed over a seven-year period in order to obtain the average lightning ground stroke densities. Some areas of the MV lines indicated a ground stroke density, which was as high as 29 strokes per year. The thematic legend in Figure 6-2 and Figure 6-3 displays the normalised ground stroke density, which is the average amount of ground strokes per year.

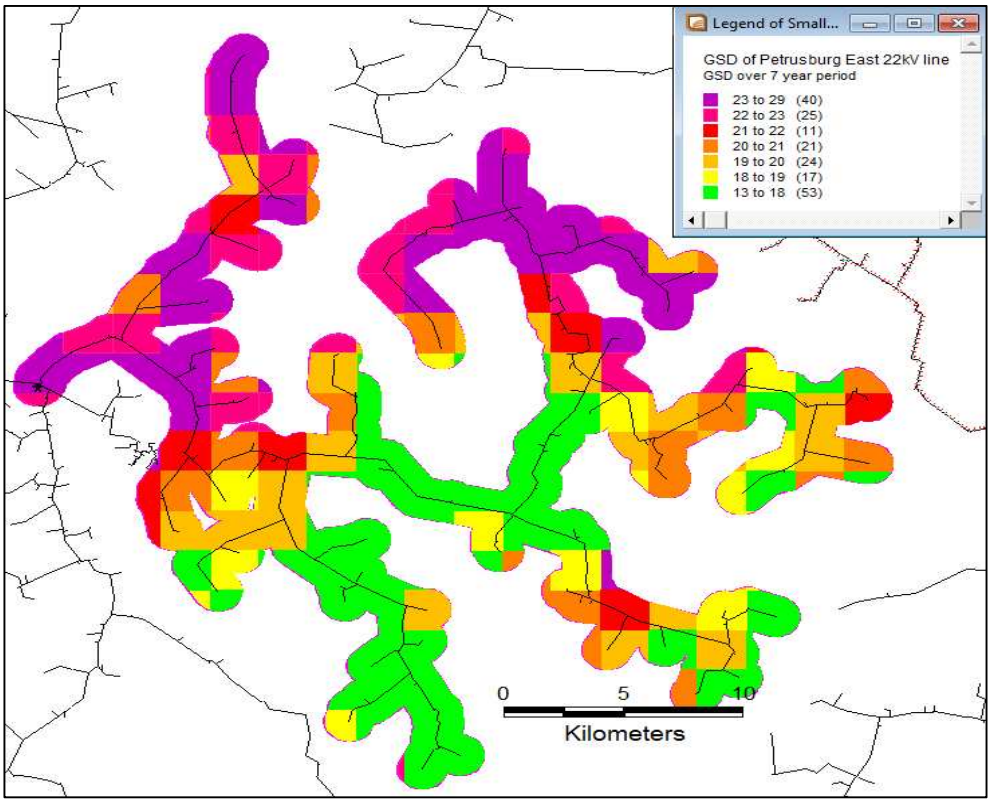

Figure 6-2 Seven-year GSD for the Petrusburg East 22 kV line (2009 – 2016)

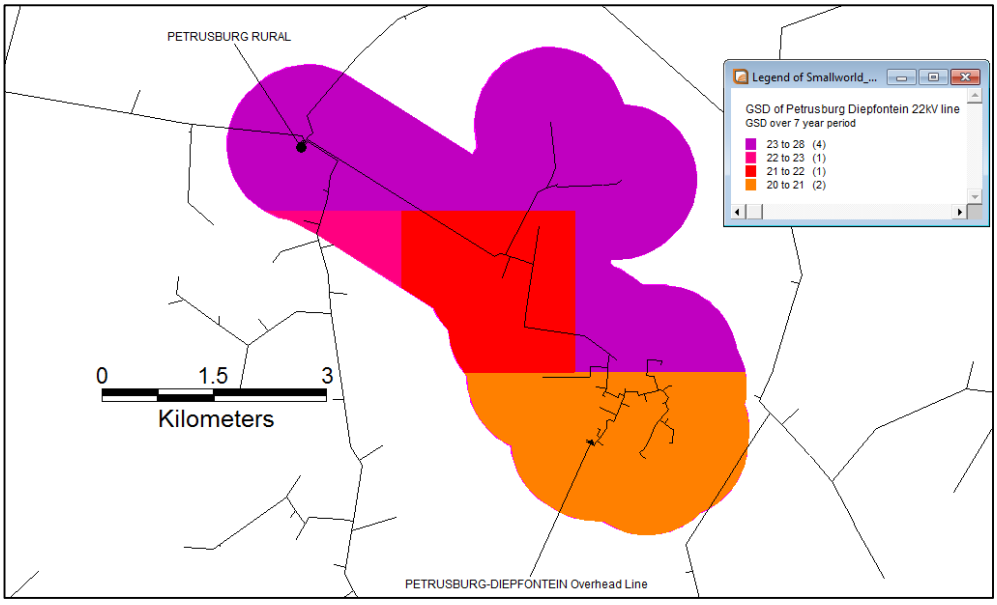

Figure 6-3 Seven-year GSD for the Diepfontein 22 kV line (2009 – 2016)

For the period of April 2015 to March 2016, all faults on the Petrusburg East and Diepfontein MV lines were analysed. This was done in order to verify the information stated in literature regarding the number of transient faults, and types of faults that are more prevalent in electrical networks [3], [4], [5], [14], [16], [18]. Table 6-4 below shows the percentage of transient faults versus permanent faults.

Table 6-4 Percentage of permanent and transient faults

MV line name	Permanent faults	Transient faults
Petrusburg East	16%	84%
Diepfontein	36%	64%

The 233 km rural Petrusburg East line has a higher percentage of transient faults compared to the 18 km urban Diepfontein line. The possible reasons for the higher amount of transient faults are:

- Larger area exposed to lightning
- Greater exposure to animals and vegetation
- Average spanning distance between poles is longer, which could lead to conductor clashing during windy conditions
- More equipment installed on the line that can fail.

Table 6-5 below shows the percentage of earth faults versus multi-phase faults encountered on the Petrusburg East and Diepfontein lines.

Table 6-5 Percentage of earth faults and multi-phase faults over a one-year period

MV line name	Earth faults	Multi-phase faults
Petrusburg East	78%	22%
Diepfontein	86%	14%

The results given in Table 6-6 indicate what the percentage fault contribution was of each phase of the Petrusburg East and Diepfontein overhead lines.

Table 6-6 Percentage phase contribution to faults over a one-year period

MV line name	Phase-A	Phase-B	Phase-C
Petrusburg East	28%	67%	5%
Diepfontein	37%	53%	10%

The results in Table 6-6 indicate that the phase-B conductor on the MV overhead lines had the most faults on it. Both lines were constructed with a T-frame configuration, where the phase-B is elevated above the other phase conductors and therefore causes it to be more exposed to lightning strikes. In the event of a phase-to-phase fault, chances are very high that the phase-B conductor will form part of the fault. The chances are very slim of a phase-A to phase-C fault occurring on a T-frame structure.

6.4 Simulation results

ATPdraw is used to model the neutral breaker and single-phase breaker schemes in order to observe the system response under fault conditions. During the simulation process, attention is paid to both the LV and MV voltage and current waveforms.

Table 6-7 displays the conductor specification, which is used in the verified and validated line models:

Table 6-7 Conductor specifications

ASCR conductor	Reactance (Ω/km)	Resistance (Ω/km)	Radius of conductor (cm)
Fox	0.45	0.86	0.4185
Mink	0.44	0.5	0.55
Hare	0.41	0.32	0.708

The physical dimensions of the T-Frame structures used in the line model, including the mid-span sagging of the overhead lines, are given in Table 6-8.

Table 6-8 Physical dimensions of T-frame structure model in ATPdraw

Phase conductor	Horisontal dimension (m)	Height of conductors at T-frame structure (m)	Height of conductors at mid-span (m)
Phase-A	0	9	8
Phase-B	0.95	9.9	8.9
Phase-C	1.9	9	8

Table 6-9 shows the fault levels used in the simulation.

Table 6-9 Fault levels on MV side of the substation transformer

Fault type	Fault current
Phase-to-phase fault	4 kA
Phase-to-earth fault	355 A

6.4.1 Neutral breaker simulations

Figure 6-4 displays the simplified ATPdraw integrated model of the neutral breaker scheme. The validated MV line – and transformer models were combined to create the integrated model. A phase-A earth fault condition is created 20 ms into the simulation. The neutral breaker is set to trip 30 ms after the earth fault is detected. The fault clears 70 ms after the neutral breaker trips, whereafter the neutral breaker recloses. The MV operating voltage was set to be 11 kV and T-frame line models were used that are strung with Mink conductor. The section of underground cable was selected to be a 95 mm^2, three-core XLPE cable.

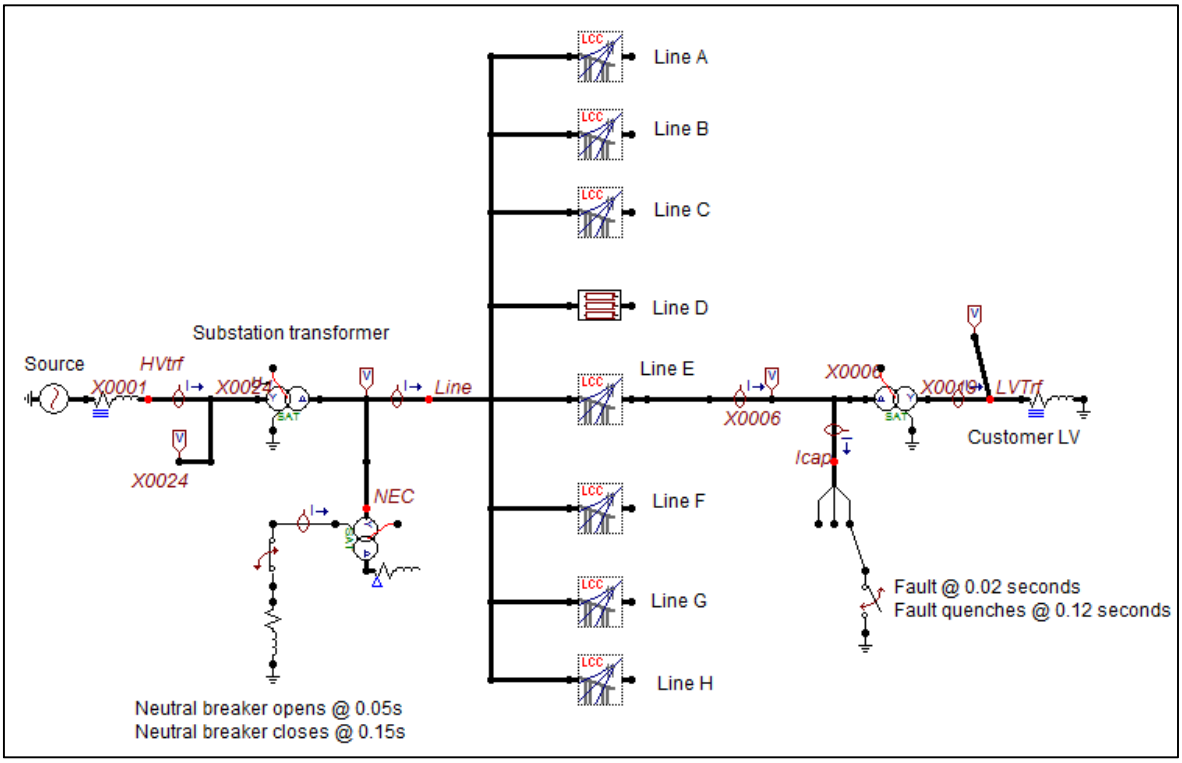

Figure 6-4 ATPdraw model of the neutral breaker scheme

The model shown in Figure 6-4 was created to replicate Thabong East substation - where the scheme will be installed. The overhead lines at Thabong East substation have a combined length of approximately 195 km and an underground cable length of 5.7 km. The capacitive current measured during the simulation was 15.1 A (rms) and is shown in Figure 6-5. Note that the capacitive current is measured during the period where the MV network is temporarily ungrounded.

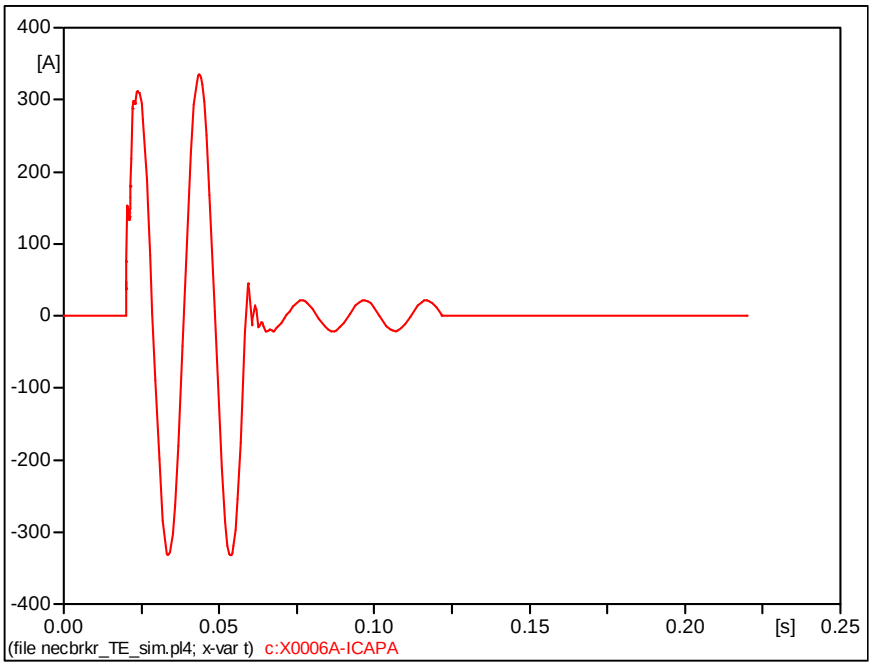

Figure 6-5 Capacitive current flowing during the ungrounding of the ATPDraw model – 15.1 A rms

The contribution of the 5.7 km underground cable towards the capacitive current is quite significant. In this case, the section of underground cable is responsible for approximately 60% of the total capacitive current, which is similar to results obtained by Määttä [47]. This is primarily due to the short distance between the cores of the cable as compared to the distances between the phase conductors of an overhead line.

The MV current and voltage waveforms at the point of the fault are shown in Figure 6-6 and Figure 6-7. Note that the voltage of the two healthy phases almost reached phase-to-phase values during the earth fault condition, as was mentioned by literature [4], [46]. It is of utmost importance to ensure that all equipment installed on the MV line is rated for phase-to-phase voltages across phase-to-earth terminals.

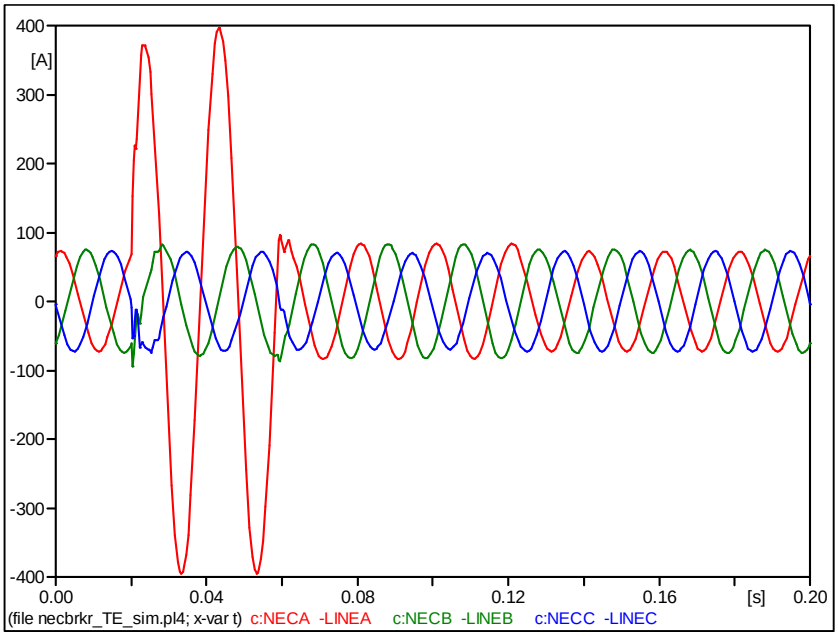

Figure 6-6 MV current waveforms of the ATPDraw model

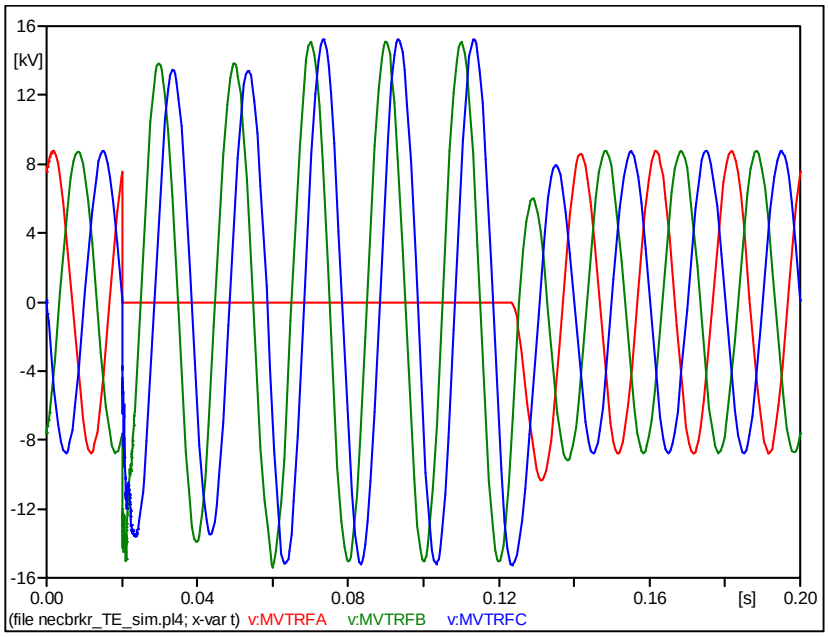

Figure 6-7 MV voltage waveforms of the ATPDraw model

The LV currents and voltages which exist on the secondary side of a Δ/Y transformer is shown in Figure 6-8 and Figure 6-9. The nominal LV phase-to-earth voltages on the secondary side of the transformer is 230 V. Note that during the period where the MV network is ungrounded it does not influence the voltages measured on the secondary side of the Δ/Y transformer.

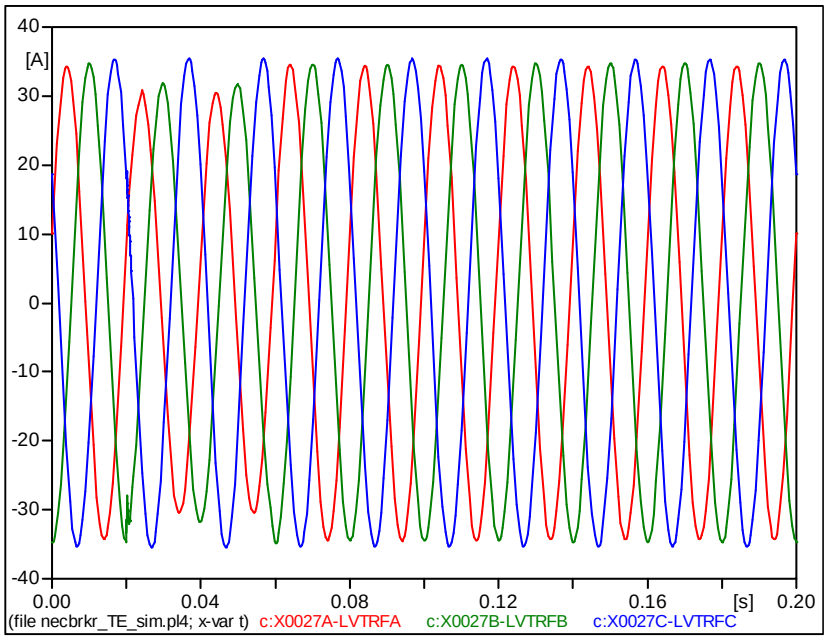

Figure 6-8 LV current waveforms of the ATPDraw model

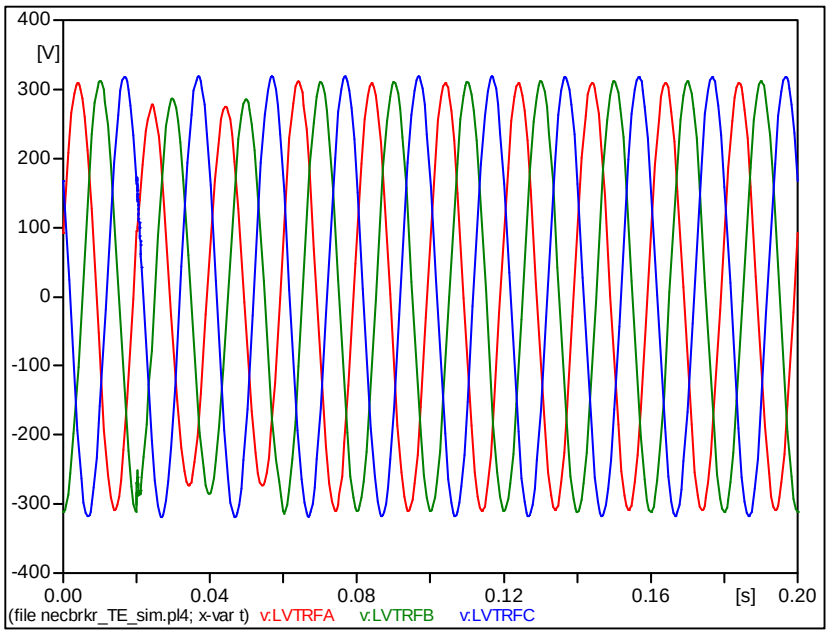

Figure 6-9 LV voltage waveforms of the ATPDraw model

During the MV earth fault condition, only a slight disturbance is noted in the LV voltage waveform as shown in Figure 6-9.

6.4.2 Single-phase breaker simulations

Figure 6-10 displays the ATPdraw integrated model of the single-phase breaker scheme. The validated MV line – and transformer models were combined to create the integrated model. A phase-to-phase fault and earth fault condition is created 20 ms into the simulation. Only the phase-A breaker is set to trip 30 ms after a fault is detected. The fault will quench 70 ms after the phase-A breaker trips, whereafter the phase-A breaker recloses. The MV operating voltage was set to be 22 kV and T-frame line models were used that are strung with Fox conductor. This model was created to replicate the Petrusburg East MV line where the scheme will be implemented.

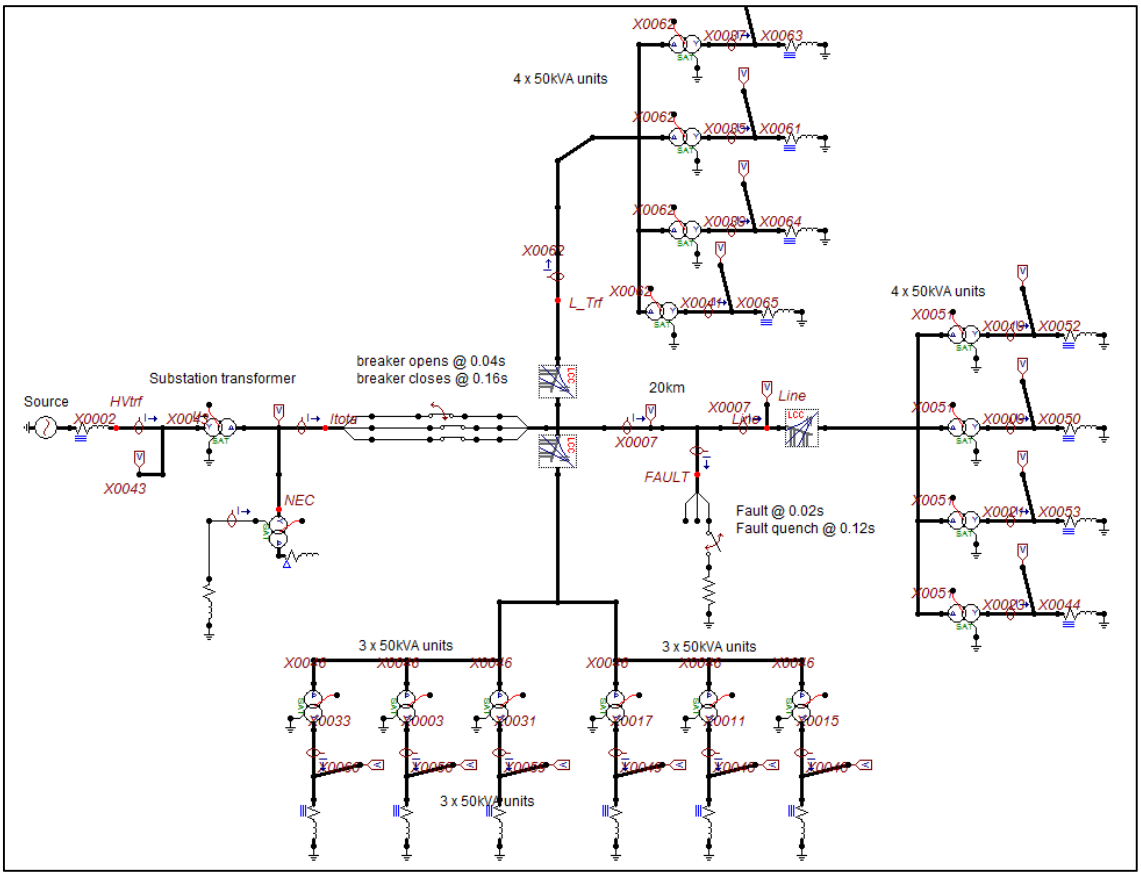

Figure 6-10 ATPdraw model of the single-phase breaker scheme with a Phase-A to Earth fault

The ATPdraw model contains fourteen 50 kVA transformers, which all operate at full load. Due to the age of the Petrusburg East line, the physical dimensions of the T-Frame structures differ from the standard, bird-friendly T-frame structures. The physical dimensions of the T-Frame structures used in the line model, including the mid-span sagging of the overhead lines are given in Table 6-10.

Table 6-10 Physical dimensions of T-frame structure model in ATPdraw

	Ph.no.	React	Rout	Resis	Horiz	Vtower	Vmid
#		[ohm/km AC]	[cm]	[ohm/km AC]	[m]	[m]	[m]
1	1	0.45	0.4185	0.86	0	8	7
2	2	0.45	0.4185	0.86	1.75	8	7
3	3	0.45	0.4185	0.86	3.5	8	7

For a phase-A to earth fault, the secondary arc current measured during the simulation was 7.4 A and the waveform is shown in Figure 6-11.

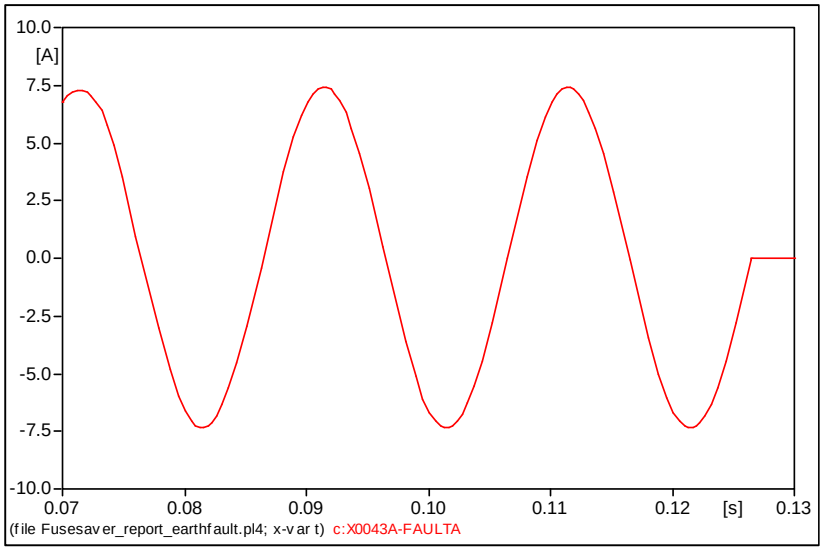

Figure 6-11 Secondary arc current measured of the ATPDraw model during earth fault condition

The MV voltage and current waveforms during the earth fault are shown in Figure 6-12 and Figure 6-13. The phase-A breaker opens 30 ms into the fault. The load current prior to the fault was approximately 17.7 A (rms) and the waveform is shown in Figure 6-14.

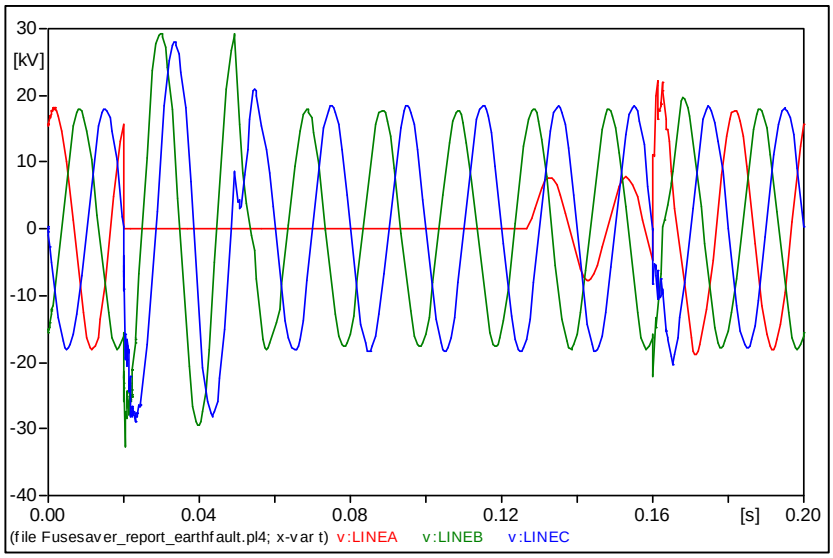

Figure 6-12 MV voltage waveforms of the ATPDraw model - Phase-A earth fault

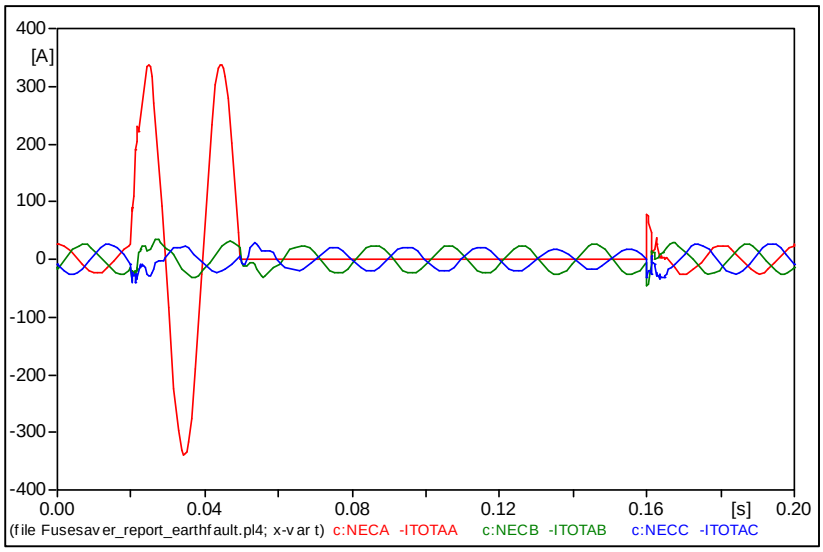

Figure 6-13 MV current waveforms of the ATPDraw model - Phase-A earth fault

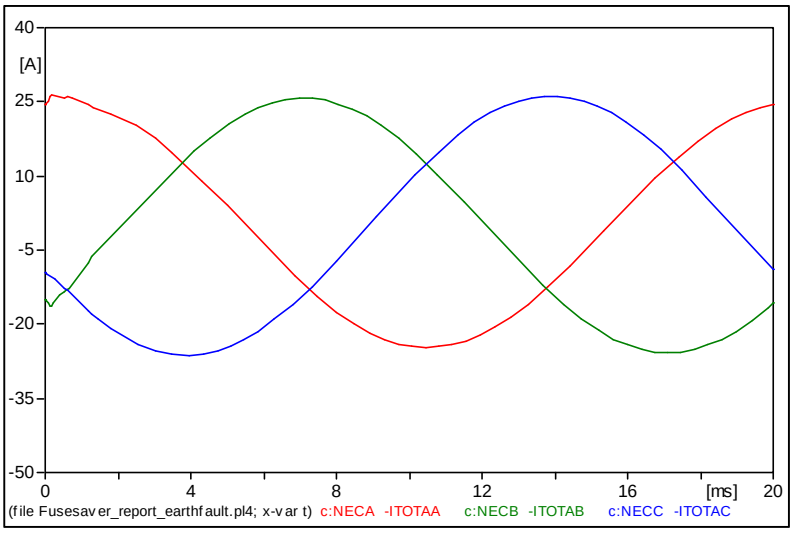

Figure 6-14 MV load current prior to the earth fault in the ATPDraw model

The LV voltages and currents which exist on the secondary side of a Δ/Y transformer during an earth fault are shown in Figure 6-15 and Figure 6-16. Note that the nominal LV phase-to-earth voltage on the secondary side of the transformer is 230 V. Even though the phase-A MV voltage is zero after the phase-A single-phase breaker trips, a reduction in only two of the phase-to-earth voltages is noted. This is a vast improvement when compared to the normal earth fault-clearing philosophy, which would have resulted in a three-second power interruption.

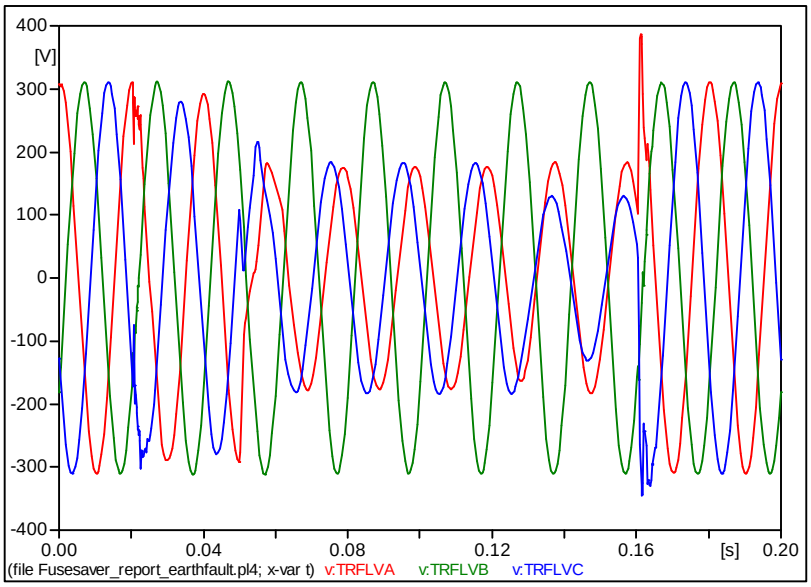

Figure 6-15 LV voltage waveforms of the ATPDraw model - Phase-to-earth fault

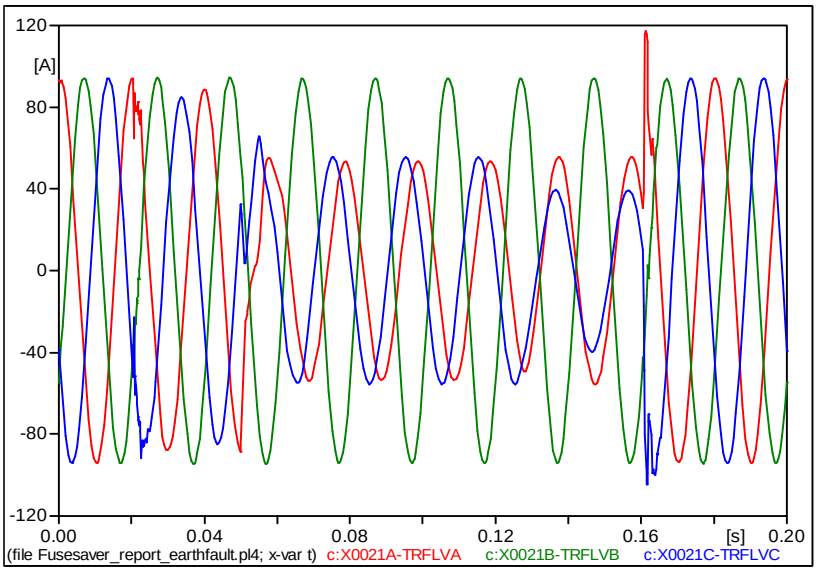

Figure 6-16 LV current waveforms of the ATPDraw model - Phase-to-earth fault

A second simulation was performed in ATPdraw for a phase-to-phase fault condition (phase-A to phase-B). The fault was created 20 ms into the simulation. Only the phase-B breaker is set to trip 30 ms after a fault is detected. The phase-to-phase fault clears 30 ms after the phase-B breaker opens, whereafter the phase-B breaker recloses. The same model shown in Figure 6-10 was used for the phase-to-phase fault simulation.

The MV voltage and current waveforms during the phase-to-phase fault is shown in Figure 6-17 and Figure 6-18.

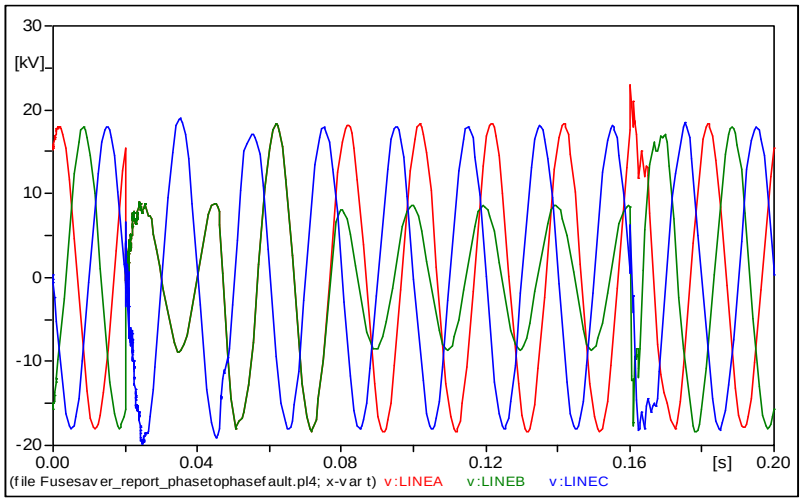

Figure 6-17 MV voltage waveforms of the ATPDraw model - Phase-to-phase fault

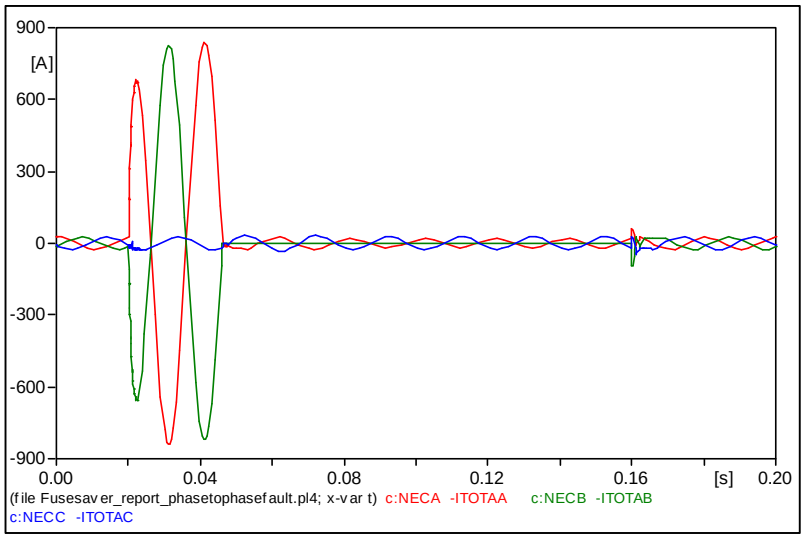

Figure 6-18 MV current waveforms of the ATPDraw model - Phase-to-phase fault

The LV voltage and current waveforms which exist on the secondary side of a Δ/Y transformer, during a phase-to-phase fault, are shown in Figure 6-19 and Figure 6-20. Note that the nominal LV phase-to-earth voltage on the secondary side of the transformer is 230 V.

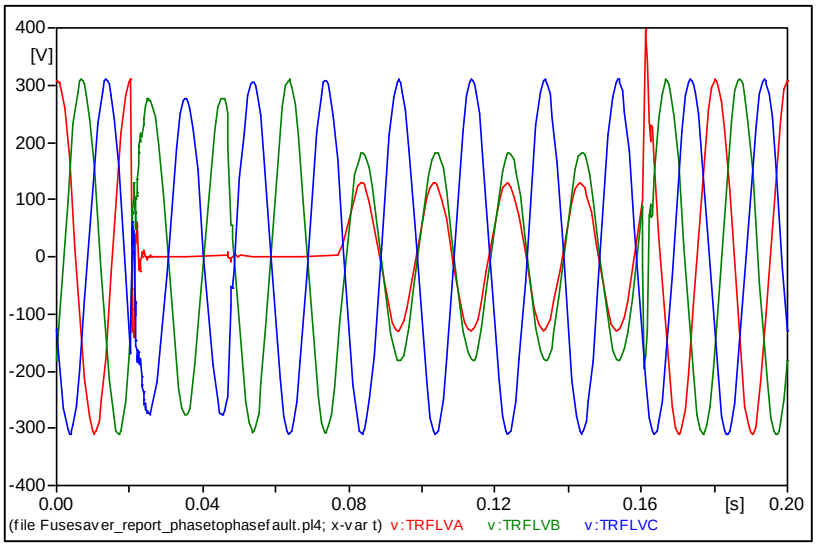

Figure 6-19 LV voltage waveforms of the ATPDraw model - Phase-to-phase fault

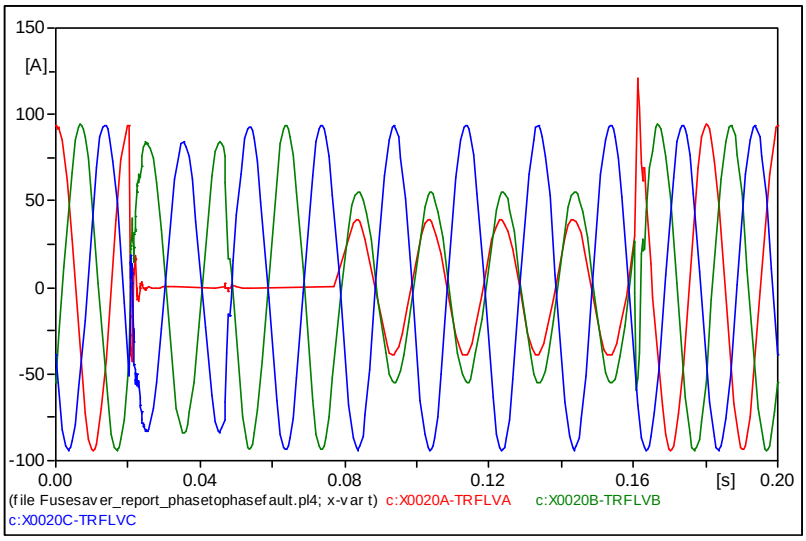

Figure 6-20 LV current waveforms of the ATPDraw model - Phase-to-phase fault

6.5 Summary – Integrated models

The neutral breaker scheme and the single-phase breaker scheme each has its own advantages and disadvantages. With regards to an earth fault condition, the neutral breaker scheme will have the least negative impact on the voltage waveforms that a customer will experience according to the simulation results. When temporarily disconnecting the MV network from earth, the voltages on the secondary side of a Δ/Y transformer might be slightly lower than normal until the E/F is cleared. Under a single-phase breaker tripping condition, two of the three LV phase voltages could drop to as low as 58% of the declared nominal voltage. However, this still affords customer plant equipment the opportunity to ride through the one-second dip when compared to a three-second power interruption.

According to the simulated results, both schemes are able to clear transient earth faults without resulting in a three-phase power outage. Only the single-phase breaker scheme is capable to clear transient phase-to-phase faults without resulting in a three-phase power outage.

The primary factor that determines the success rate of the neutral breaker scheme is the magnitude of capacitive current flowing when MV network is ungrounded. Although there is also capacitive current present with regards to the operation of the single-phase breaker scheme, it is to a lesser extent. The primary factor influencing the success rate of the single-phase breaker scheme is the amount of current being back fed into the fault, through the Δ/Y transformers.

--- Chapter 7 ---

Measured results

In order to verify and validate the simulated results of the integrated models, both schemes were installed on MV networks. The testing of the schemes involved creating faults on overhead MV lines. A number of continuous logging QOS waveform recorders were installed during each test at different locations in order to obtain all the required data.

Three sets of tests were conducted to evaluate the neutral breaker scheme. A permanent earth fault was created in order to determine whether the scheme protection philosophy functions and integrates correctly with other breakers in the same network. A transient earth fault was also created in order to determine how fast such a fault quenches. Lastly, a phase-to-phase fault was created in order to determine whether the neutral breaker is able to clear a phase-to-phase fault condition.

Two sets of tests were conducted to evaluate the single-phase breaker scheme. A transient earth fault condition was created in order to determine how fast the fault current can be cleared. A transient phase-to-phase fault condition was also created in order to determine how fast the fault current can be cleared by only opening one of the two affected phases.

7.1 Neutral breaker tests

7.1.1 Test site layout

The neutral breaker tests were performed by placing one of the existing MV breakers on bypass. The E/F was created on the secondary side of a bypassed breaker to ensure the continuity of supply to the customers during the testing of the neutral breaker scheme. A second advantage was that the breaker could be closed remotely onto the created E/F. This reduces the risk of an operator being exposed to step and touch potentials in the case where the breaker is closed manually. A continuous logging QOS recorder was installed on the MV busbars of the substation and the transformer MV CTs were used to measure the fault current during the test as shown in Figure 7-1.

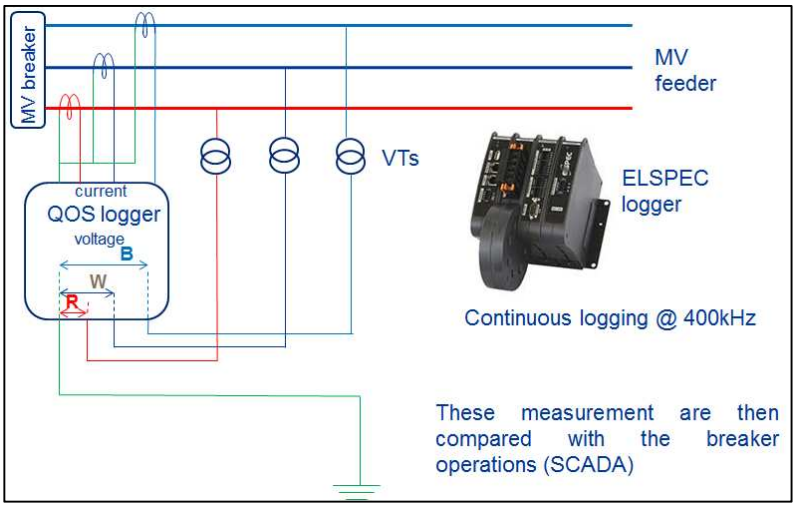

Figure 7-1 Setup of QOS recorder at substation

A second continuous logging QOS recorder was installed at the breaker where the E/F was simulated. The voltage of the overhead line was measured by means of a voltage divider as shown in Figure 7-2. Two resistors were used to step the high voltage down to a measurable 110 V. The earth fault current was measured by using a rogowski coil.

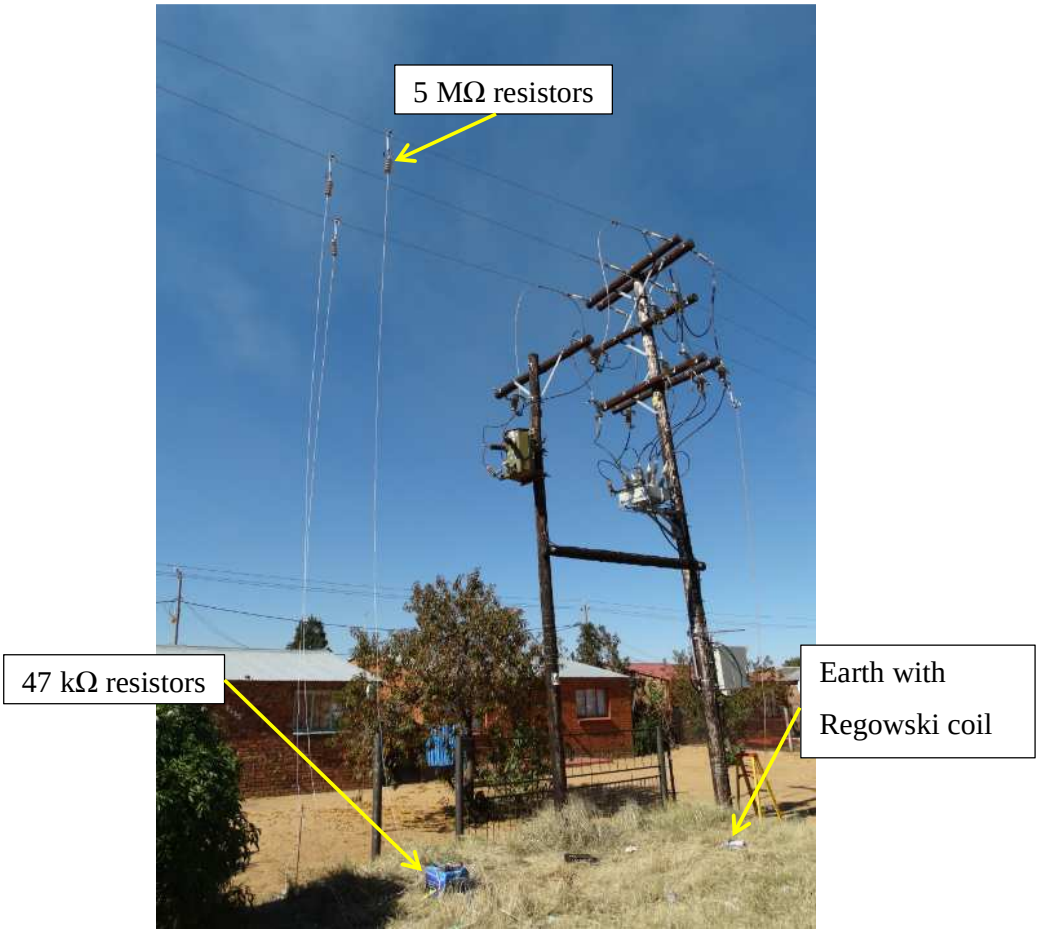

Figure 7-2 Photo of field test setup including the QOS logger and voltage divider

In order to create a temporary earth fault condition, a thin piece of wire was spanned across the sheds of a 22 kV insulator. The one end of the insulator was connected to one of the MV overhead conductor phases. The other end of the insulator was connected to the crow foot earthing arrangement of the breaker installation. This was done in order to ensure that the earthing resistance is kept as low as possible to reduce the risks of step and touch potential.

When closing the breaker onto the fault, the thin wire spanned across the insulator burns off immediately, resulting in an electrical arc forming. The electric arc bridges the insulator and will only quench if the secondary arc current is below 35 A in an ungrounded network [5]. An overview of this setup is shown in Figure 7-3.

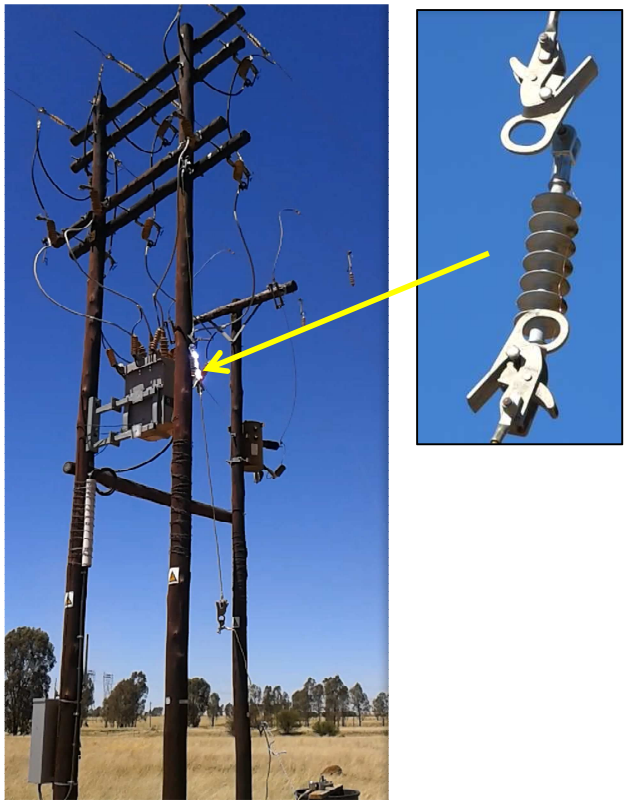

Figure 7-3 MV insulator with thin copper wire across sheds to initiate earth fault

7.1.2 Tests performed

Three sets of tests were performed to ensure that the neutral breaker scheme functions correctly with regards to:

- Transient earth fault
- Permanent earth fault
- Phase-to-phase fault

In principle, for an earth fault current (10 A or higher) on the MV network, the neutral breaker trips instantaneously and remains in the open position for two-seconds. During this time the earth fault should clear if the fault is temporary in nature. After this, the neutral breaker closes and remains in the closed position for 60 seconds to allow normal system protection to operate and isolate the fault in the case of a permanent fault on the MV network.

7.1.3 Commissioning test results

When creating the transient phase-to-earth fault on the Repeater 11 kV line, which is supplied from Theunissen Munic substation, the neutral breaker cleared the fault successfully before any other breaker on the MV line tripped for the fault. Figure 7-4 shows the voltage- and current waveform measured at the substation and Figure 7-5 shows the voltage- and current waveform measured at the fault location on the line.

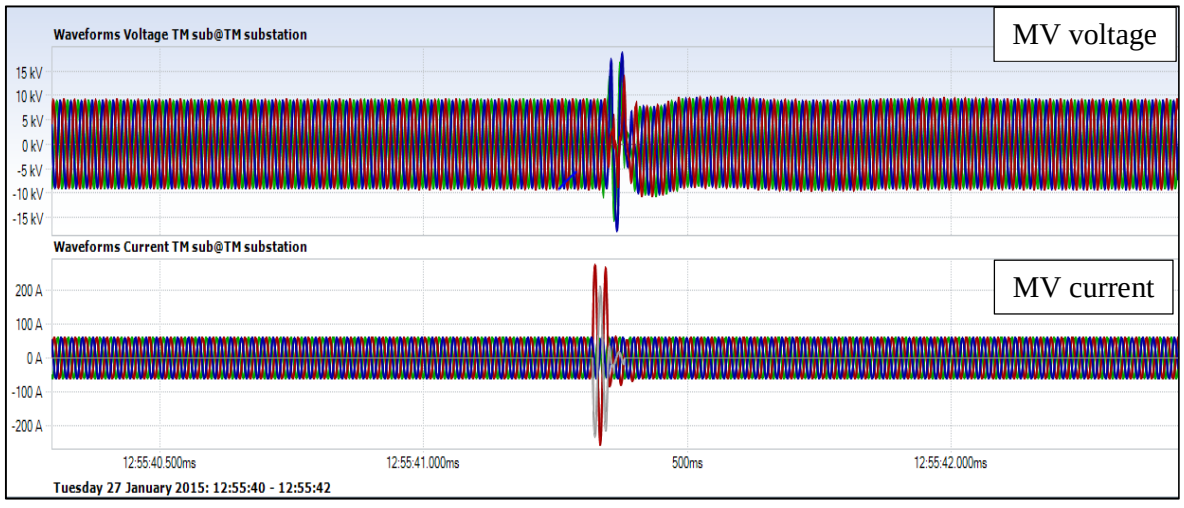

Figure 7-4 Transient earth fault cleared by neutral breaker on TGPO line (voltage and current waveforms measured at substation)

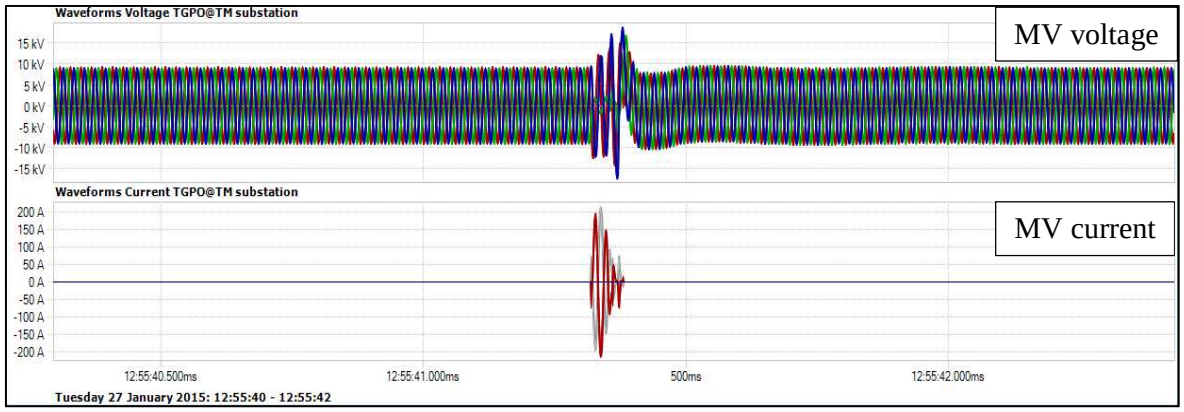

Figure 7-5 Transient earth fault cleared by neutral breaker on TGPO line (voltage and current waveforms measured at fault location)

Figure 7-6 below shows the earth fault event in more detail, as measured at the fault location. The earth fault cleared in approximately 60 ms. The voltages of the two healthy phases rise as the E/F fault starts. The neutral breaker opens approximately 30 ms after the fault starts and temporarily unearths the MV network for two-seconds. As the neutral reference point shifts, full phase-to-phase voltages can be measured across phase-to-earth terminals up until the arc quenches [4].

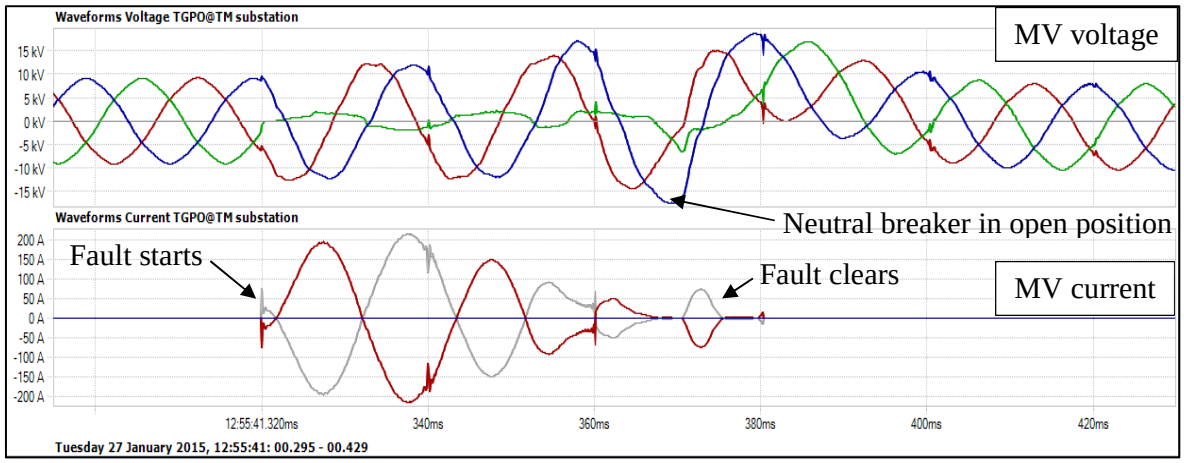

Figure 7-6 Waveforms of transient fault (measured at fault location)

A video camera with a recording rate of 60 frames per second was used to visually record the earth fault event. Figure 7-7 shows three consecutive frames from the video recording that is displayed below the measured waveforms of the transient fault event.

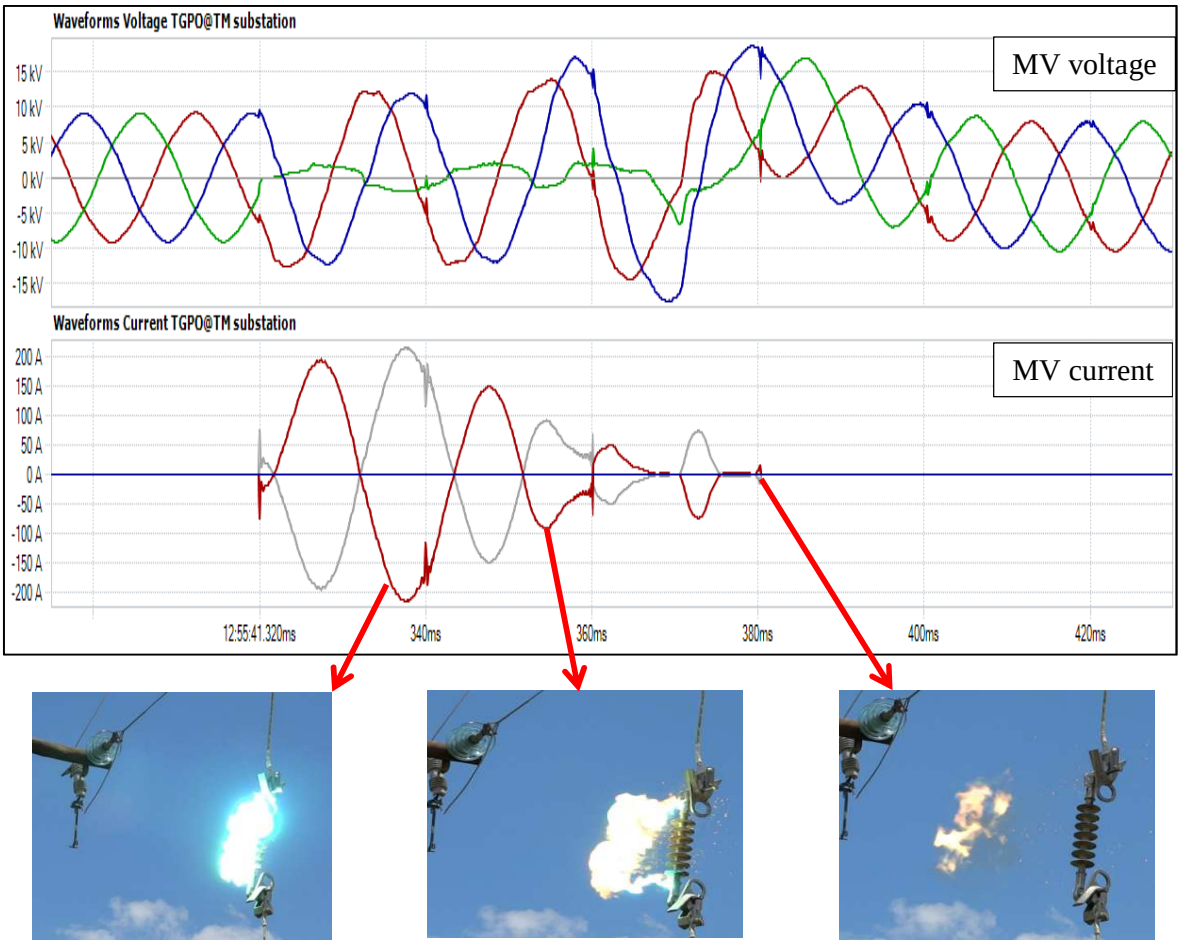

Figure 7-7 Detailed waveforms of transient fault condition with electric arc

The breaker where the E/F occurred was programmed with the protection settings in Table 7-1:

Table 7-1 E/F protection settings of breaker at TGPO97-71-2

E/F protection parameter	Value
Time multiplier	0.1
Pickup current	30 A
Protection curve	Standard Inverse - IMDT

For an earth fault current of 144 A, the calculated trip time of the breaker at TGPO97-71-2 is 475 ms. The calculated trip time is the sum of the IDMT protection trip time plus the 30 ms it takes for the breaker mechanism to physically open. The neutral breaker fault-clearing time of 60 ms is a vast improvement when compared to the conventional 475 ms fault-clearing time.

A similar test was performed where a transient E/F was created on a 22 kV network. Figure 7-8 shows the voltage and current waveforms measured at the substation and also the LV voltage waveform measured at the customer point of supply. The neutral breaker opens approximately

50 ms after the earth fault starts and unearths the network for two-seconds. While the MV network is temporarily ungrounded nominal system voltage is measured on the secondary side of the Δ/Y transformers in the electrical network.

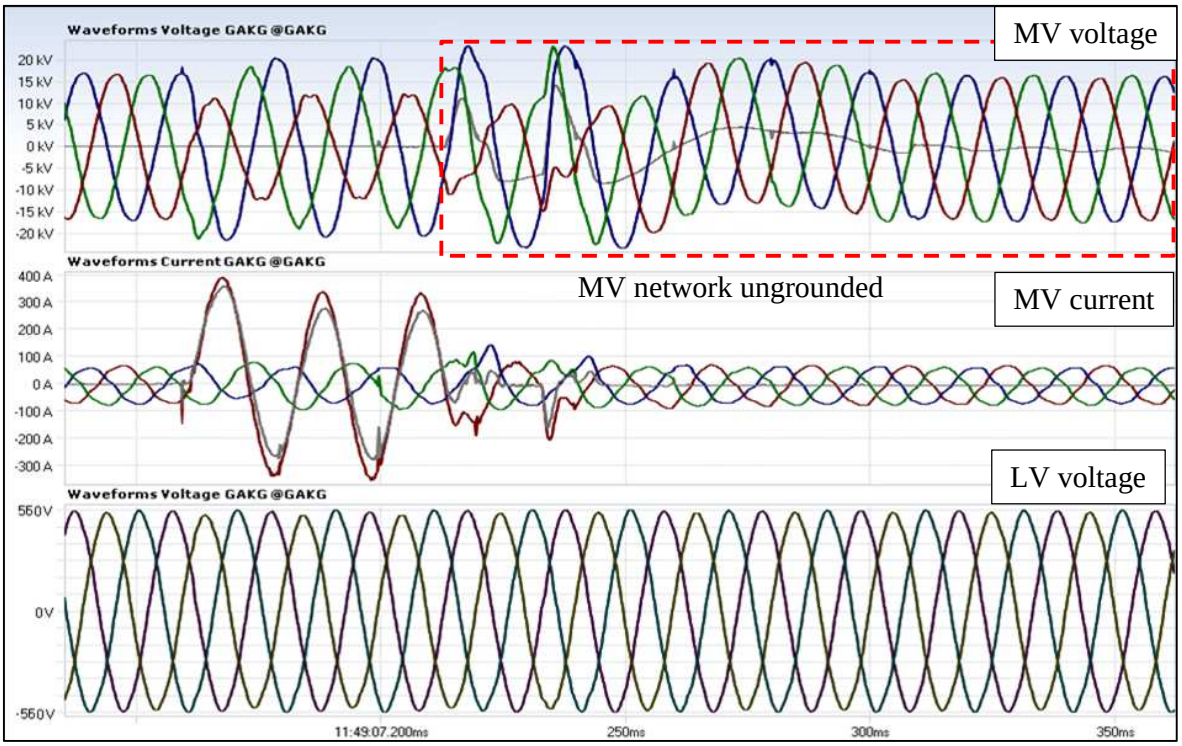

Figure 7-8 Transient earth fault cleared by neutral breaker

When creating the permanent phase-to-earth fault on the Repeater 11 kV line, which is supplied from Theunissen Munic substation, the neutral breaker protection scheme functioned correctly. The neutral breaker tripped for the E/F and remained in the open position for two-seconds, where after it closed again. After reclosing, the neutral breaker remained in the closed position for 60 seconds, enabling the TGPO97-71-2 line breaker to trip and isolate the permanent E/F. The voltage and current waveforms recorded during the permanent earth fault event are shown in Figure 7-9.

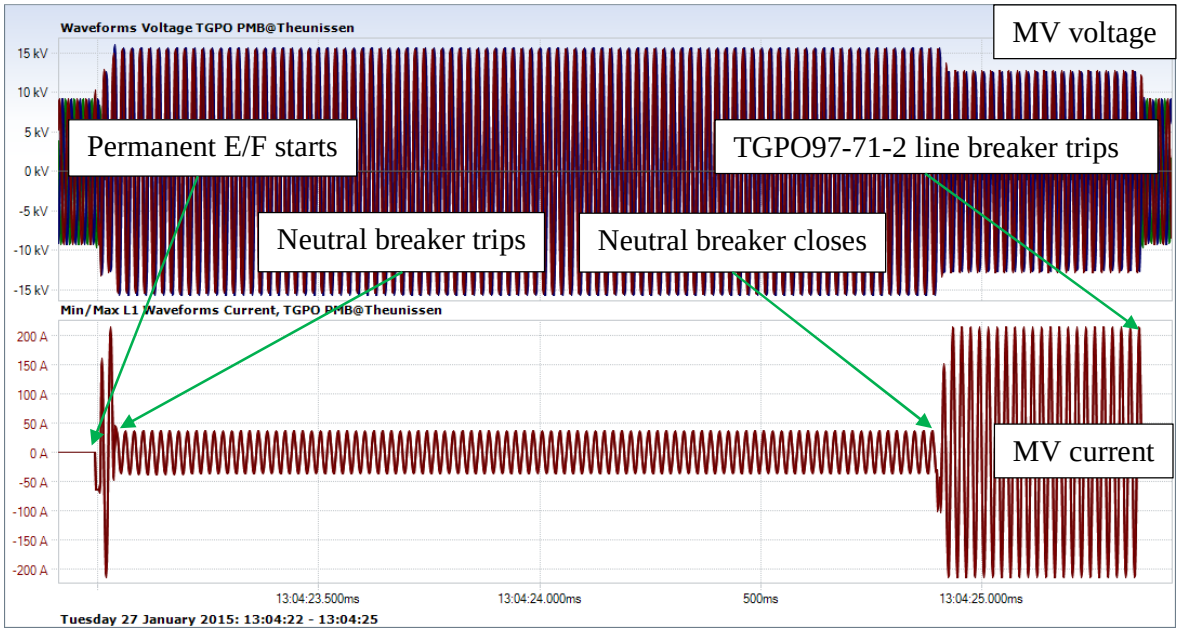

Figure 7-9 Permanent earth fault on the 11 kV Repeater line

During a phase-to-phase fault, the neutral breaker scheme can only attempt to clear the earth fault component. The phase-to-phase fault current is not influenced by the tripping of the neutral breaker. Such a recorded event is shown in Figure 7-10. The phase-to-phase fault was cleared by one of the line breakers located at TBP140-3 on the Brandfort pumps 11 kV line, supplied from Theunissen Munic substation.

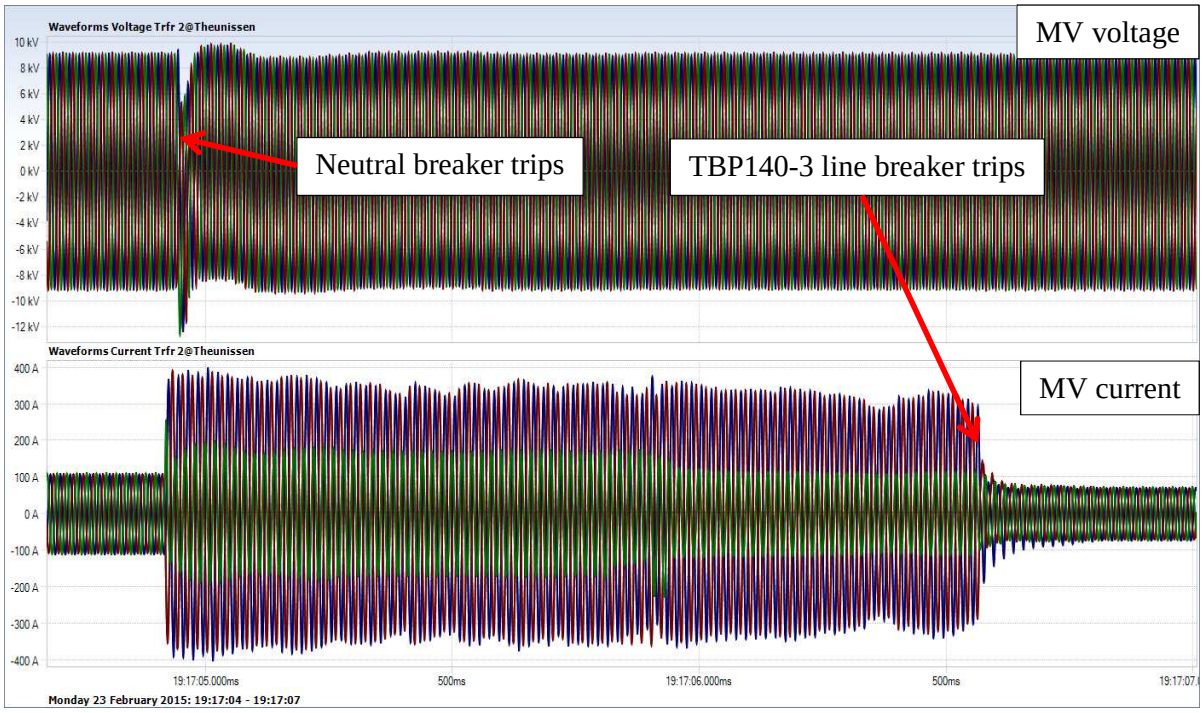

Figure 7-10 Phase-to-phase fault - not cleared by neutral breaker

7.2 Single-phase breaker tests

7.2.1 Test site layout

The single-phase breaker tests were performed by placing one of the existing MV breakers on bypass. Both the E/F and phase-to-phase faults were created on the secondary side of the bypassed breaker. A continuous logging QOS recorder was installed on the MV busbar of the substation and the transformer MV CT's were used to measure the current during the test.

A second continuous logging QOS recorder was installed at the point where the faults were created. The fault current was measured by means of Rogowski coils. A third continuous logging QOS recorder was also installed in a LV meter kiosk to monitor the LV voltage waveforms at the customer point of supply.

In order to create a temporary phase-to-phase fault, the same process was followed as with the neutral breaker scheme. A thin piece of wire was spanned across the sheds of a 22 kV insulator to create a temporary phase-to-phase fault. The insulator was connected between two MV overhead line phases, on the secondary side of the bypassed breaker.

When closing the breaker onto the fault, the thin wire bridging the insulator burns off immediately, causing an electrical arc to form. The electrical arc easily bridges the sheds of the insulator and will only quench if the secondary arc current is low enough. An overview of this setup is shown in Figure 7-11.

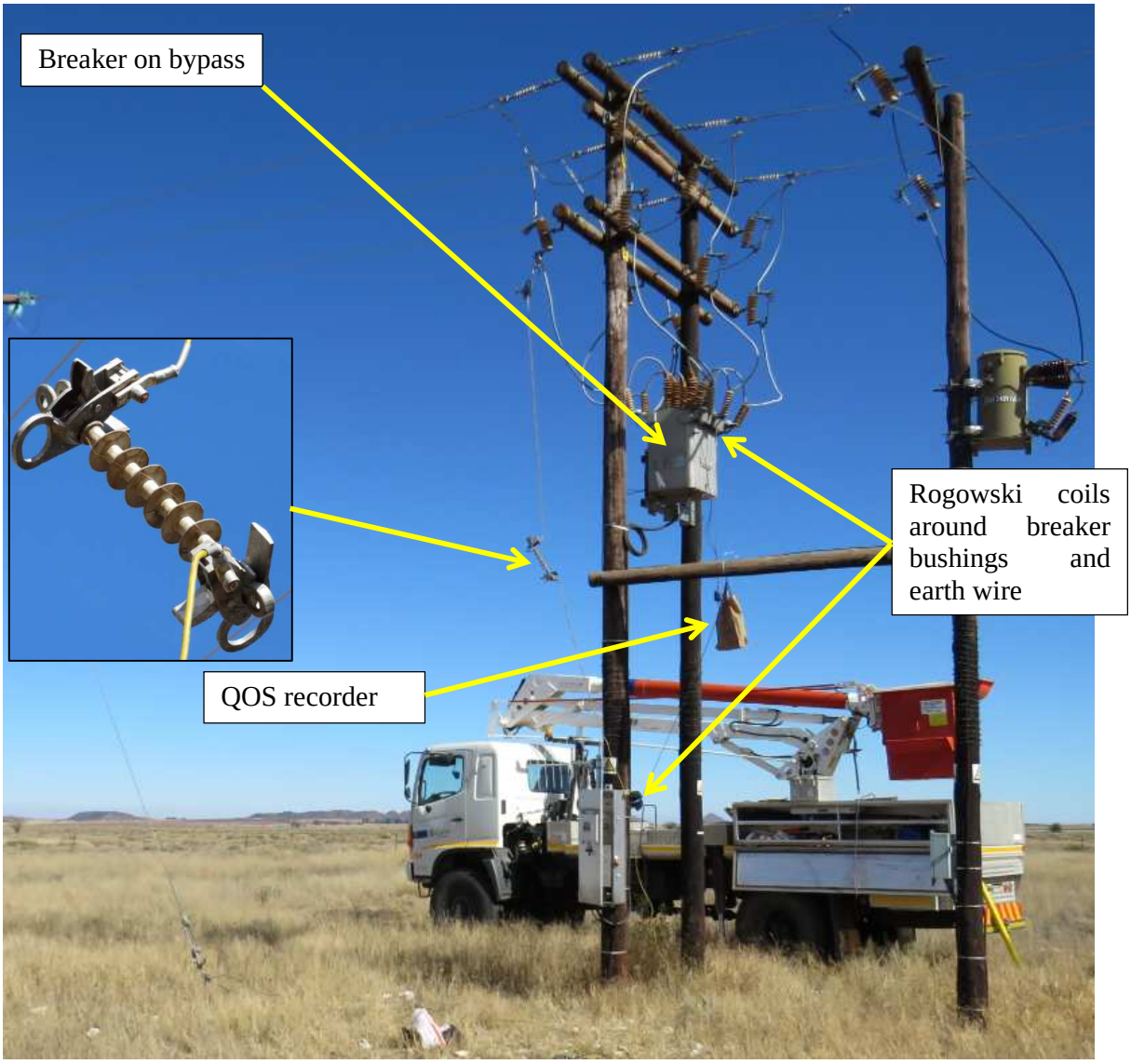

Figure 7-11 MV insulator with thin wire across insulator to initiate transient earth fault

7.2.2 Tests performed

Two sets of tests were performed to ensure that the single-phase breaker protection scheme operates correctly during:

- Transient earth faults
- Transient phase-to-phase faults

In principle, for an earth fault or phase-to-phase fault (80 A or higher), the respective single-phase breaker must trip instantaneously and remain in the open position for one-second. During this period the transient fault should quench, provided that the secondary arc current is low enough [4], [5]. After the single-phase breaker closes it remains in the closed position for 60 seconds before being able to trip again. This time allows normal system protection to operate and isolate the permanent fault from the MV network.

7.2.3 Commissioning test results – Transient earth fault

When creating a transient earth fault on the Petrusburg East 22 kV line, which is supplied by Petrusburg substation, the phase-A breaker cleared the fault successfully. The voltage and current waveforms recorded during the earth fault event are shown in Figure 7-12. The first and second waveform is the MV voltage and current measured at the substation and the last waveform is the voltage measured on the secondary side of a Δ/Y transformer.

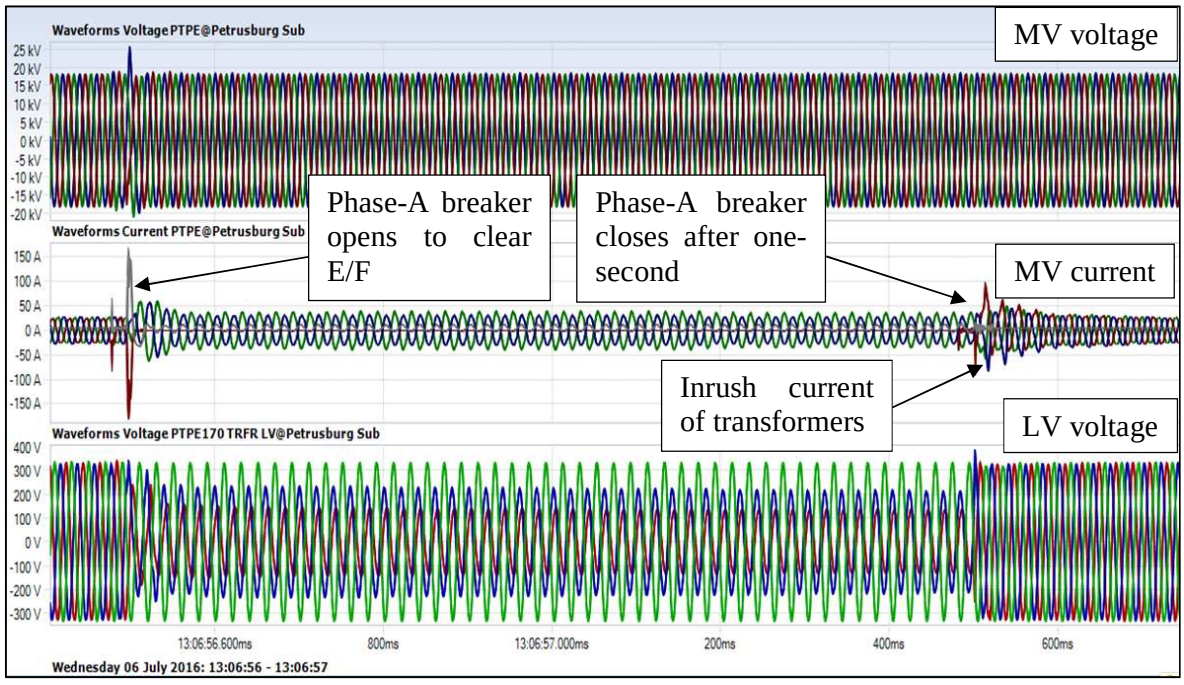

Figure 7-12 Transient fault cleared by single-phase breaker on PTPE line

Figure 7-13 shows a more detailed view of the earth fault and it can be seen that the earth fault clears within 10 ms.

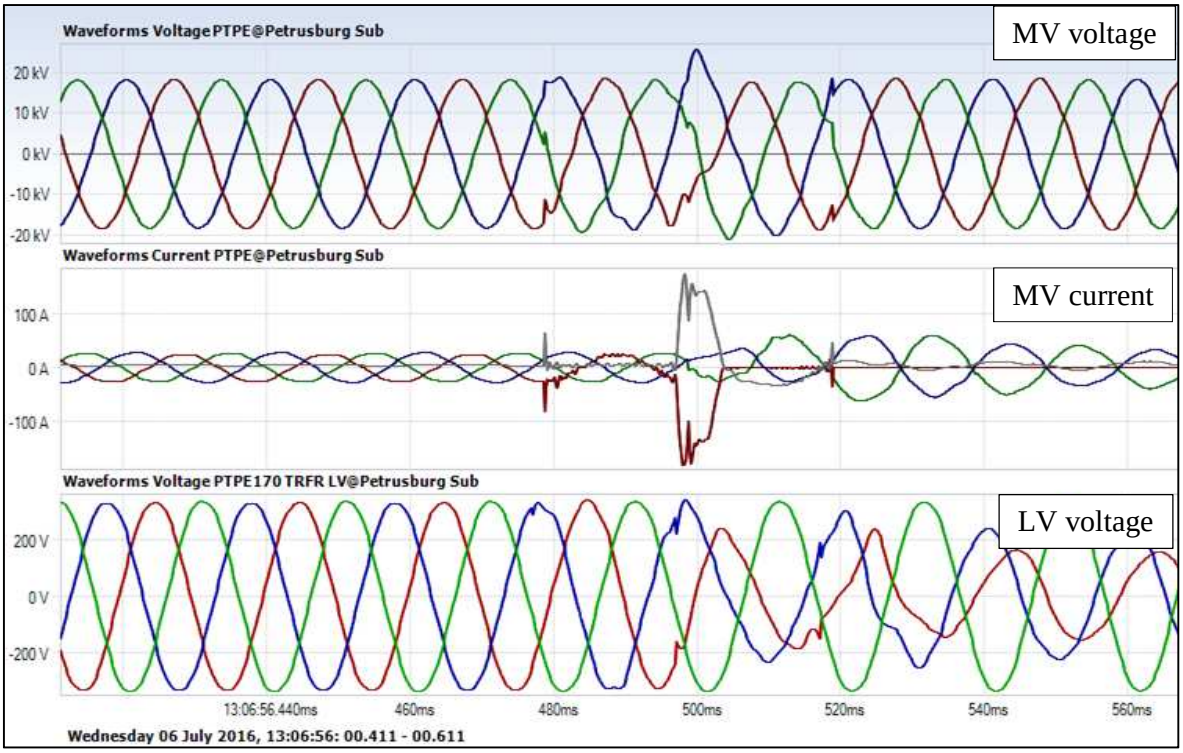

Figure 7-13 Waveforms of transient fault showing that fault current cleared within 10 ms

Figure 7-14 shows the recorded MV voltage waveform and sum of the transformer feedback current measured at the substation while the phase-A single-phase breaker is in the open position for one-second. Figure 7-14 also includes voltage measured on the secondary side of a Δ/Y transformer.

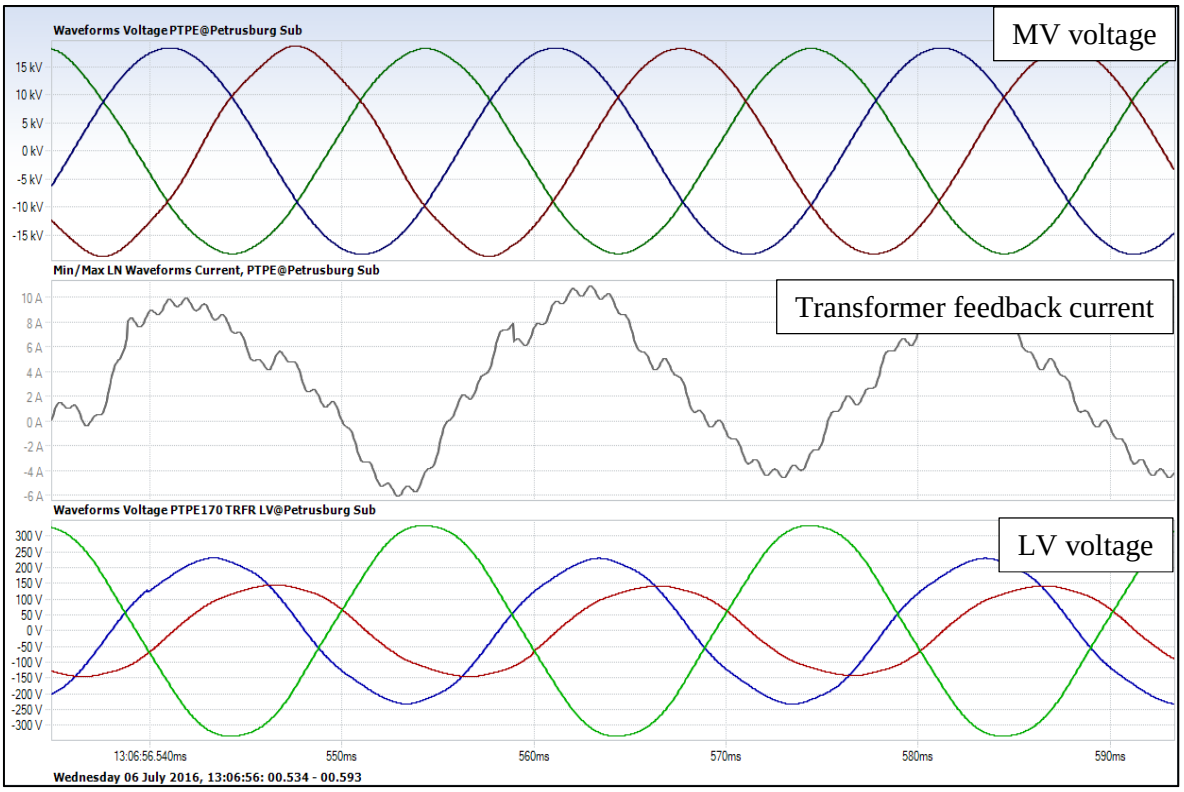

Figure 7-14 Voltage and current waveforms while phase-A breaker is open for one-second

The recordings in Figure 7-12 and Figure 7-13 indicate that the earth fault was cleared in approximately 10 ms. As soon as the phase-A breaker opens for one-second, one can observe a decrease in two of the phase-to-earth LV voltages on the transformer LV side. The current due to magnetic and capacitive coupling was measured to be 5.65 A (rms) during the period when the phase-A breaker was in the open position. As soon as the breaker successfully recloses, one can observe an increase in current - which decays in a period of 60 ms. This current can be ascribed to the three-phase energising of the pole mounted transformers on the 22 kV line. A high speed video was taken of the earth fault that was created. Four consecutive frames in the video are shown on the measured fault recording in Figure 7-15.

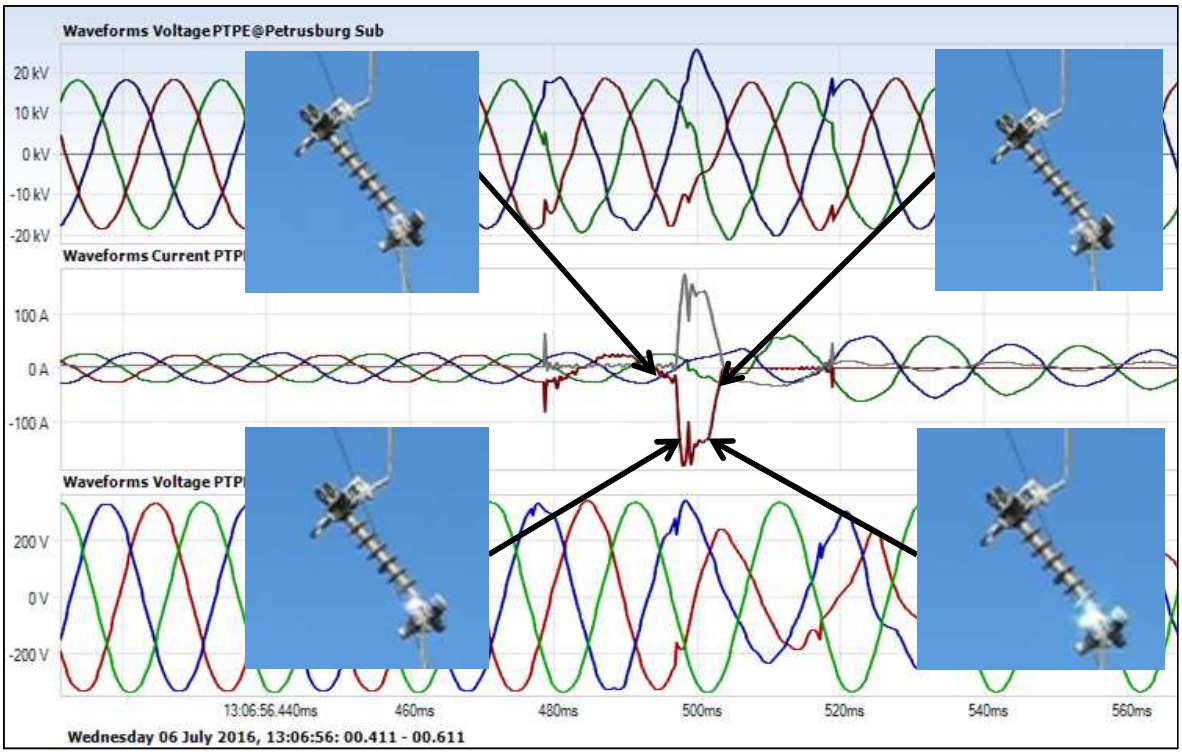

Figure 7-15 Waveforms of transient earth fault with electric arc that is barely noticeable

The breaker where the E/F occurred was programmed with the following protection settings:

Table 7-2 E/F Protection settings of breaker at PTPE168-1

E/F protection parameter	Value
Time multiplier	0.15
Pickup current	40 A
Protection curve	Standard inverse - IMDT

For an earth fault current of 130 A, the calculated trip time of the breaker at PTPE168-1 would be approximately 910 ms. The 910 ms includes the sum of the IDMT protection trip time plus the 30 ms it takes for the breaker mechanism to physically open. The single-phase breaker fault-clearing time of 10 ms is a vast improvement when compared to the conventional 910 ms fault-clearing time. The fast clearing time reduces the arcing energy quite substantially. The voltage dip that would have propagated on the neighbouring 22 kV lines for 910 ms is now limited to only 10 ms.

7.2.4 Commissioning test results – Transient phase-to-phase fault

In order to allow plant equipment to ride through a phase-to-phase fault condition, it is important that only one of the two affected single-phase breakers trip. As mentioned in Chapter 3, the phase-B breaker is set to trip faster than the other two single-phase breakers. This will ensure that the Δ/Y transformers still receive normal system supply on two of the three phases. When creating a transient phase-A to phase-B fault on the Petrusburg East 22 kV line, only the phase-B breaker trips. The tripping of only the phase-B single-phase breaker clears the phase-to-phase fault successfully. The voltage and current waveforms recorded during the phase-to-phase fault are shown in Figure 7-16. The recordings indicate that the phase-to-phase fault was cleared in approximately 40 ms. As soon as the phase-B breaker opens, one can observe a decrease in two of the phase-to-earth LV voltages. As soon as the breaker successfully recloses, one can observe an increase in current - which decays in a period of 60 ms. This current can be ascribed due to the three-phase energising of the pole mounted transformers on the 22 kV line.

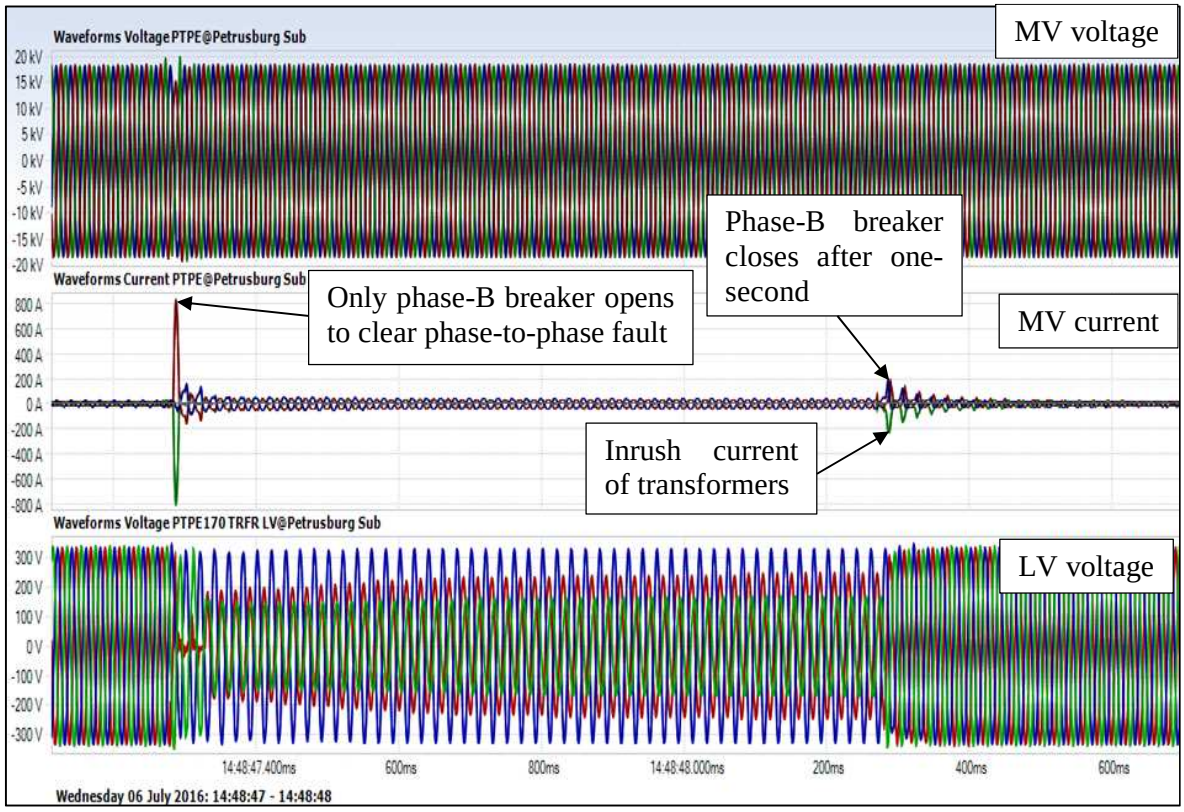

Figure 7-16 Transient phase-to-phase fault cleared by phase-B single-phase breaker on PTPE line

Figure 7-17 shows the waveforms of the phase-to-phase fault, that cleared in 40 ms, in greater detail.

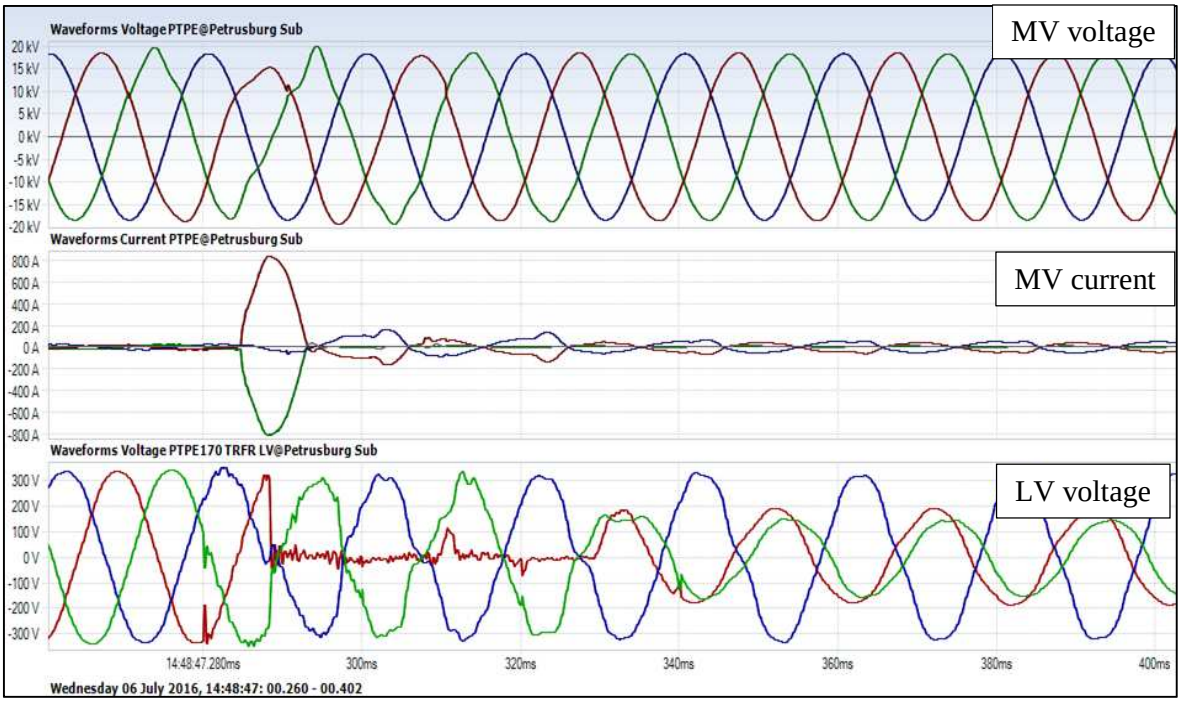

Figure 7-17 Waveforms of transient phase-to-phase fault that cleared in 40 ms

Figure 7-18 shows the recorded MV voltage waveform and transformer feedback current waveforms measured at the substation while the phase-B single-phase breaker is in the open position for one-second. Figure 7-18 also includes voltage measured on the secondary side of a Δ/Y transformer. The sum of the transformer feedback current was measured to be approximately 5 A (rms).

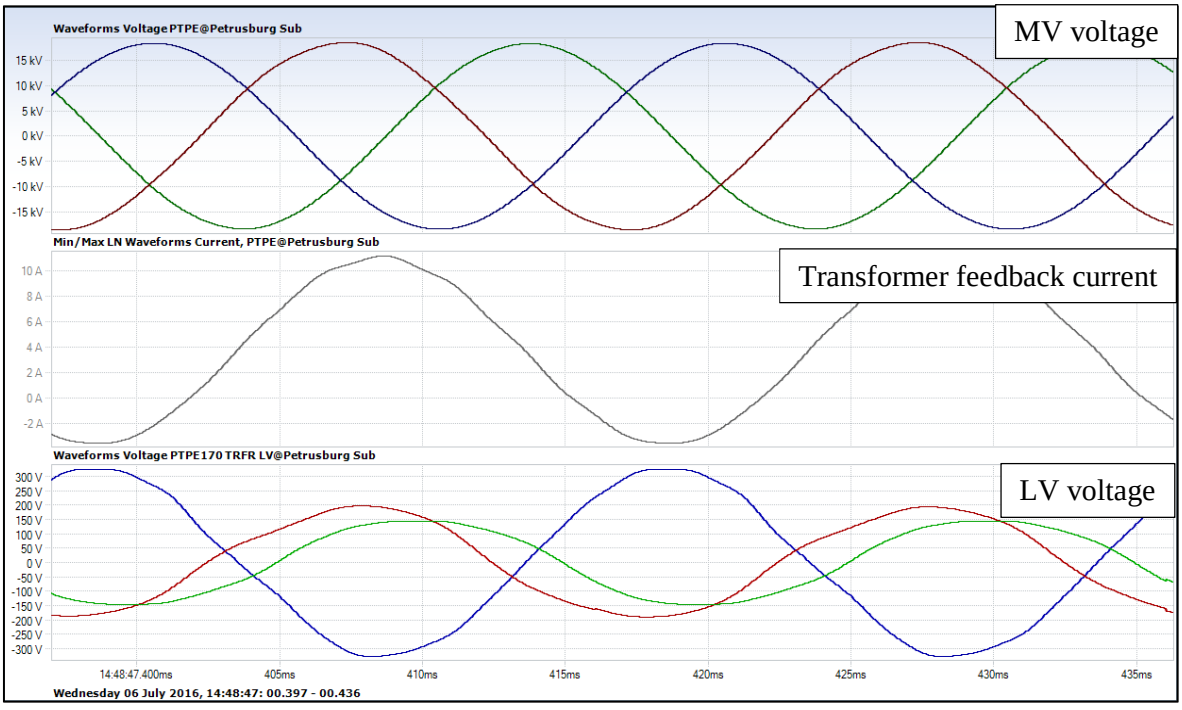

Figure 7-18 Voltage and current waveforms while phase-B breaker is open for one-second

A high-speed video was taken of the phase-to-phase fault that was created. Some of the frames in the video are shown below the measured fault recording in Figure 7-19.

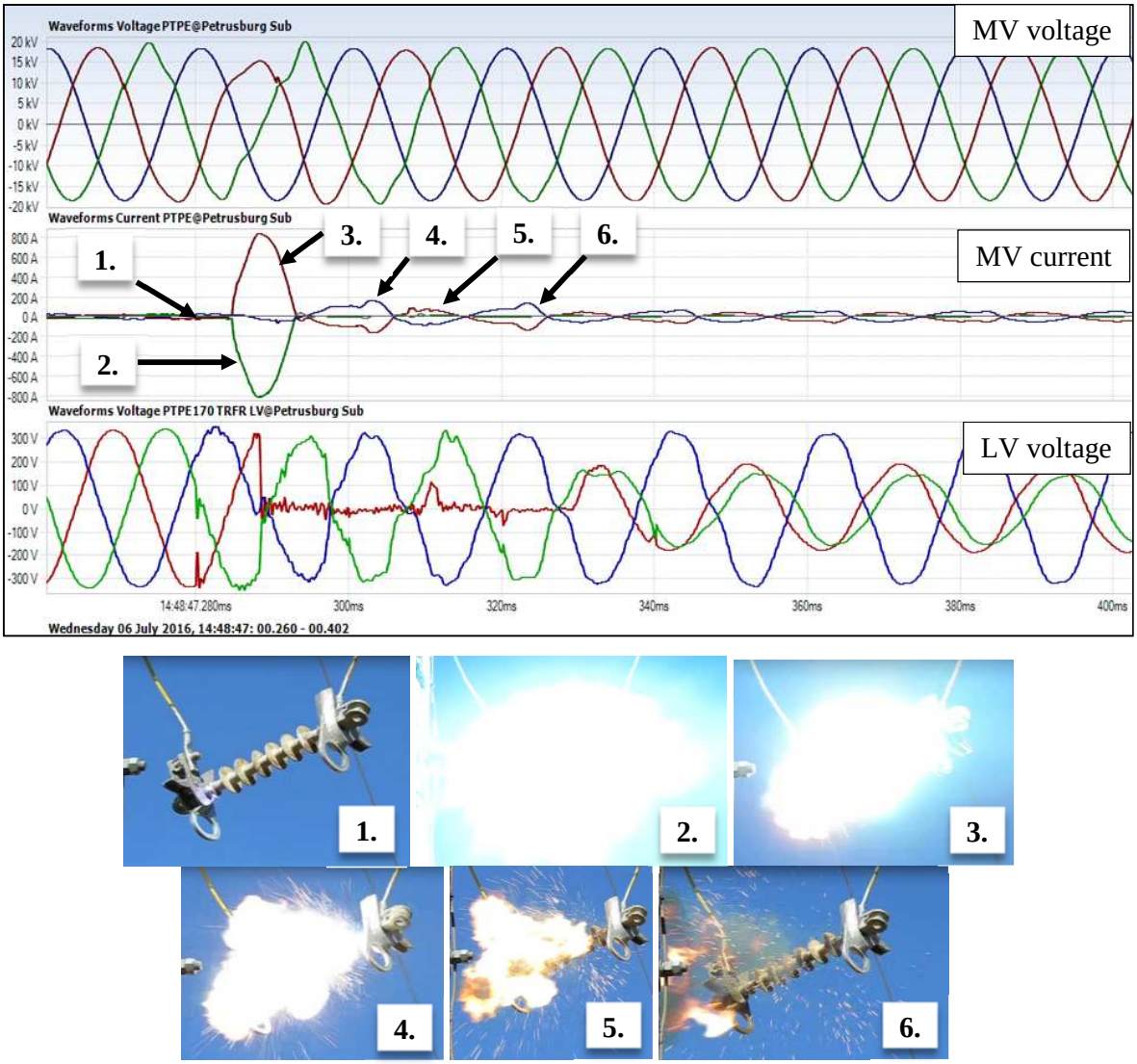

Figure 7-19 Waveforms of transient phase-to-phase fault as well as photos of the electric arc

The breaker where the fault occurred was programmed with the following protection settings:

Table 7-3 O/C protection settings of breaker at PTPE168-1

O/C protection parameter	Value
Time multiplier	0.2
Pickup current	80 A
Protection curve	Standard inverse - IMDT

For a fault current of 565 A, the calculated trip time of the breaker at PTPE168-1 would be approximately 732 ms. The 732 ms includes the sum of the IDMT protection trip time plus the 30 ms it takes for the breaker mechanism to physically open. The single-phase breaker fault-

clearing time of 40 ms is a vast improvement when compared to the conventional 732 ms fault-clearing time. The fast-clearing time reduces the arcing energy quite substantially. The voltage dip that would have propagated on the neighbouring 22 kV lines for 732 ms is now limited to only 40 ms.

7.3 Summary – Measured results

The earth fault-clearing capabilities of both the neutral – and single-phase breaker schemes prove to be very effective. While the MV network is temporarily ungrounded during the operation of the neutral breaker scheme, nominal system voltage is measured on the secondary side of the Δ/Y transformers in the network. When one of the single-phase breakers opens to clear a transient earth fault, two of the phase-to-earth LV voltages reduce by roughly 43%.

The phase-to-phase fault-clearing capability of the single-phase breaker scheme proves to be very effective. This can be ascribed to the fast fault-clearing of the scheme. Secondly, only one of the MV phases will be disconnected for one-second during a phase-to-phase fault. This is a substantial improvement compared to a conventional power interruption of a few seconds. The neutral breaker scheme does not have the capability to clear a phase-to-phase fault, however it can aid in removing the earth fault component within a multi-phase to earth fault.

Both schemes contribute to the improvement of power quality in the networks where they are installed. These schemes limit the effects of voltage dip propagation to neighbouring lines as transient faults are cleared from the MV network much faster. By implementing fast tripping in both schemes, it greatly reduces the arc energy when compared to normal IDMT protection philosophies. This fast fault-clearing time also reduces the amount of ionised air created during an electrical arc and therefore reduces the risk of a transient fault becoming a permanent fault.

The measured results from chapter 7, and simulated results from chapter 6, with regards to both schemes, correlate well. The simulated MV voltage and current waveforms match the voltage and current waveforms measured during the field testing. The simulated secondary arc current (5.3 A rms) of the single-phase breaker scheme correlates well with the measured results (5.65 A and 5 A rms). The slight difference can be ascribed to the loading difference of the MV line at the time when the fault occurred. The loading difference will influence the magnitude of the feedback current through the transformer windings into the fault. The simulated LV voltage waveforms under fault conditions also align with that of the measured results. The slight variation in the magnitude of the LV voltage waveforms can be ascribed to a difference in transformer tap positions and the loading of the transformers.

--- Chapter 8 ---

Conclusion and Recommendations

8.1 Overview

To conclude on the objective of the dissertation, Chapter 8 compares the neutral breaker and single-phase breaker schemes with each other. The comparison includes the following:

- Transient earth fault-clearing capabilities
- Transient phase-to-phase fault-clearing capabilities
- Impact on power quality
- Advantages of each scheme
- Limitations of each scheme
- Proposed locations to implement each scheme.

Chapter 8 also includes relevant recommendations that are made with regards to improving the operation of both schemes.

8.2 Conclusion

8.2.1 Neutral breaker scheme

The earth fault-clearing capabilities of the neutral breaker scheme proved to be very effective. Unfortunately, the neutral breaker scheme does not have the capability to clear a phase-to-phase fault. The scheme only aids in removing the earth fault component of a multi-phase to earth fault.

The power quality issues that the neutral breaker scheme addresses is a reduction in both momentary and sustained interruptions that are caused by earth faults. This scheme also reduces the length of a voltage dip caused by an earth fault on all lines that are connected to the same NECR. The speed with which the neutral breaker scheme trips is less than 60 ms after sensing an earth fault condition.

After the commissioning of the neutral breaker scheme at Thabong East, Thabong Bulk, Kutlwanong, Meloding and Theunissen Munic substations, the following results were obtained within the period of a year:

Table 8-1 Transient faults cleared by neutral breaker scheme

Substation name	Number of earth faults	Number of earth faults cleared by neutral breaker
Thabong Bulk 132/11 kV	27	24
Thabong East 132/11 kV	85	73
Meloding 132/11 kV	105	89
Kutlwanong 132/11 kV	29	17
Theunissen Munic 88/11 kV	45	41
Total	**291**	**244**

Figure 8-1 gives the ratio between the permanent and transient earth faults which were successfully cleared by the neutral breaker scheme.

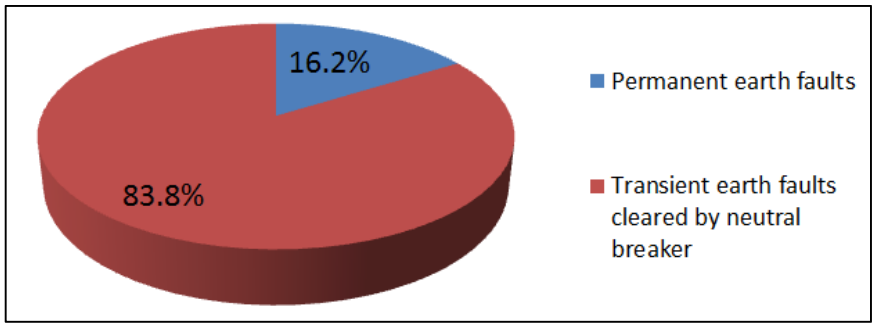

Figure 8-1 Ratio between permanent and transient earth faults cleared by neutral breaker

From the results shown in Table 8-1 and Figure 8-1, as many as 83.8% of earth faults were successfully cleared by the neutral breaker scheme without causing a momentary interruption to customers. This equates to a total of 244 less power interruptions experienced by customers. The neutral breaker scheme also significantly reduced the length of voltage dips caused by the 244 earth fault events, to as little as 60 ms. This is a vast improvement in terms of power quality and network reliability with regards to transient earth faults on MV networks.

The fast fault-clearing time of the neutral breaker scheme results in less damage caused to upstream equipment. The time it normally takes for an earth fault protection to operate for a high impedance earth fault is reduced from the seconds-range to the milliseconds-range. By implementing the neutral breaker scheme, it could reduce burn wounds on animals or humans by a factor of up to fifty times in a case where inadvertent contact was made with a live conductor.

During the earth fault condition, customers might experience a slight disturbance with regards to their LV voltage waveform for a few milliseconds. However, as soon as the transient fault

quenches, customers will experience normal system voltages on their LV network, even though the MV network might still be ungrounded for a two-seconds.

The scheme coverage of the neutral breaker includes all MV lines that are connected to the substation NECR at which the scheme is installed as schematically shown in Figure 8-2.

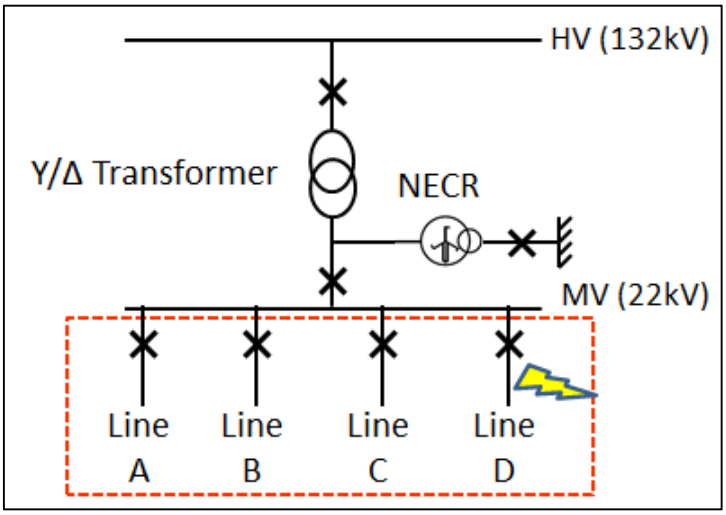

Figure 8-2 Neutral breaker scheme coverage

To ensure for the effective clearing of transient faults, it is recommended that the scheme not be installed in MV networks where the capacitive coupling current exceeds 35 A. Therefore, the sum of the overhead line lengths must not exceed 600 km for an 11 kV network, and 300 km for a 22 kV network. If cables are present within an MV network, this must be taken into account as the capacitive coupling of cables can be up to 80 times more compared to overhead lines. During the period when the neutral breaker is in the open position, the magnetic coupling of transformers that are installed on the MV lines will not influence the magnitude of the secondary arc current. The secondary arc current is dependent on the capacitive coupling current only.

8.2.2 Single-phase breaker scheme

The earth fault and phase-to-phase fault-clearing capabilities of the single-phase breaker scheme proved to be very effective. One of the factors responsible for the success of the scheme is the time in which a fault is cleared. The fast fault-clearing time of the single-phase breakers (less than 30 ms), also results in less damage being caused to upstream equipment, and equipment located at the point of the fault.

In terms of a power outage, customers who primarily utilise three-phase equipment will only experience a one-second interruption on one phase, as compared to a standard three-phase power interruption of at least three-seconds. Another advantage of this scheme is that voltage dip

propagation to parallel lines is reduced. The length of a voltage dip experienced by parallel lines is now only a few milliseconds instead of three-seconds. This allows plant equipment to ride through the voltage dip. The depth of the voltage dip cannot be altered by the implementation of this scheme. The depth of the voltage dip depends on the fault level of the electrical network.

Four months of voltage dip data was analysed at the Petrusburg substation; the focus being only on voltage dips caused by faults on the PTPE and PTDI lines. The information used to create a scatter plot was obtained from the continuous logging QOS recorder, which measured the MV busbars voltage at the substation. A summary of the voltage dips is given in Table 8-2. The voltage dip scatter plot is shown in Figure 8-3.

Table 8-2 Summary of voltage dips after implementing single-phase breaker schemes

Voltage dip category	Number of dips
Insignificant	14
Y	7
X1	3
X2	1
S	1
T	2
Z1	4
Z2	3
Total	35

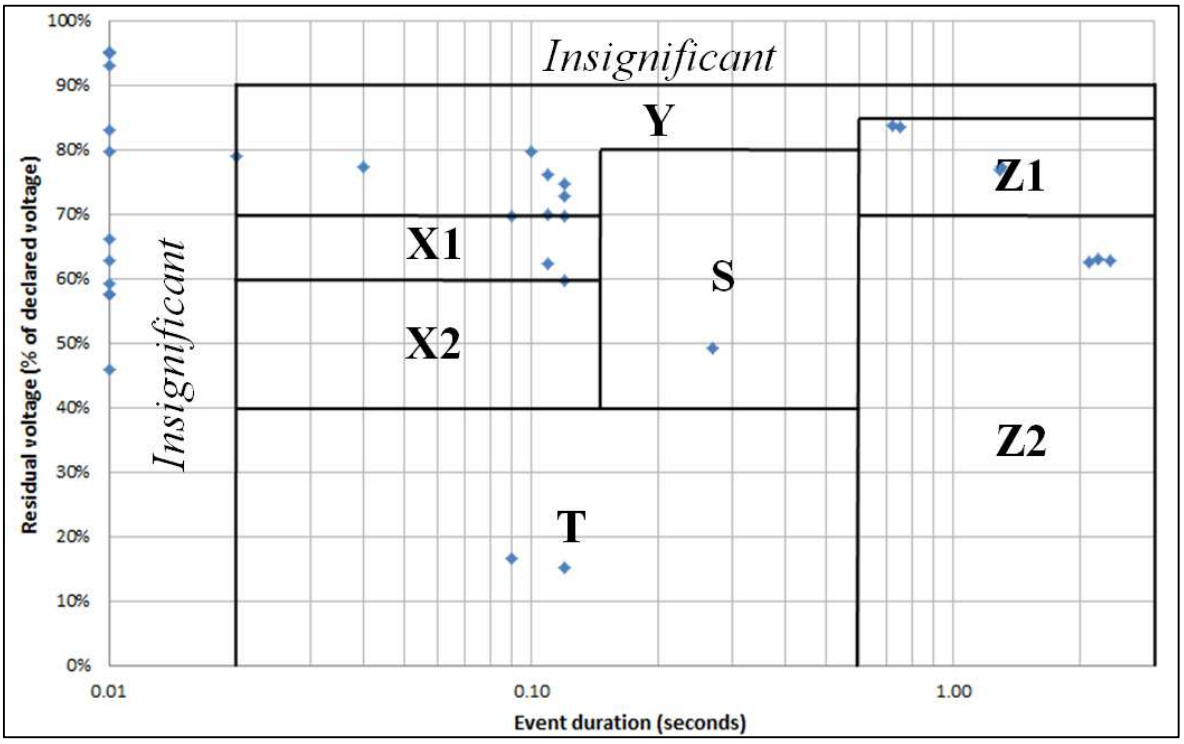

Figure 8-3 Voltage dip scatter plot at Petrusburg substation after implementing single-phase breaker scheme

One should note that 60% of all measured voltage dips can be seen as being insignificant (which includes Y-class dips). This is due to the fast fault-clearing time of the single-phase breaker scheme. The voltage dip length of 26 of the measured dips was drastically reduced by the operation of the single-phase breaker scheme that successfully cleared the transient faults. This resulted in customers not experiencing a three-second power interruption compared to the functioning of normal breaker operations. Figure 8-4 below shows the ratio between the different fault types that caused voltage dips at Petrusburg substation.

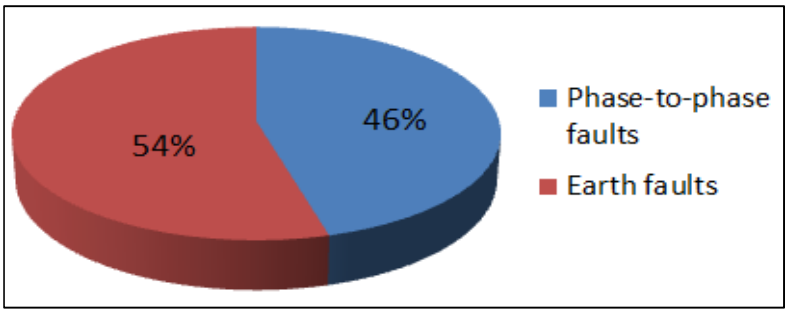

Figure 8-4 Ratio between earth – and phase-to-phase faults on PTDI and PTPE lines

Figure 8-5 shows the ratio between the permanent earth faults and transient earth faults that were cleared by the single-phase breaker scheme.

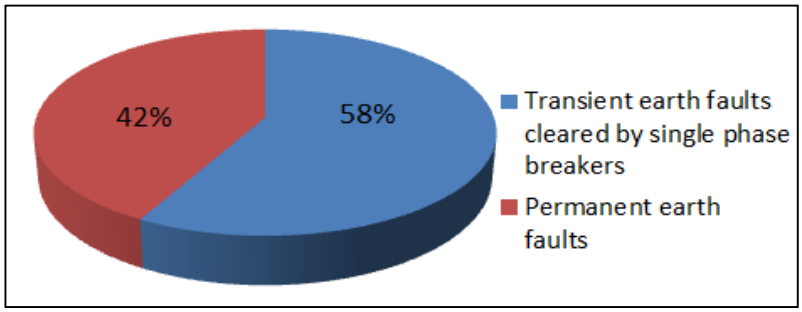

Figure 8-5 Ratio between permanent and transient earth faults cleared by single-phase breakers

Figure 8-6 shows the ratio between the permanent phase-to-phase faults and transient phase-to-phase faults that were cleared by the single-phase breaker scheme.

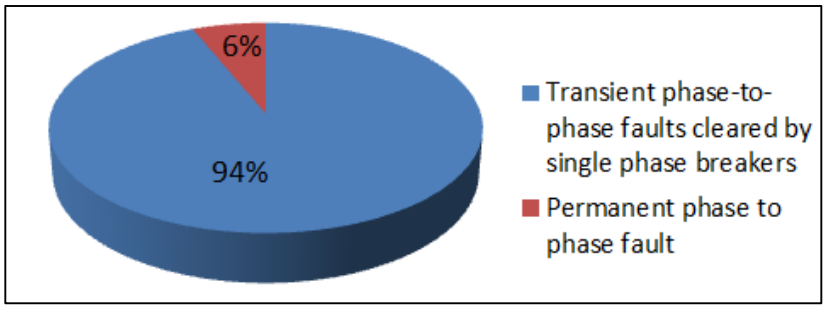

Figure 8-6 Ratio between permanent and transient phase-to-phase faults cleared by single-phase breakers

In some cases, the earth fault current magnitude was below the current pickup setting of the single-phase breaker scheme. This caused the single-phase breakers not to trip for a high impedance earth fault. Phase-to-phase faults have a higher fault current magnitude compared to earth faults, which are limited by the NECR. Therefore the single-phase breaker cleared a higher percentage of phase-to-phase faults compared to earth faults.

Another voltage dip scatter plot was created in order to determine what the voltage dip profile at the Petrusburg substation would have been if the single-phase breakers were not installed. The fault current magnitudes, substation fault levels and breaker protection settings were used to determine what the length of the voltage dips would have been. The hypothetical scatter plot is shown in Figure 8-7 with the voltage dip summary given in Table 8-3.

Table 8-3 Summary of voltage dips if single-phase breaker scheme was not implemented

Voltage dip category	Number of dips
Insignificant	4
Y	1
X1	0
X2	0
S	10
T	0
Z1	10
Z2	10
Total	35

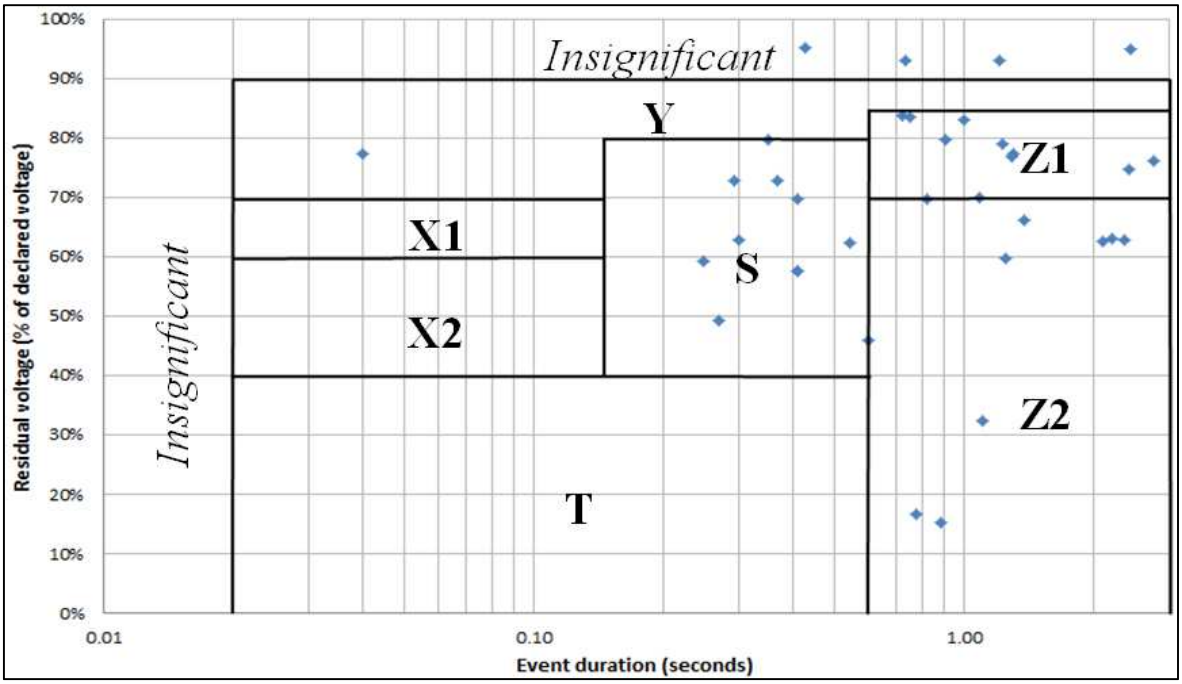

Figure 8-7 Hypothetical voltage dip scatter plot at Petrusburg substation if single-phase breaker scheme was not implemented

The measured voltage dip scatter plot of Figure 8-3 is combined with the hypothetical dip scatter plot of Figure 8-7 to illustrate the improvement of voltage dip performance. The combined dip scatter plot can be seen in Figure 8-8. Note that the blue diamond shaped markers indicate the voltage dips measured at Petrusburg substation with the single-phase breaker scheme in operation. The red square shaped markers indicate the hypothetical voltage dip scatter plot, which would have been present if the single-phase breaker scheme was not installed.

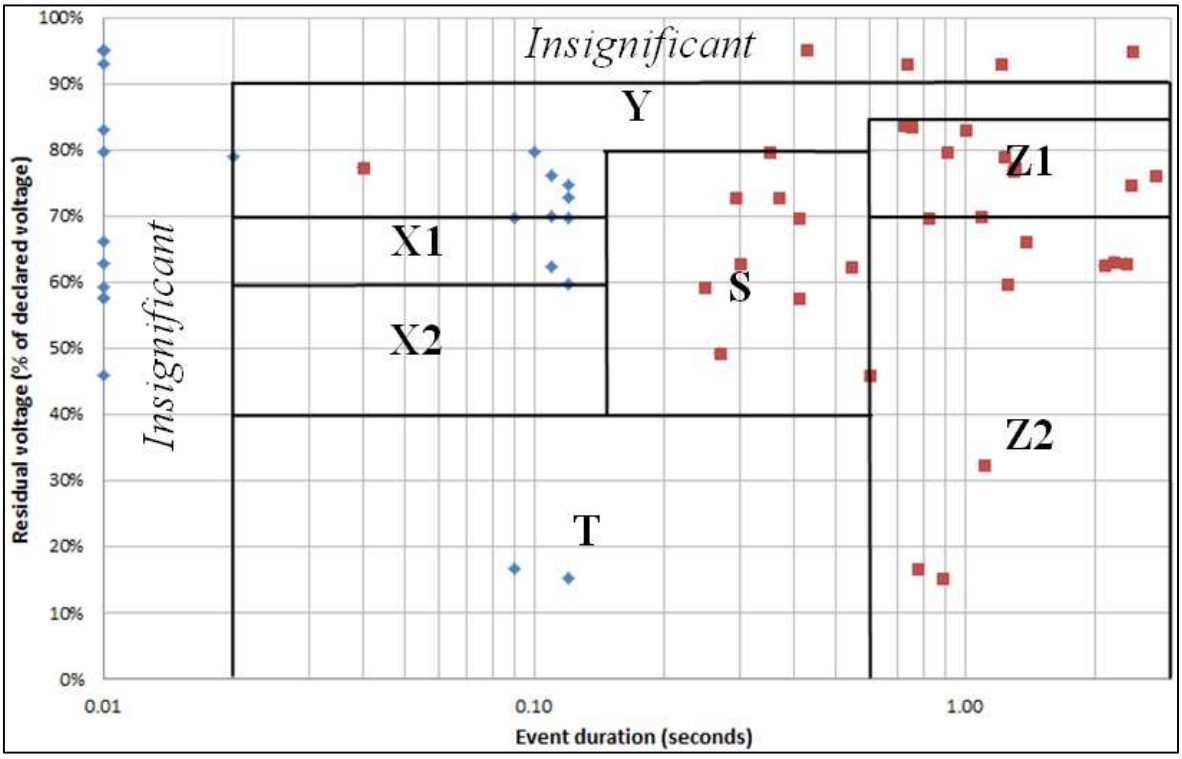

Figure 8-8 Comparison of voltage dip scatter plot results

Table 8-4 below shows a comparison between the measured voltage dip results from Table 8-2 and the hypothetical voltage dips from Table 8-3.

Table 8-4 Comparison of voltage dip results

Voltage dip category	Number of voltage dips measured at substation after implementing single-phase breaker scheme	Number of hypothetical voltage dips at Petrusburg substation if single-phase breaker scheme was not implemented
Insignificant	14	4
Y	7	1
X1	3	0
X2	1	0
S	1	10
T	2	0
Z1	4	10
Z2	3	10

Table 8-4 illustrates that the single-phase breaker scheme reduces the effects of voltage dip propagation quite substantially. With the scheme being implemented, the voltage dips are much shorter - which affords plant equipment the opportunity to ride through the voltage dips caused by faults on the MV network.

Table 8-5 shows a comparison of momentary interruptions on the PTDI and PTPE lines. The comparison took three scenarios into consideration. Note that 19 of the 35 events were earth faults.

Table 8-5 Comparison of momentary interruptions on MV lines

Line name:	PTPE	PTDI
Single-phase breaker scheme implemented: Number of momentary interruptions	8	1
No scheme implemented: Number of hypothetical momentary interruptions	23	12
Neutral breaker scheme implemented: Number of hypothetical momentary interruptions	7	9

Implementing only the single-phase breaker scheme resulted in 74.3% less power interruptions experienced by customers compared to not implementing any scheme. Implementing only the neutral breaker scheme resulted in 54% less power interruptions being experienced by customers when compared to not implementing any scheme.

The scheme coverage of the single-phase breaker is limited to the MV line on which the scheme is installed, as graphically shown in Figure 8-9.

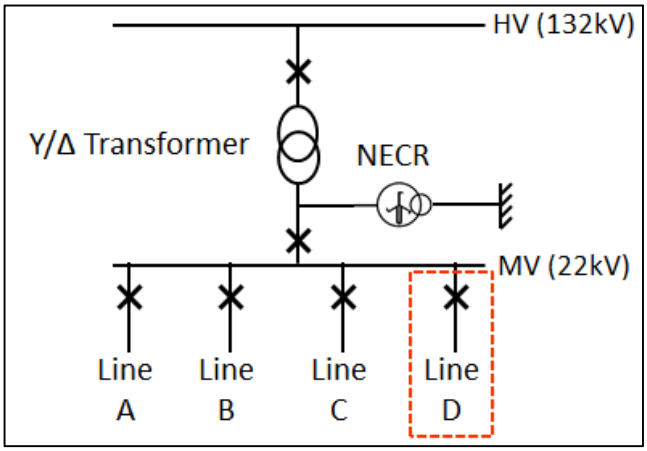

Figure 8-9 A Single-phase breaker scheme installed on Line D will only clear faults on Line D

With the single-phase breaker scheme installed the MV network remains grounded at all times and therefore the capacitive coupling of the overhead line under fault conditions is much less when compared to an ungrounded network. The main contributor to the secondary arc current for

the single-phase breaker scheme is the magnitude of the transformer feedback currents. The capacitive coupling of the MV overhead line does not significantly contribute towards the secondary arc current. Therefore, to ensure that transient faults are cleared, it is recommended that the feedback current due to the magnetic coupling of Δ/Y transformers not exceed 35 A.

8.2.3 Scheme comparison

Neutral tripping is effective in the clearing of earth faults and high-impedance earth faults. It was found that by implementing neutral tripping, as many as 83.4% of earth faults were successfully cleared. The fault-clearing effectiveness of neutral tripping is primarily determined by the capacitive coupling of the MV network.

Single-phase tripping is effective in the clearing of earth faults and phase-to-phase faults. It was found that by implementing single-phase tripping, 58% of earth faults and 94% of phase-to-phase faults were successfully cleared. The fault-clearing effectiveness of single-phase tripping is primarily determined by the feedback current magnitudes of the Δ/Y transformers on the MV line. In contrast to the neutral tripping, the capacitive coupling contribution in single-phase tripping is much less.

Implementing these methods of transient fault clearing results in less stress being placed on breakers, conductors and transformers within the MV network. The efficiency with which transient faults are cleared positively influences network reliability, since transient faults are cleared before they can develop into permanent faults. The speed with which transient faults are cleared improves the power quality of the MV network with regards to voltage dips, sustained and momentary interruptions.

The neutral breaker scheme results in a reduction of power interruptions and voltage dips caused by earth faults. The power quality of all MV lines connected to the same NECR will be improved. The neutral breaker scheme is capable of clearing transient faults in 60 ms.

The single-phase breaker scheme results in a reduction of voltage dip length on all neighbouring feeders. The MV line on which the fault occurs will experience a one-second single-phase event instead of a three-phase power interruption. The single-phase breaker scheme is capable of clearing transient faults in less than 40 ms.

A summary of the comparison between the neutral breaker and single-phase breaker schemes is given in Table 8-6.

Table 8-6 Neutral tripping and single-phase tripping comparison

	Neutral breaker	Single-phase breaker
Capable of clearing E/F	Yes	Yes
➢ Fault-clearing time	60 ms	10 ms - 40 ms
➢ Power quality impact	No negative impact on customer LV voltage. Reduces length of voltage dips caused by earth faults. Reduces number of momentary interruptions experienced by customers due to earth faults.	Creates a single-phase event for all customers on line for one-second. Allows plant equipment to ride through fault condition. Reduces the length of voltage dips that propagate to neighbouring lines. Reduces number of momentary interruptions experienced by customers due to earth faults.
Capable of clearing high-impedance E/F	Yes	No
Capable of clearing phase-to-phase fault	No	Yes
➢ Fault-clearing time	N/A	10 ms – 40 ms
➢ Power quality impact	N/A	Creates a single phasing event for all customers on line for one-second. Allows plant equipment to ride through fault condition. Reduces the length of voltage dips that are propagated to neighbouring lines. Reduces number of momentary interruptions experienced by customers due to phase-to-phase faults.
Scheme coverage	Scheme clears earth faults on all lines that are connected to the same NECR.	Clears faults only on MV line where scheme is installed.
Limitations	Scheme success rate limited by magnitude of capacitive current Secondary arc current must be less than 35 A.	Scheme success rate limited by transformer feedback currents. Secondary arc current must be less than 35 A.
Mounting location	In substation yard	Mounted on overhead line
Proposed site implementation	Short overhead lines supplying a large amount of customers (townships).	Long rural overhead lines.

8.3 Recommendations

The following recommendations can be made with regards to the work that was performed during this study that may be useful for similar future work:

- When any test is performed on MV networks, safety is the first priority, especially when faults are created in order to test the operation of equipment. Special care needs to be taken with regards to step and touch potential during an earth fault condition
- When implementing the neutral breaker scheme, it is important to ensure that all equipment installed on the MV network is rated for phase-to-phase voltages across phase-to-earth terminals.
- While monitoring the performance of the single-phase breaker scheme, it was observed that faults normally quenched within 40 ms after a breaker opens. Therefore, if the one-second open time of the single-phase breaker can be reduced to 80 ms, it will substantially reduce the single-phase condition experienced by customers. The reclose time of the single-phase breakers could not be set lower than one-second due to hardware constraints.
- A software constraint that was encountered with the single-phase breakers used was that the tripping time of the breaker can be adjusted in steps of 100 ms only. It will be profitable if the breaker trip time can be adjusted in 10 ms increments. This will allow a person to set the minimum trip time to 70 ms, which will allow the breaker not to trip for transformer inrush currents, since the inrush current usually decays to a value below the O/C pickup setting within 60 ms.
- It is important to ensure that the protection philosophy of the neutral breaker and single-phase breaker schemes can integrate with existing network protection philosophies.
- It will be beneficial to install single-phase breakers on all lines that are supplied from the same substation to optimise the reduction of voltage dip propagation.

8.4 Closure

The research done in this dissertation was successful in showing the contribution towards power quality by developing a protection philosophy for the neutral breaker and single-phase breaker schemes. Momentary interruptions, voltage dip propagations and voltage dip times will be reduced. One of the advantages of the single-phase breaker scheme is that three-phase LV motors will be able to ride through the single-phase event, which will reduce the overall plant downtime of customers.

The neutral breaker and single-phase breaker schemes performed well in clearing transient faults from MV networks. This greatly contributes towards limiting the amount of equipment damage caused by transient faults on MV networks due to the fast fault-clearing capabilities of the schemes.

Both the schemes have a significant contribution to the safety of humans and animals in the case where inadvertent contact is made with the MV network, because of the fast fault-clearing capabilities of the schemes.

References

[1] Eskom, "The integrated annual report 2015," Eskom Holdings, Sandton, March 2015.

[2] W. L. Vosloo and J. P. Holtzhausen, High voltage engineering – Practice and Theory, 2011.

[3] R. Smeets and P. Knol, "Verification of lifetime arcing stress withstand of circuit breakers through testing," in *Cigre 6th Southern Africa Regional conference*, Cape Town, Paper no. P402, August 2009.

[4] J. P. Scholtz, "Improved transient earth fault clearing on solid and resistance earthed MV networks," M.S. thesis, University of Cape Town, Cape Town, 2011.

[5] S. Hänninen, "Single phase earth faults in high impedance grounded networks," Ph.D. dissertation, VTT Publications, Vaasa, Finland, 2001.

[6] J. C. Pfeiffer, "Arc flash," Pfeiffer Engineering Co., Louisville, Kentucky, pp. 1 - 20, 2008.

[7] C. J. van der Mescht and W. J. D. van Schalkwyk, "Clearing of transient faults in MV networks," in *CUT 18th Research Seminar*, Bloemfontein, pp. 1-17, October 2015 .

[8] IEEE, "IEEE 1584 -2002 Guide for Performing Arc Flash Hazard Calculations," IEEE standards, September 2002.

[9] M. F. McGranaghan, D. R. Mueller and M. J. Samotyj, "Voltage sags in industrial power systems," *IEEE Transactions on Industry Applications*, vol. 29, p. 379–403, 1993.

[10] R. C. Leborgne, G. Olguin, J. M. Filho and H. J. Bollen, "Effect of PQ-monitor Connection on Voltage Dip Indices: PN vs PP Voltages," *Electrical Power Quality and Utilisation*, vol. II, pp. 17 - 26, 2006.

[11] J. Lamoree, D. Mueller, P. Vinett and W. Jones, "Voltage sag analysis case studies," Electrotek Concepts Inc., Knoxville, Tennessee, pp. 1 - 7.

[12] NERSA, "NRS 048-2:Part 2 Electricity Supply – Quality of Supply," Eskom, Pretoria, 2007.

[13] L. Zhang and H. J. Bollen, "Characteristics of Voltage Dips (Sags) in Power Systems," *IEEE Transactions on Power Delivery*, vol. 15, pp. 827 - 832, April 2000.

[14] J. Kennedy, P. Ciufo and A. Agalgaonkar, "A review of protection systems for distribution networks embedded with renewable generation," *Renewable and Sustainable Energy Reviews*, pp. 1308-1317, 2016.

[15] M. Lehtonen, S. Hänninen and T. Hakola, "Earth Faults and Related Disturbances in Distribution Networks," IEEE, Espoo, Finland, pp. 1181 - 1186, 2001.

[16] Coopers, Electrical Distribution system protection, Coopers power systems, 1990.

[17] Eskom Holdings SoC, *Eskom NEPS system*, FSOU region: Eskom, 2016.

[18] J. D. Glover, M. S. Sarma and T. J. Overbye, Power system analysis and design, Toronto, Ontario: Thomson learning, 2008.

[19] M. Kizilcay, G. Ban, L. Prikler and P. Handl, "Interaction of the secondary arc with the transmission system during Single-phase auto reclosure," in *IEEE Bologna Power Tech conference*, Italy, June 2003.

[20] IEEE, "Single phase tripping and reclosing of transmission lines IEEE committee report," *Transactions of Power Delivery*, vol. 7, no. 1, pp. 182 - 192, January 1992.

[21] K. Ngamsanroaj and S. Premrudeeprechacharn, "Transient study for single phase reclosing using arc model on the Thailand 500kV transmission lines from Mae Moh to Tha Ta Ko," in *International Conference on Power Systems Transients (IPST2009)*, Japan, 2009.

[22] J. Serfontein, "Basic Power system protection," Eskom, Bloemfontein.

[23] D. G. Loucks and J. Collins, "What you need to know about arc flashes," Eaton, pp. 1 - 8, July 2013.

[24] R. A. Wilson, J. Keisala, R. Harju and S. Ganesan, "Tripping with the Speed of Light: Arc Flash Protection," ABB, Finland.

[25] P. Ferracci, "Ferroresonance," Schneider Electric, Technical collection - Cahier Technique no.190, pp. 5 - 19 , March 1998.

[26] S. van Zyl, P. Groenewald and R. McCurrach, "Protection settings philosophy for Medium Voltage distribution networks," Eskom, Sandton, pp. 12 - 29, March 2015 .

[27] V. Cohen, Application guide for the protection of L.V. Distribution systems, Johannesburg: Circuit breaker industries Ltd, 2002.

[28] W. J. Dirkse van Schalkwyk and J. M. van Coller, "An investigation into a more optimal choice of BIL on MV feeders," in *Cigre Conference*, October 2013.

[29] T. A. Short, Electric Power Distribution Handbook, Boca Raton, FL: CRC Press, 2003.

[30] J. Pretorius, "Cost-benefit analysis of recloser placements for network reliability," M.S. thesis, University of Cape Town, Cape Town, 2014.

[31] S. H. Ngqungqa, "A critical evaluation and analysis of methods of determining the number of times that lightning will strike a structure," M.S. thesis, University of Witwatersrand, Johannesburg, 2005.

[32] NASA, "GHRC: Lightning Characteristics.," NASA, 23 March 2016. [Online]. Available: http://thunder.msfc.nasa.gov/primer/primer2.html. [Accessed 23 March 2016].

[33] F. Heidler, W. Zischank, Z. Flisowski, C. Bouquegneau and C. Mazzetti, "Parameters of lighting current given in IEC 62305 – Background, Experience and Outlook," in *29th International Conference on Lightning Protection*, Uppsala, Sweden, pp. 1 - 22, June 2008.

[34] A. J. Gonzales, G. C. Kung, C. Raczkowski, C. W. Tylor and D. Thonn, "Effects of Single and Three Pole Switching and High Speed Reclosing on Turbine Generator Shafts and Blades," *IEEE Trans. Power Apparatus and Systems*, vol. PAS 103, no. 11, pp. 3218-3228, November 1984.

[35] M. E. Zevallos and M. C. Tavares, "Single-phase Auto-reclosing studies: Influence of Transversal parameters of a transmission system on the secondary arc current reduction," University of Campinas, Campinas, pp. 1 - 8, 2005.

[36] T. Pniok and M. Kizilcay, "Digital Simulation of Fault Arcs in Power Systems," *ETEP Journal*, vol. 1, pp. 55-60, 1991.

[37] T. Y. Vinokurova, O. A. Dobryagina, E. S. Shagurina and V. A. Shuin, "Selective complex single-phase earth fault protection for distribution medium-voltage networks," Ivanovo

State Power Engineering University, Ivanovo, Russia.

[38] P. E. Sutherland and T. A. Short, "Effects of single-phase reclosing on Industrial loads," in *Industry applications conference, 41st IAS annual meeting*, pp. 2636 - 2644, 2006.

[39] M. Val Escudero, I. Dudurych and M. Redfern, "Understanding ferroresonance," in *39th International Universities Power Engineering Conference*, 2004.

[40] V. Valverde, G. Buigues, A. J. Mazón, I. Zamora and I. Albizu, "Ferroresonant Configurations in Power Systems," in *International Conference on Renewable Energies and Power Quality (CREPQ'12)*, Spain, March 2012.

[41] S. Santoso, R. C. Dugan, T. E. Grebe and P. Nedwick, "Modeling ferroresonance phenomena in an underground distribution system," in *IEEE IPST '01*, Rio de Janeiro, Brazil, June 2001.

[42] A. Norouzi, "Open phase conditions in transformers analysis and protection algorithm," in *MIPSYCON conference*, Markham, ON, pp. 1 - 14, 2013.

[43] Alstom, "Network Protection & Automation Guide," Alstom Grid, May 2011.

[44] A. Britten, M. Korber and R. Ramnarain, "Coupling," in *Eskom Power Series - The planning, design and construction of overhead power lines*, Sandton, Crown Publications cc, Eskom Holdings Ltd, February 2005, p. 311.

[45] F. Mariani, S. Bisnath and J. Reynders, Inductive instrument transformers and protective applications, Johannesburg: Crown Publications, 2007.

[46] J. Roberts, H. J. Altuve and D. Hou, "Review of ground fault protection methods for grounded, ungrounded, and compensated distribution systems," Schweitzer Engineering Laboratories, Inc., Pullman, USA, 2001.

[47] E. Määttä, "Earth fault protection of compensated rural area cabled Medium Voltage networks," M. S. thesis, University of Vaasa, Vaasa, 2014.

[48] J. D. Jackson, Classical Electrodynamics, Wiley, 1975.

[49] M. van der Mescht, "Capacitive coupling on overhead power lines," in *CUT 18th research seminar*, Bloemfontein, October 2015.

[50] W. T. J. Hulshorst, E. L. M. Smeets and J. A. Wolse, "Benchmarking on PQ desk survey: What PQ levels do different types of customer need?," KEMA Nederland B.V, Arnhem, Netherlands, June 2007.

[51] Eskom, "Grid connection code for renewable power plants (RPPs) connected to the electricity transmission system (TS) or the distribution system (DS) in South Africa - Version 2.8," Eskom Transmission Division, Sandton, July 2014.

[52] M. F. McGranaghan, Electrical power quality, McGraw-Hill, 2004.

[53] W. J. Dirkse van Schalkwyk and J. M. van Coller, "Choice of MV feeder BIL to maximize QoS and minimize failure," in *Cired - 23rd International Conference on Electricity Distribution*, Lyon, Paper no. 0998, June 2015.

[54] A. A. Ansari and D. M. Deshpande, "Investigation of performance of 3-phase asynchronous machine under voltage unbalance," *Journal of Theoretical and Applied Information Technology*, vol. 6, no. 1, pp. 21-26, 2009.

[55] A. Pichai, "Effects of unbalanced voltage on induction motor operating points under different load torque profiles," in *13th International Conference on Electrical Engineering/Electronics, Computer, Telecommunications and Information Technology (ECTI-CON)*, Thailand, 2016.

[56] A. Chauhan, P. Thakur and D. Raveendhra, "Assessment of induction motor performance under supply voltage unbalance: A review," in *Engineering and Systems (SCES)*, Dehradun, India, 2013.

[57] M. Lehtonen and T. Hakola, Neutral earthing and power system protection: Earthing solutions and protective relaying in medium voltage distribution networks., Vaasa, Finland: ABB, 1996.

[58] J. E. Allen and S. K. Waldorf, "Arcing Ground Tests on a Normally Ungrounded 13kV 3-Phase Bus," *IEEE Transactions*, vol. 65, May 1946.

[59] M. J. Heathcote, The J & P Transformer Book, Woburn: Reed Educational and Professional Publishing Ltd, 1998.

[60] S. van Zyl, "High resistance neutral earthing of MV networks with embedded generation," *Energize*, pp. 28-30, Jan/Feb 2009.

[61] IEEE, Power system protection, England: MacDonald & Co., 1995.

[62] W. J. Dirkse van Schalkwyk, "The placing of line surge arresters and fuses on11 and 22kV lines to protect equipment against lightning," M.S. thesis, Stellenbosch University, Stellenbosch, March 2001.

[63] M. du Preez and W. J. Dirkse van Schalkwyk, "Lightning and Power Frequency Performance of MV Pole Mounted Transformers," in *Cigre: 7th SOUTHERN AFRICA REGIONAL CONFERENCE*, Somerset West, October 2013.

[64] Y. Y. Iossel, E. S. Kochanov and M. G. Strunskiy, The Calculation of Electrical Capacitance, Ohio: National Technical Information Service, Springfield, August 1971.

[65] F. Kiessling, P. Nefzger, J. F. Nolasco and U. Kaintzyk, Overhead Power Lines: Planning, Design, Construction, Berlin, Heidelberg: Springer, 2003.

A. Appendix A – Transient fault data

Two years of historical data obtained from Eskom's NEPS database was used to produce the figures shown in Figure A-1, Figure A-2, Figure A-3, Figure A-4 and Figure A-5. Transient faults include, but are not limited to, the following root cause categories:

- Overhead line problem
- No fault found
- Conductor problem
- Adverse weather
- Lightning

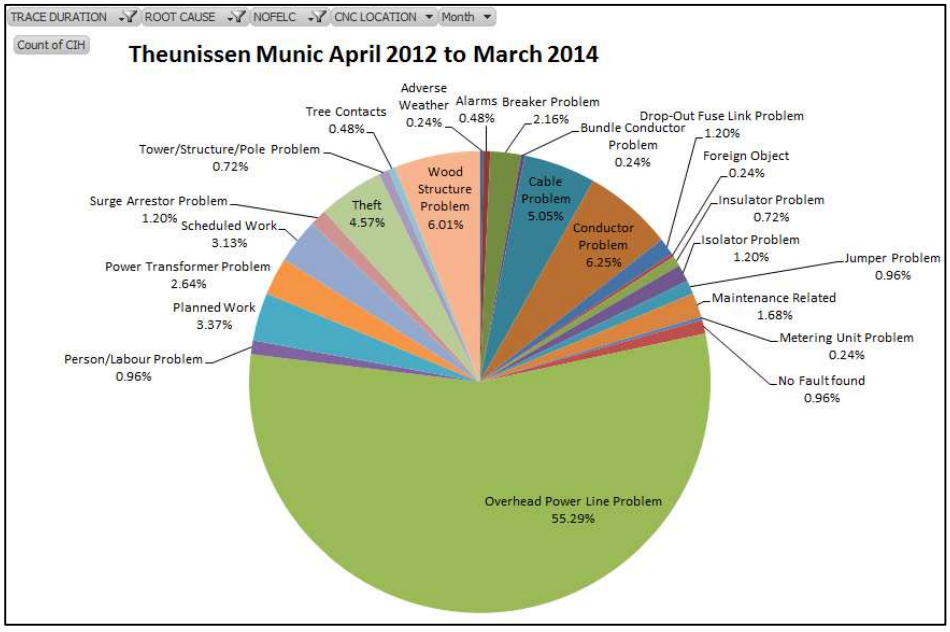

Figure A-1 Root causes which resulted in customer interruptions at Theunissen Munic substation (total of 416 events)

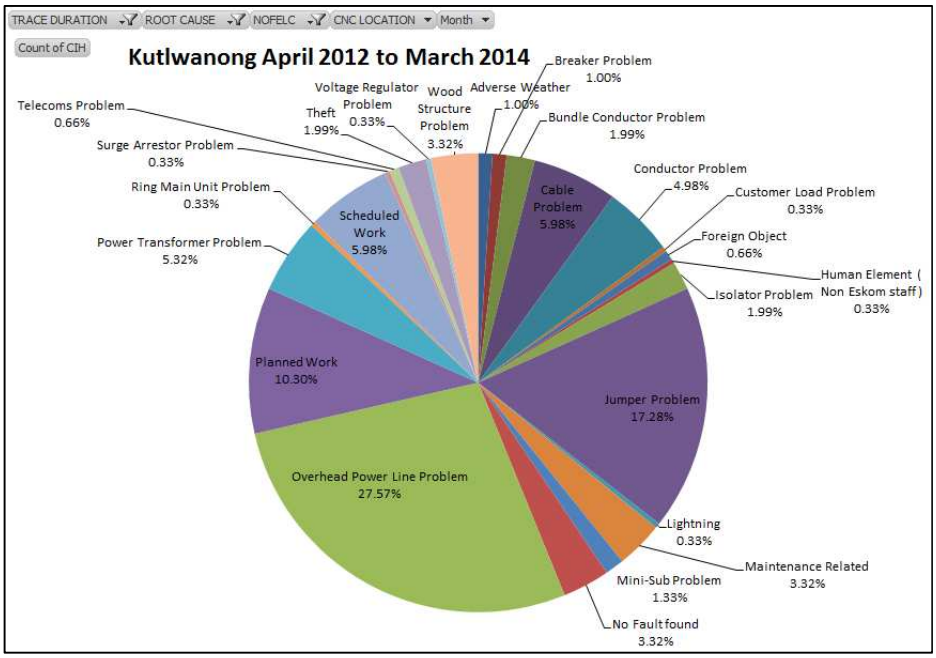

Figure A-2 Root causes which resulted in customer interruptions at Kutlwanong substation (total of 301 events)

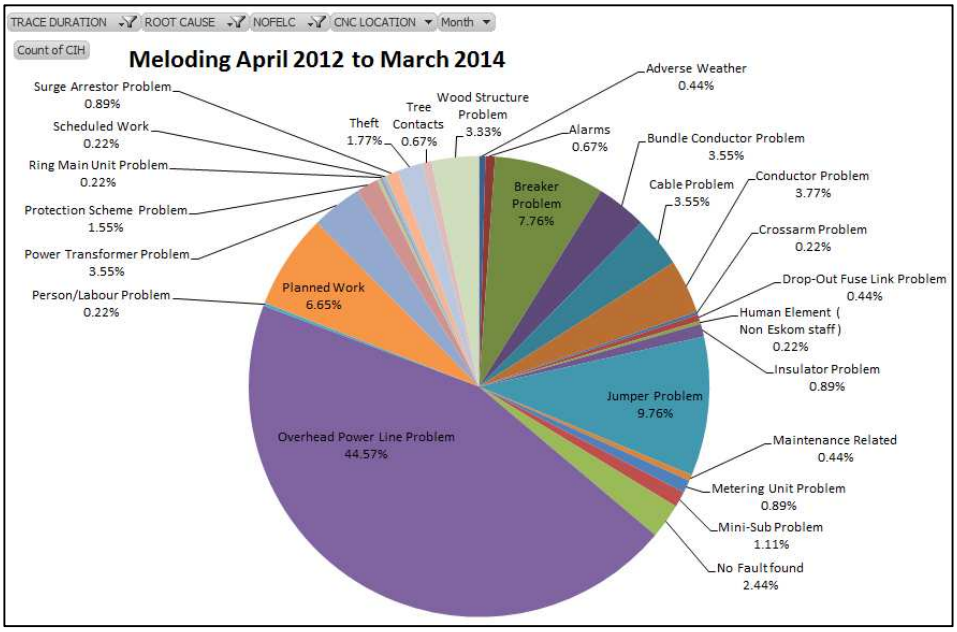

Figure A-3 Root causes which resulted in customer interruptions at Meloding substation (total of 451 events)

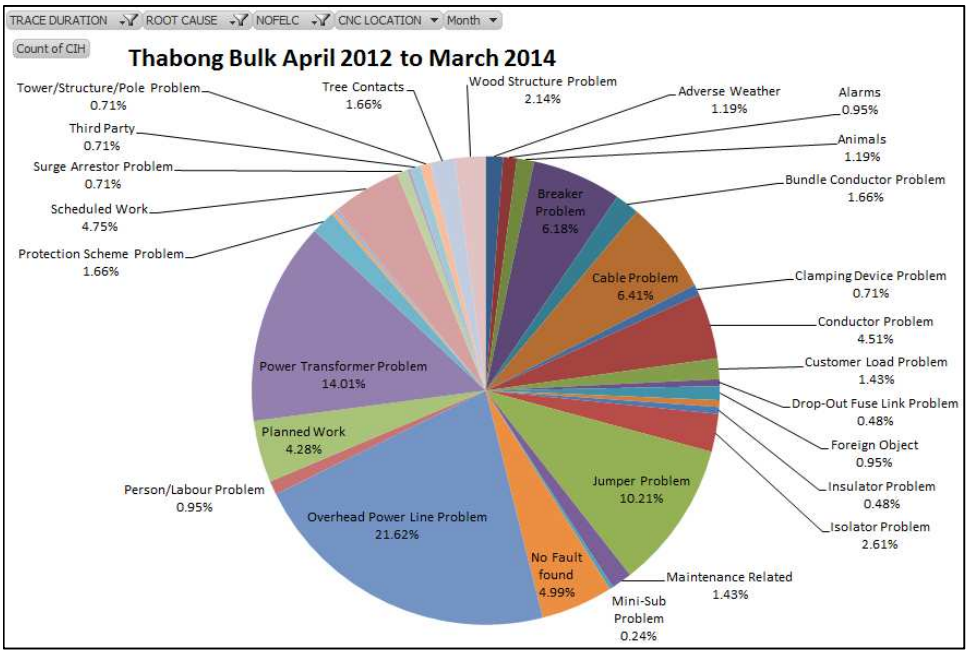

Figure A-4 Root causes which resulted in customer interruptions at Thabong Bulk substation (total of 421 events)

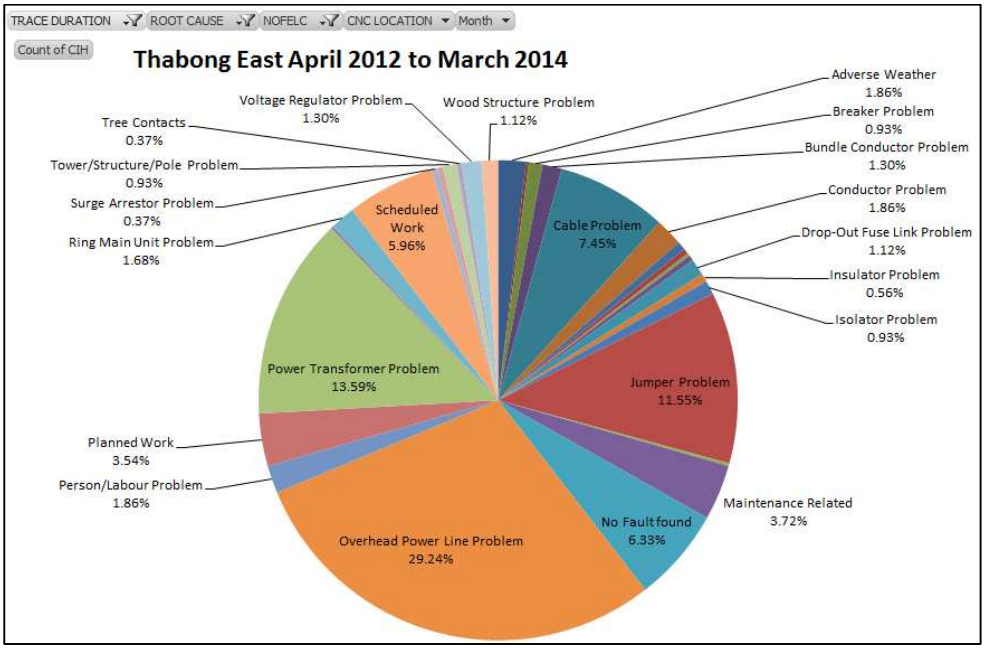

Figure A-5 Root causes which resulted in customer interruptions at Thabong East substation (total of 537 events)

B. Appendix B – Lightning analysis

A gridded exposure lightning analysis was performed on all MV lines that are connected to the proposed substations listed in Table 6-3 by using the FALLS system. The gridded exposure analysis in Figure B-1, Figure B-2, Figure B-3, Figure B-4 and Figure B-5 show the lightning ground stroke density with an applied 2 km x 2 km grid. The analysis was performed over a five-year period in order to obtain the average lightning ground stroke densities. Some areas of the MV lines indicated a ground stroke density, which was as high as 30 strokes per year. The thematic legend in Figure B-1, Figure B-2, Figure B-3, Figure B-4 and Figure B-5 displays the normalised ground stroke density, which is the average amount of ground strokes per year

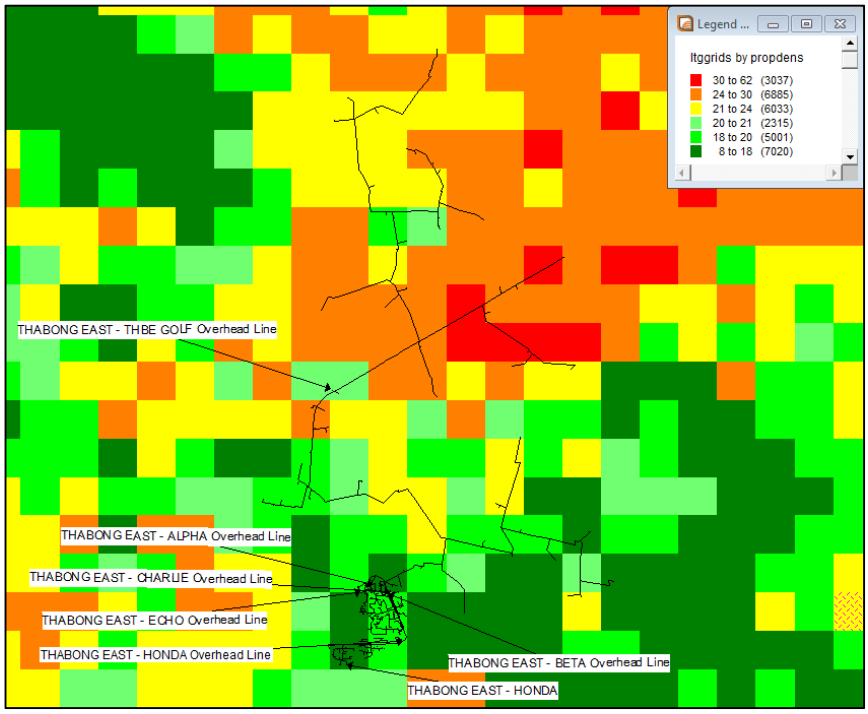

Figure B-1 Five year GSD for Thabong East substation MV lines (2009 – 2014)

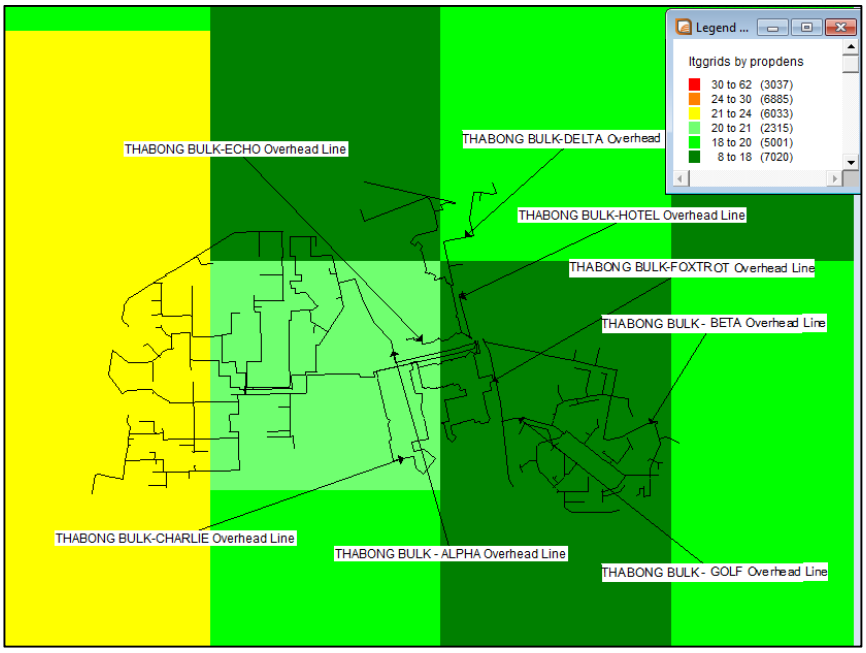

Figure B-2 Five year GSD for Thabong Bulk substation MV lines (2009 – 2014)

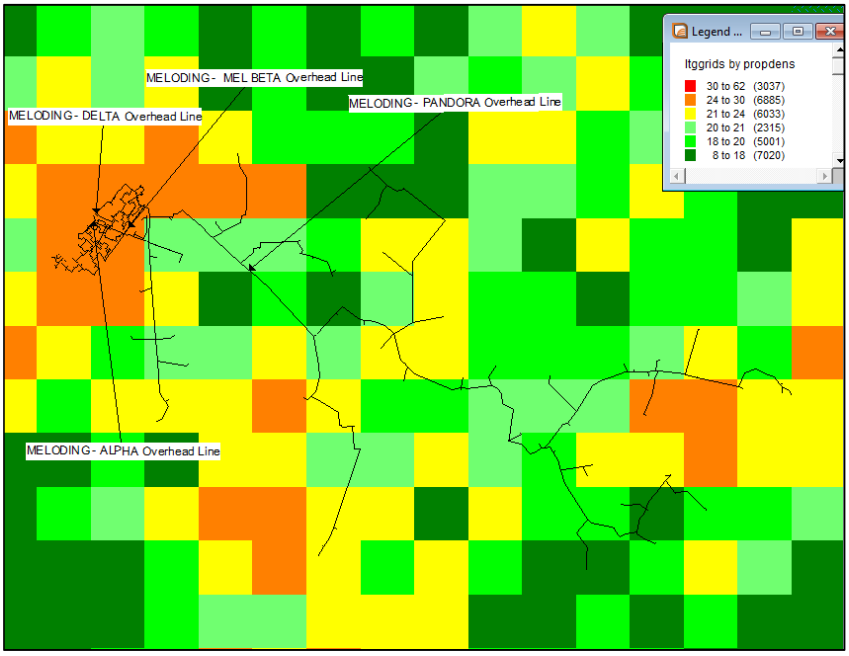

Figure B-3 Five year GSD for Meloding substation MV lines (2009 – 2014)

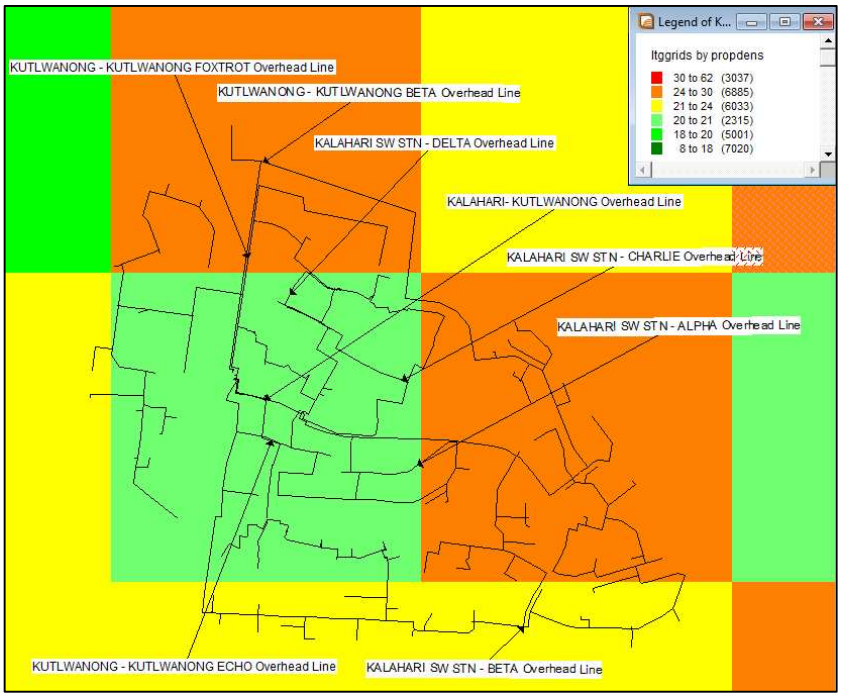

Figure B-4 Five year GSD for Kutlwanong substation MV lines (2009 – 2014)

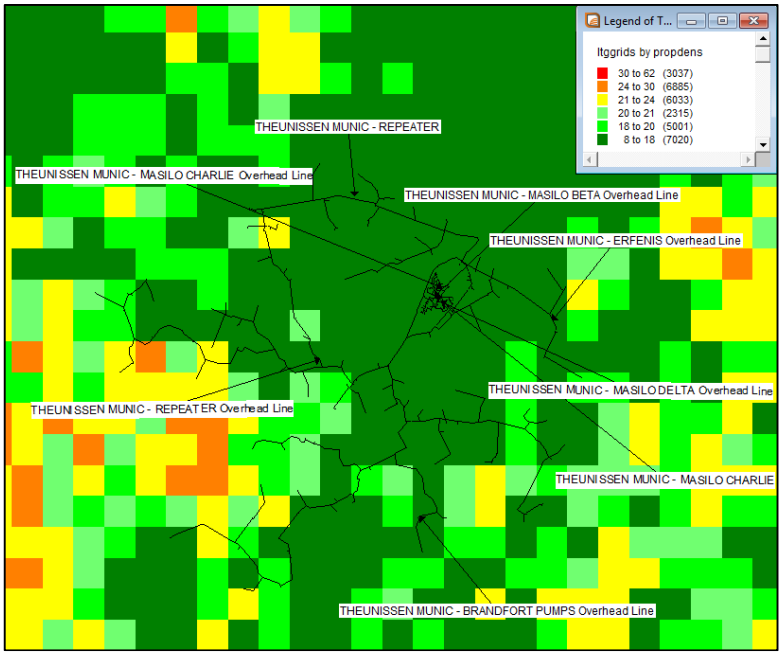

Figure B-5 Five year GSD for Theunissen Munic substation MV lines (2009 – 2014)